Quaternary geology and paleoseismology in the Fucino and L'Aquila basins

6th INQUA International Workshop on Active Tectonics Paleoseismology and Archaeoseismology
Pescina (AQ) - Italy

GFT - *Geological Field Trips*

Quaternary geology and Paleoseismology in the Fucino and L'Aquila basins

6th INQUA, 19-24 April 2015, Pescina (AQ) - Fucino basin

Sara Amoroso[1], Filippo Bernardini[2], Anna Maria Blumetti[3], Riccardo Civico[4], Carlo Doglioni[5], Fabrizio Galadini[1], Paolo Galli[6], Laura Graziani[4], Luca Guerrieri[3], Paolo Messina[7], Alessandro Maria Michetti[8], Francesco Potenza[9], Stefano Pucci[4], Gerald Roberts[10], Leonello Serva[11], Alessandra Smedile[1], Luca Smeraglia[5], Andrea Tertulliani[4], Giacomo Tironi[12], Fabio Villani[1], Eutizio Vittori[3]

[1] INGV, L'Aquila. [2] INGV, Bologna. [3] ISPRA, Rome. [4] INGV, Rome. [5] Dip. Sc. della Terra, Univ. "La Sapienza", Rome. [6] Dip. Prot. Civile, Rome. [7] CNR-IGAG, Montelibretti, Rome. [8] Univ. dell'Insubria, Como. [9] Dep. of Civil, Arch. Env. Eng., Univ. of L'Aquila. [10] Birbeck Univ., London, UK. [11] Independent Consultant, Rome. [12] Studio Eng. Giacomo Tironi, L'Aquila.

Corresponding Author e-mail address: luca.guerrieri@isprambiente.it

geological field trips 2016 - 8(1.2)

2

publishing group

INDEX

4

information

Abstract

This 2 days-long field trip aims at exploring field evidence of active tectonics, paleoseismology and Quaternary geology in the Fucino and L'Aquila intermountain basins and adjacent areas, within the inner sector of Central Apennines, characterized by extensional tectonics since at least 3 Ma. Each basin is the result of repeated strong earthquakes over a geological time interval, where the 1915 and 2009 earthquakes are only the latest seismic events recorded respectively in the Fucino and L'Aquila areas. Paleoseismic investigations have found clear evidence of several past earthquakes in the Late Quaternary to Holocene period. Active tectonics has strongly imprinted also the long-term landscape evolution, as clearly shown by numerous geomorphic and stratigraphic features.

Due to the very rich local historical and seismological database, and to the extensive Quaternary tectonics and earthquake geology research conducted in the last decades by several Italian and international teams, the area visited by this field trip is today one of the best studied paleoseismological field laboratories in the world. The Fucino and L'Aquila basins preserve excellent exposures of earthquake environmental effects (mainly surface faulting), their cumulative effect on the landscape, and their interaction with the urban history and environment. This is therefore a key region for understanding the role played by earthquake environmental effects in the Quaternary evolution of actively deforming regions, also as a major contribution to seismic risk mitigation strategies.

Keywords: *Quaternary geology, paleoseismology, tectonic terraces, intermountain basin, surface faulting, fault scarp, seismic hazard*

Riassunto

L'escursione ha una durata di due giorni ed è focalizzata sull'evoluzione quaternaria, la tettonica attiva e la paleosismologia dei bacini intermontani del Fucino e de L'Aquila ed aree limitrofe (Appennino Centrale).

La tettonica estensionale è attiva in quest'area da almeno 3 milioni di anni. Ciascun bacino, delimitato da versanti e scarpate di faglia, è il risultato della sommatoria di più eventi di fagliazione superficiale in un intervallo di tempo geologico in cui gli eventi del 1915 e del 2009 sono i più recenti che hanno prodotto fagliazione in superficie nei due bacini.

Grazie alla grande disponibilità di dati storici e sismologici ed alle numerose ricerche sulla tettonica attiva e paleosismologia condotte negli ultimi decenni da numerosi gruppi di ricercatori italiani e stranieri, la zona attraversata dall'escursione è una delle più conosciute dal punto di vista paleosismologico. Queste indagini hanno consentito di riconoscere le evidenze stratigrafiche di diversi terremoti avvenuti nel periodo tardo Quaternario – Olocene. La tettonica attiva ha inoltre fortemente condizionato anche l'evoluzione a lungo termine del paesaggio, come chiaramente mostrato da numerose caratteristiche stratigrafiche e geomorfologiche.

Nei bacini del Fucino e de L'Aquila sono dunque riconoscibili gli effetti geologici cosismici (prevalentemente fagliazione superficiale), ed il loro effetto cumulato sul paesaggio, e la loro interazione con la storia urbana e l'ambiente. Per questo motivo, è considerata una regione chiave per la comprensione del ruolo giocato dagli effetti geologici cosismici nell'evoluzione quaternaria di regioni in deformazione attiva, anche come importante contributo alle strategie di mitigazione del rischio sismico.

Parole chiave: *geologia del Quaternario, paleosismologia, terrazzi tettonici, bacini intermontani, superfice di faglia, scarpata di faglia, pericolosità sismica*

geological field trips 2016 - 8(1.2)

5

information

Program

The area covered by this field trip is located in Abruzzo (Central Italy), and in particular in the L'Aquila province. This area can be easily reached by the A24 (Roma-L'Aquila-Teramo) and A25 (Roma-Pescara) motorways. The area can also be reached by train, stopping at the stations of Avezzano and Pescina, on the line Roma-Pescara. The first day of the excursion focuses on the Fucino basin: after a panoramic view from its western border (Stop 1.1), the geomorphic and paleoseismic evolution of the northern border will be examined in detail along the Magnola fault (Stop 1.2) and along the Cerchio-Pescina-Parasano fault (Stop 1.3). The remaining stops will explore in detail the paleoseismic evidence along the eastern border, including the evidence of the 1915 coseismic rupture, and in particular along the Serrone fault (Stop 1.4) and the San Benedetto-Gioia de' Marsi fault (Stops 1.5 and 1.6).

In the second day, we will move to the L'Aquila basin and middle Aterno Valley. Specific focus will be on active tectonics and paleoseismology along the middle Aterno Valley fault (Stops 2.1 and 2.2). Stops 2.3, 2.4 and 2.5 will detail the Quaternary geology of the same area. In the afternoon, we will move to L'Aquila city center, to observe the macroseismic effects caused by the 2009 L'Aquila earthquake (Stops 2.6 to Stops 2.11).

General information

The best periods to undertake this field trip, in terms of climatic and expected weather conditions, are April-June and September-October. In July and August, temperatures are hot. In November and winter temperatures are cold and climate is wetter with frequent snowfalls.

The average weather conditions are the following: Spring: T min = 5 °C, T max = 18 °C, Rainfall = 60 mm per month, Humidity = 72 %; Summer: T min = 15 °C, T max = 29 °C, Rainfall = 40 mm per month, Humidity = 70 %, Sudden storms can be frequent; Fall: T min = 6 °C, T max = 16 °C, Rainfall = 75 mm per month, Humidity = 75 %.

In all seasons a waterproof coat/jacket is recommended. From June to September sun protection and hats are recommended.

All participants need comfortable hiking boots. A rucksack is necessary to carry rain protection, spare clothing (T-shirt or a fleece/sweater), a packed lunch, water and snacks.

Safety

The aim of this document is to collate key information into a simple format for use by field and on-call staff in the event of an accident.

Safety in the field is closely related to awareness of potential difficulties, fitness and use of appropriate equipment. Safety is a personal responsibility and all participants should be aware of the following issues.
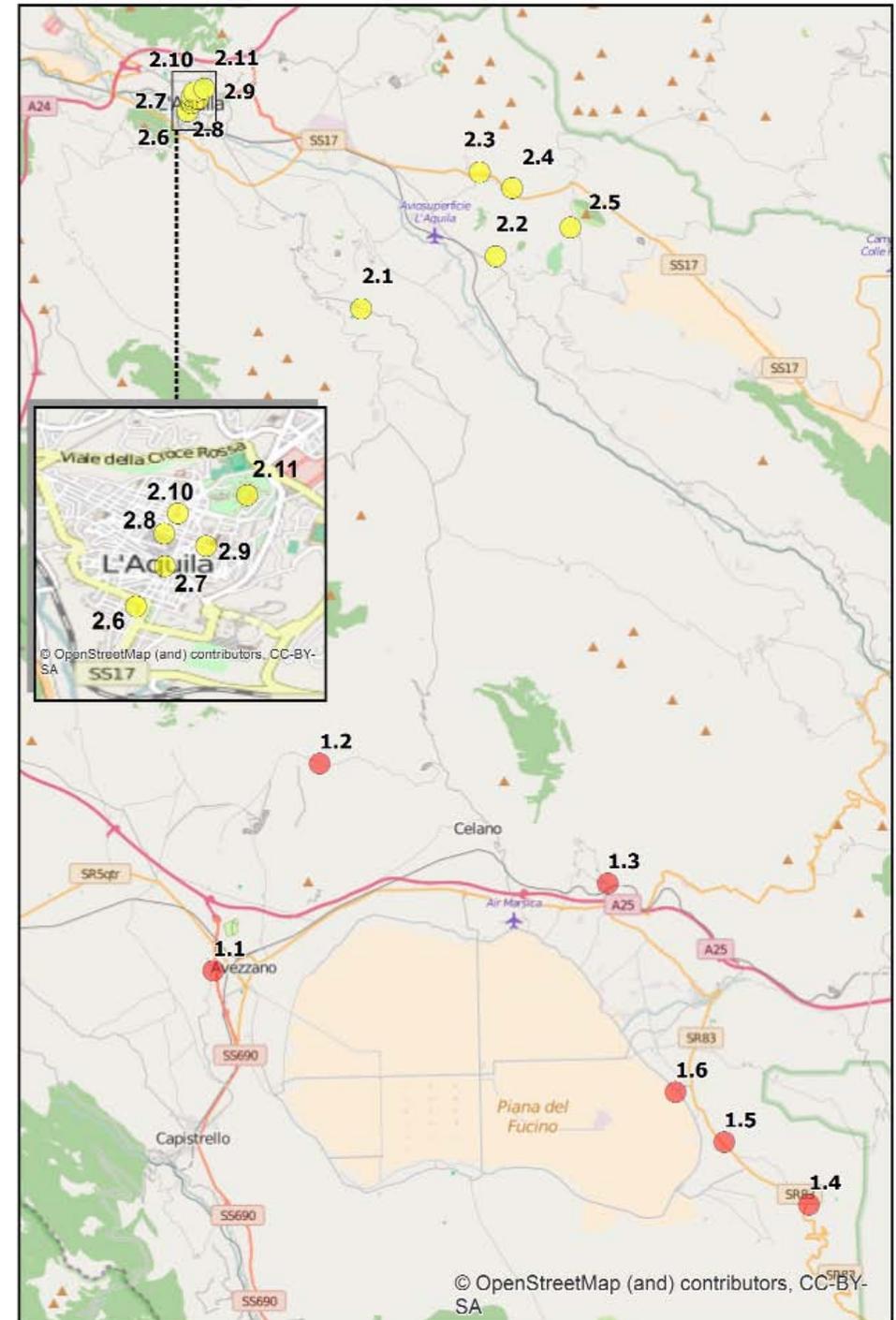
- The excursion takes place at moderate altitudes (between 650 and 1100 meters a.s.l.).
- Most of the outcrops are along the road and long walks are never scheduled
- Trainer or running shoes are unsuitable footwear in the field.
- A waterproof coat/jacket is essential.
- Each vehicle needs to carry one basic first aid kit.
- Mobile/cellular phone coverage is good although in some remote places there is no signal.

Emergency Services

In case of emergency please contact the following numbers (valid all over Italy)
- Medical Emergency/Ambulance: 118
- Police: 113 or 112
- Firemen: 115

Medical Facilities in the area

The nearest hospitals are
- 1st day (Fucino): Ospedale SS. Filippo e Nicola, Via G. di Vittorio, 67051 Avezzano (AQ), Tel.: +39-0862-3681
- 2nd day (L'Aquila): Ospedale Regionale San Salvatore, Via Vetoio, 1, 67100 Coppito, L' Aquila (AQ), Tel.: +39-08634991

1. Geological and geodynamic framework of Central Apennines

The Central Apennines are the midmost part of the Apennines chain, a NW-SE oriented, late Oligocene-Present fold and thrust belt, that composes the backbone of the Italian peninsula (Fig. 1).

The Meso-Cenozoic stratigraphical successions cropping out in Central Apennines developed on the southern Neotethyan passive margin, where a basin-platform system developed in the area as a consequence of a rifting stage that affected the whole Neotethyan region during the lower Jurassic. The paleogeography related to the lower Jurassic basin-platform system was persistent until early Tertiary times.

Fig. 1 - Synthetic tectonic map of Italy and surrounding seas; **1)** foreland areas; **2)** foredeep deposits; **3)** domains characterized by a compressional tectonic regime; **4)** Alpine orogen; **5)** areas affected by extensional tectonics: these areas can be considered as a back-arc basin system developed in response to the eastward roll-back of the west-directed Apenninic subduction; **6)** crystalline basement; **7)** oceanic crust in the Provençal basin (Miocene in age) and in the Tyrrhenian Sea (Plio-Pleistocene in age) and old mesozoic oceanic crust in the Ionian basin; **8)** Apenninic water divide; **9)** main thrusts; **10)** faults. From Scrocca et al., 2003.

8

excursion notes

Fig. 2 - Geological map of the central Apennines. **1)** Plio-Pleistocene marine and continental deposits; **2)** Pleistocene volcanics; **3)** buried Pliocene marine sediments; **4)** clastic deposits related to the Messinian/Early Pliocene thrust-top basins; **5)** Messinian clastic deposits and evaporites; **6)** foredeep siliciclastic deposits of undifferentiated age (Upper Miocene); **7)** Meso-Cenozoic shallow-water limestones; **8)** Meso-Cenozoic deep-water limestones; **9)** thrust; **10)** undifferentiated fault; **11)** isobaths in meters of the base of the Pliocene deposits. Dotted line indicates the trace of CROP 11 project (Fig. 5). Modified from Cosentino et al., 2010.

The pre-rifting Triassic rocks, outcropping in Central Apennines belong to shallow water carbonate platform and euxinic basins paleo-environments that led to depositions of shallow-marine carbonates, dolostones and sulfates about 1.5-2 km thick (Bally et al., 1986). The lower Jurassic tectonic phase related to the Neotethys Jurassic rifting is evident in the Mesozoic stratigraphic records of Central Apennines (Cosentino et al., 2010).

The shallow-water platform domain was broken-up and new platform-basin systems developed, being characterized by downthrown sectors dominated by transitional to deep-water sedimentation, with deposition of limestones, marly limestones, and marls (Fig. 2, Gran Sasso Chain, Morrone Mts., Le Mainarde Mts. and Majella area), and upthrown sectors with shallow-water carbonate platform deposits (Fig. 2, Lepini Mts., Ausoni Mts., Aurunci Mts., Ernici Mts., Simbruini Mts. and Marsica area). The early-medium Cretaceous regional paleogeography was quite similar to that of the late Jurassic and the platform-basin systems led to the deposition of thick shallow- and deep-water carbonate successions (up to 4-6 km thick, Bally et al., 1986).

In the platform domain, a late Cretaceous-early Miocene hiatus was followed by deposition of early Miocene paraconformable carbonates, deposited along a carbonate ramp (Civitelli & Brandano, 2005), while in the deeper domains sedimentation continued throughout the Paleogene.

During Eocene-Oligocene times a critical scenario developed in the proto-western Mediterranean area, with the existence of the S-SE-directed Alpine subduction system (approaching the end of its existence) and the young NW-dipping Apennine subduction system starting its activity (Doglioni et al., 1998; Carminati et al., 2012), which possibly developed along the retrobelt of the Alpine orogeny (Fig. 3). This means that two subduction systems, with nearly opposite polarity, were present in a relatively narrow area for a short time.

During the late Miocene, the southern Neotethyan passive margin was involved in the evolution of the Apennines, that accreted the sedimentary cover of the passive margin during the "eastward" roll-back of the NW-dipping Apennines subduction system (Fig. 4) (Doglioni, 1991). This was also confirmed by the
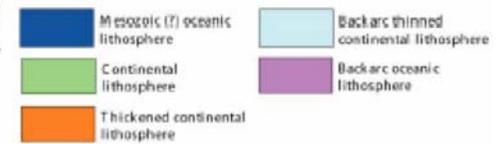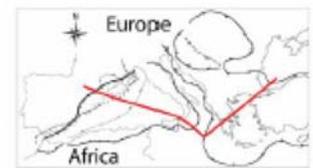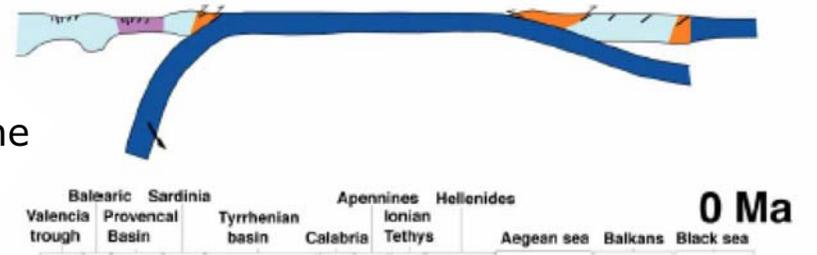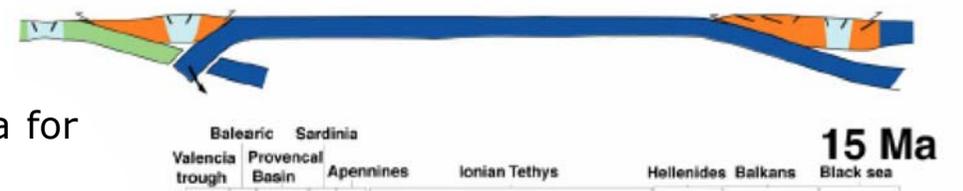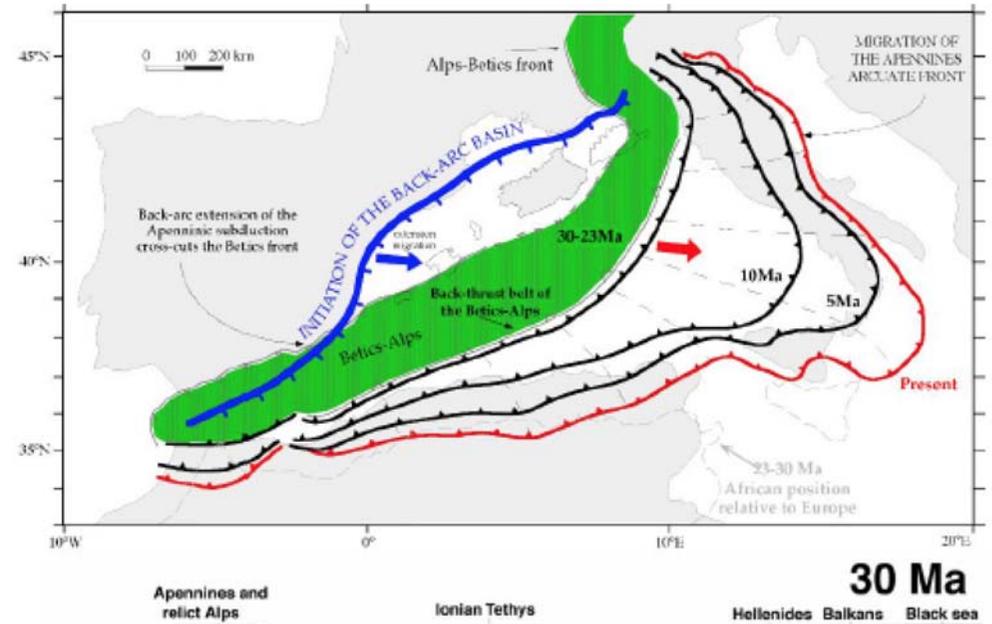
Fig. 3 - The early "east"-directed Alpine subduction was followed by the Apennines "west"-directed subduction, which developed along the retrobelt of the preexisting Alps. The slab is steeper underneath the Apennines, possibly due to the "westward" drift of the lithosphere relative to the mantle (From Carminati & Doglioni, 2005).

interpretation of CROP 11 line (Fig. 5), a deep seismic profile across the Central Apennines (Fig. 2). The Apennines slab roll-back induced subsidence and boudinage of large portions of the Alps that have been scattered and dismembered into the Apennines-related backarc basin: the Provencal and the Tyrrhenian (Fig. 3) (Doglioni et al., 1998).

Within this geodynamical setting, in the Central Apennines tectonically-controlled sedimentary basins are developed with the deposition of hemipelagic marls in a foreland environment (Carminati et al., 2007), followed by deposition of turbidites composed of siliciclastic sandstones in a foredeep setting ahead the propagating deformative front (Patacca & Scandone, 1989; Cipollari & Cosentino, 1991; Patacca et al., 1991; Milli & Moscatelli,
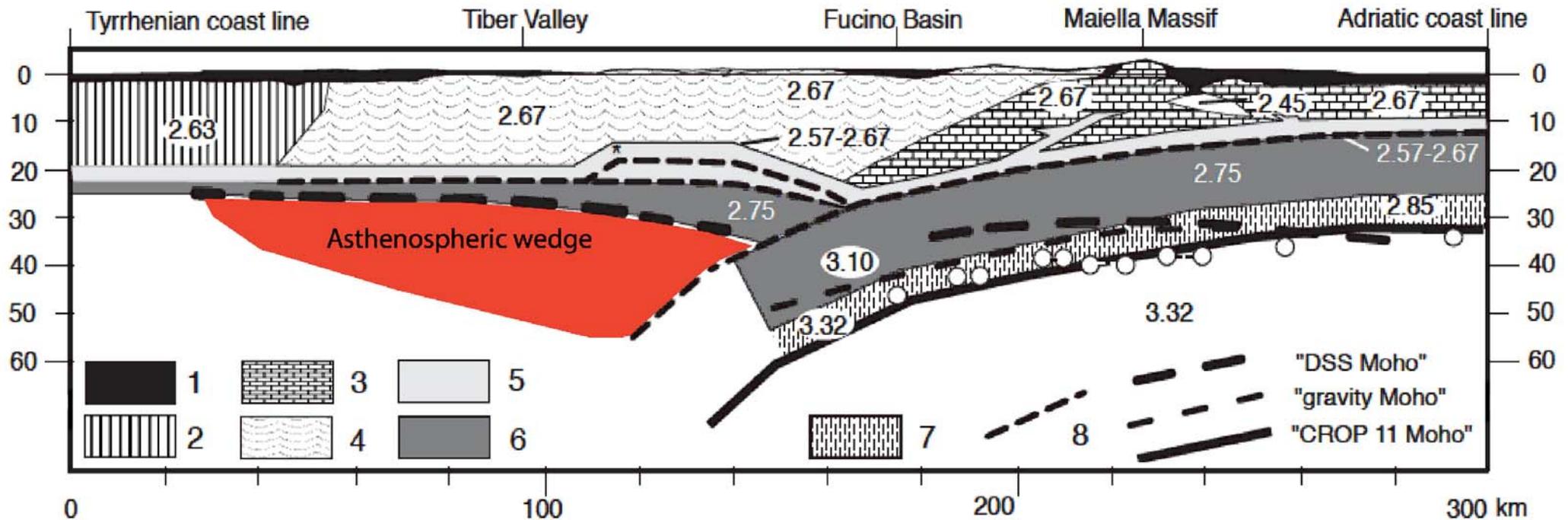
Fig. 4 - Tectonic models of subduction of the Adriatic continental crust. **1)** "stripped units" in the gravity model; **2)** Tyrrhenian upper crust; **3)** Apulian Platform units; **4)** other carbonate units (or having similar density): upper part of the Paleozoic- Triassic sequence, involved in thrusting deformation; **5)** Lower part of the sediantary cover; **6)** lower part of the Paleozoic-Triassic sequence, undeformed, and crystalline basement; **7)** lower crust; **8)** Apennine sole-thrust. Density values (g/cm³) and distribution are from the gravity model of Di Luzio et al., 2009. Circles indicate local estimates of Moho depth from stations 6-12 and FRES projected on the CROP 11 profile. From Di Luzio et al., 2009.
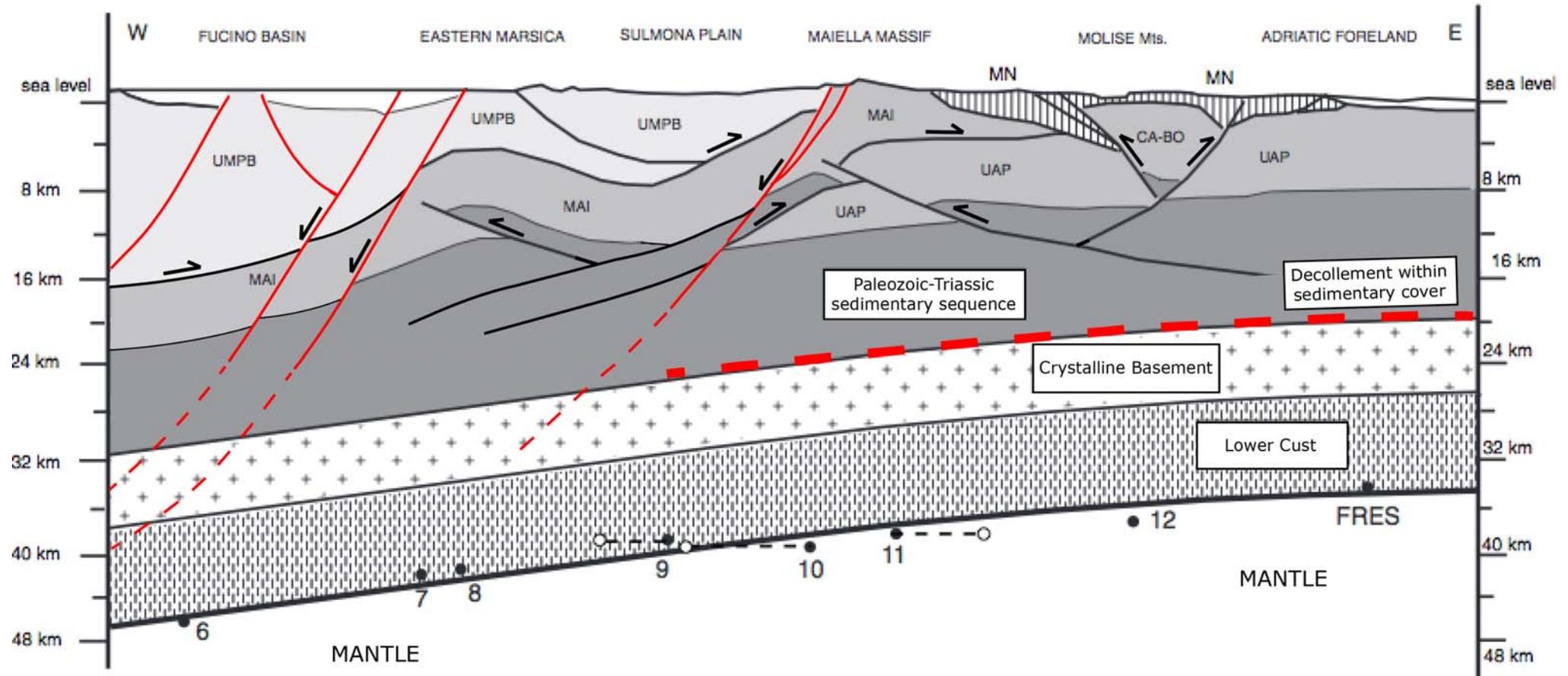
Fig. 5 - Crustal geologic section along the CROP 11 profile from the axial zone of the belt (Fucino basin) to the Adriatic foreland (See Fig. 2 for the location of CROP 11 trace). Carbonatic units involved in the Apennine deformation: **CA-BO**=Casoli-Bomba unit, **MAI** = Maiella unit, **UAP** = Undifferentiated Apulian Platform. Siliciclastic units involved in the Apennine deformation: **MN** = Molise nappes, **UMPB** = Undifferentiated Mio-Pliocene belt; **P-T** Paleozoic-Triassic sequence; **C.B.** = Cristalline Basement; **L.C.** = Lower Crust; Moho depths estimated from receiver functions are projected on the CROP 11 following the shallow structural axis (black circles) and the minimum-distance path (white circles). Red faults are the main extensional faults, bordering intra-mountain basins, cutting throughout the crust. Modified From Di Luzio et al., 2009.
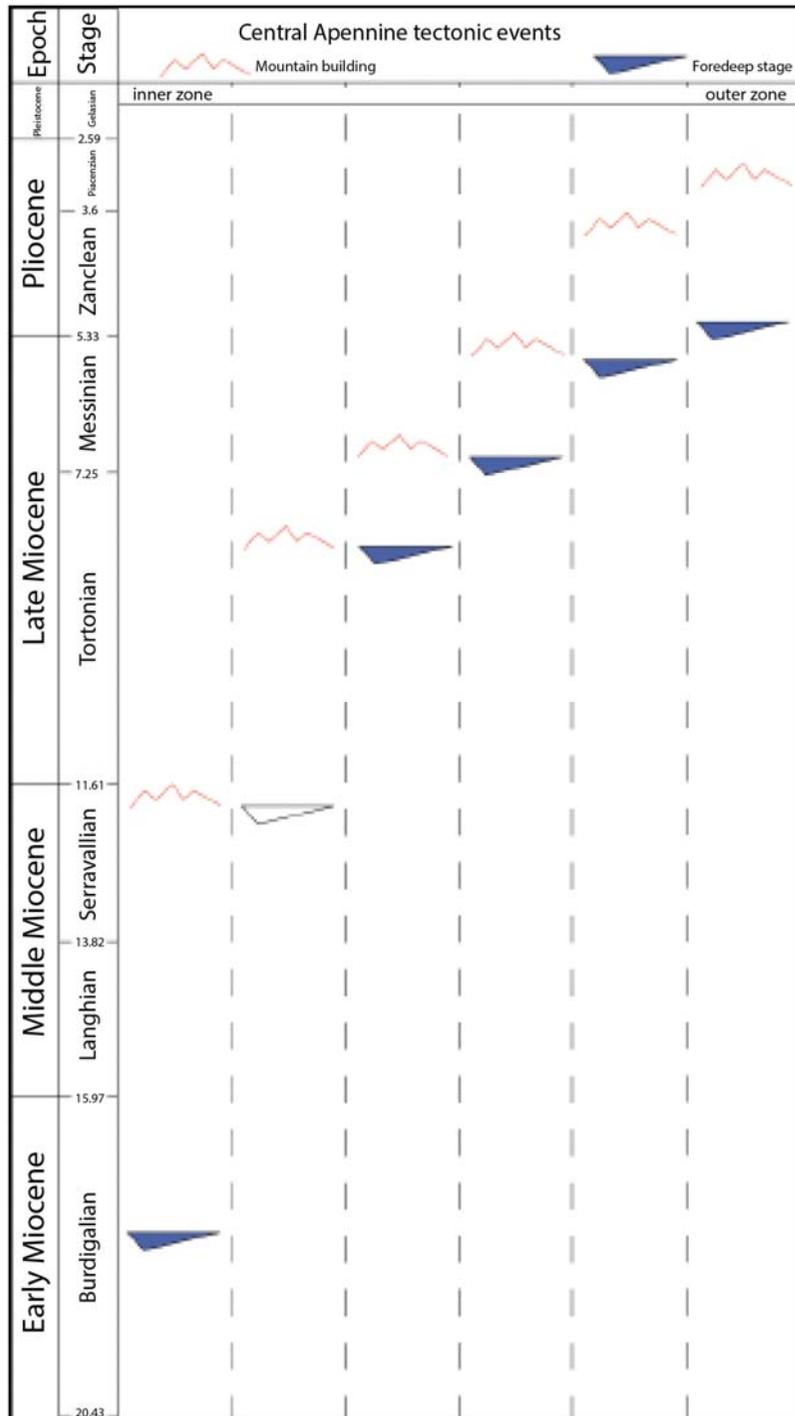
2000; Critelli et al., 2007). North-eastward migration of thrust fronts (Cipollari et al., 1995) developed different tectonic units that brought carbonate ridges, oriented NW-SE, onto turbiditic basins (Fig. 2) (Ricci Lucchi, 1986; Boccaletti et al., 1990; Cipollari et al., 1995; Patacca & Scandone, 2001; Cosentino et al., 2010).

Across the suite of both extensional and compressive tectonic features, a space-time rejuvenation of the deformative front, from the western to the eastern part of the Apennines, is recognizable (Fig. 6) (Cavinato & De Celles, 1999; Cipollari et al., 1995).

Following the kinematics of W-dipping subduction and applying the westward drift of the lithosphere, the Apennines should float above a new asthenospheric mantle, which replaced the subducted lithosphere, causing the uplift of the accretionary wedge of the Apennines chain (Fig. 7) (Doglioni, 1991). Nowadays the Apennines are characterized by a frontal active accretionary wedge, below the Adriatic sea, whereas the inland elevated ridge is instead in uplift and extension, controlled by tensional regime oriented about NE-SW (Fig. 1) (Doglioni & Flores, 1995).

Fig. 6 - Chronostratigraphical scheme adopted for the analysis of the syn-tectonic terrigenous deposits of the Central Apennines. In the right half, the recognized Central Apennine tectonic events are shown. For the Serravallian foredeep stage (in white) no siliciclastic deposits are recognizable in the study area. From Cosentino et al., 2010.

13

excursion notes
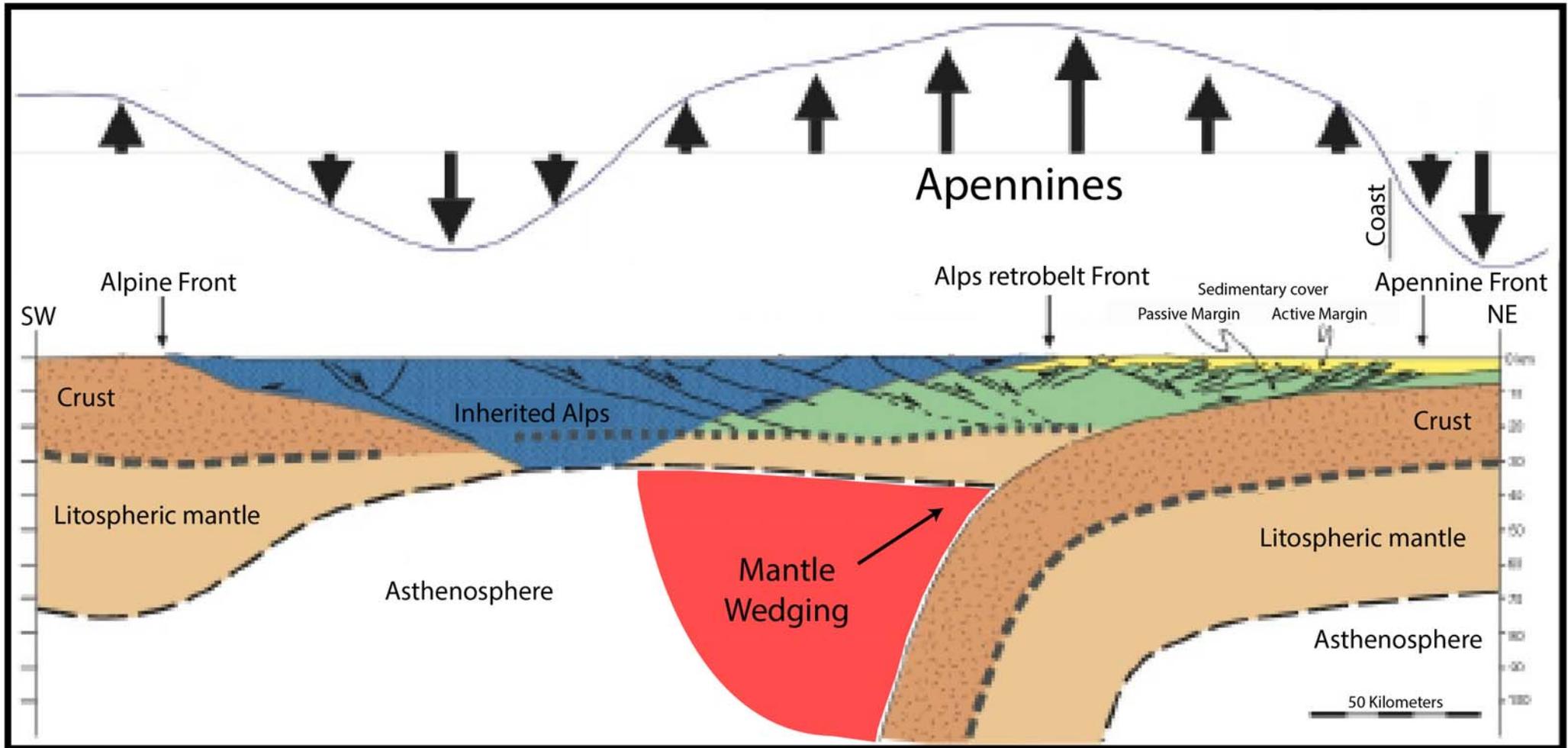
Fig. 7 - Cross section from Corsica (SW), through Tyrrhenian Sea and across the Apennines (NE). The Apennines prism (light green) developed along the retrobelt of the Alpine orogen (the blue double-wedge in the center of the section). The alpine orogen was boudinated and stretched by the backarc rift. Above the cross section are reported the vertical movements. From Carminati et al., 2010.

Throughout the Central Apennines the eastward migrating compression is coeval with extension, coupled with a clear eastward migration of rifting in the back-arc basin of the Tyrrhenian Sea associated with extensive volcanism (Fig. 7 and Fig. 4) (Doglioni & Flores, 1995). This is generally inferred from the age of the different intra-mountain sedimentary basins filled by alluvial and lacustrine sediments (e.g., Fucino, Sulmona and
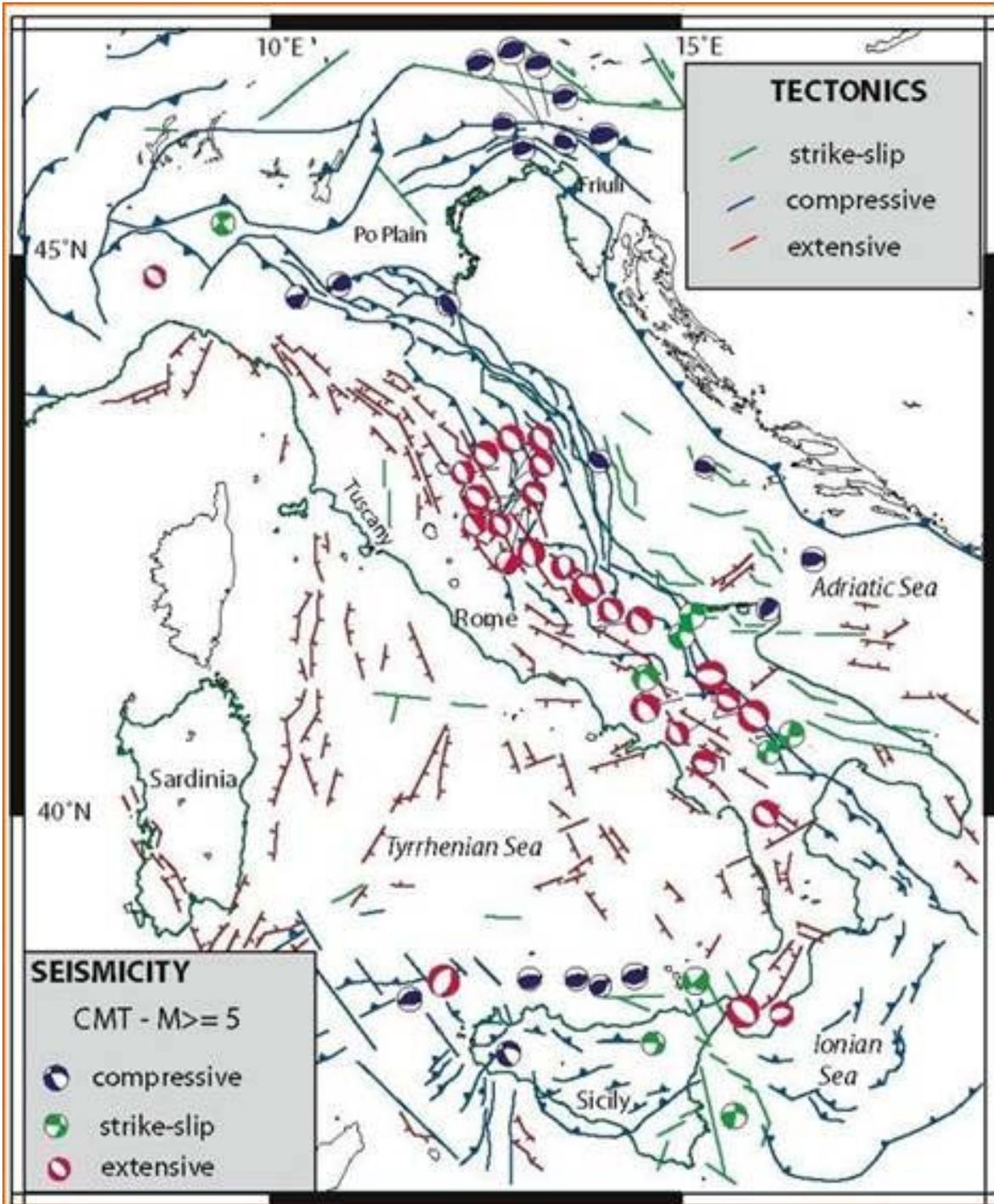
L'Aquila basins), initiated by the extensional tectonic activity affecting the Central Apennine area since the late Messinian and still active. Along a transect transverse to the Central Apennine, the onset of these extension-related basins becomes younger going from the Tyrrhenian to the Adriatic side of the chain (Cavinato et al., 1994; Cavinato & De Celles, 1999).

These intra-mountain basins are mainly bordered by NW-SE oriented and SW-dipping normal faults (Fig. 5) cutting throughout the crust, generating most of the seismicity in the region (Cavinato et al., 2002) (e.g., Fucino earthquake, 1915, Mw 7.0; L'Aquila earthquake, 2009, Mw 6.3). Extensional regime is concentrated in the intra-mountain zone whereas compressional regime is confined in the external zone along the buried active decolléments of the accretionary wedge (Fig. 8) (Lavecchia et al., 1994).

Fig. 8 - Centroid moment tensor solutions available for the Central Apennine area. Note the extensional earthquake in the intra-mountain zone and the compressional earthquake confined in the external zone. Modified after Cinti et al., 2004.

2. The Fucino basin

Tectonic setting

The Fucino basin is a typical intermountain normal-fault-bounded structure within the Apennines segmented normal fault system, which extends from Tuscany south to the Calabrian Arc and represents one of the most seismically active provinces of the Mediterranean region. Major normal faults representing nearest segments of this system are the M.Magnola - M.Velino fault to the NW («D» in Fig. 9; Morewood and Roberts, 2000) and the Sangro Valley fault to the SE.

Seismic reflection profiles (Mostardini & Merlini, 1988; Cavinato et al., 2002) indicate that the Fucino structure is a half graben controlled by the master fault along the NE border of the basin (Fig. 10), i.e. the San Benedetto-Gioia dei Marsi normal fault (Beneo, 1939; «A» in Fig. 9) and parallel subsidiary faults (e.g. the Parasano-Cerchio fault; «B» in Fig. 9). Within this style of faulting, tectonic inversion (Quaternary normal slip on pre-existing reverse faults) is very well documented, for instance along the SW range front of the Velino Massif (e.g., Nijman, 1971; Raffy, 1979). Normal faulting appears to have been ongoing during the whole Quaternary and is still active today. This is documented by (a) displacement and tilting of lacustrine formations and slope deposit sequences, (b) progressive offset of young sediments along Holocene normal fault scarps revealed by trench investigations and (c) observation of coseismic and paleoseismic surface faulting events (January 13, 1915, M 7 Avezzano earthquake and related paleoseismic studies; Oddone, 1915; Serva et al.,1988; Galadini et al.,1995; Michetti et al., 1996; Galadini et al., 1997a; Galadini & Galli, 1999; Galli et al., 2012; Figs 9, 11 and Table 1). These data show that the two major normal fault segments (Celano-San Benedetto-Gioia dei Marsi and M. Magnola-M.Velino faults) are characterized by Middle Pleistocene to present slip-rates of 0.5 to 2.0 mm/yr and total Quaternary offset in the order of 2000 m (Cavinato et al., 2002; Papanikolaou et al., 2005).

Geomorphologic setting

The Fucino basin (Figs 9 and 11) is the largest tectonic basin of the Abruzzi region. It lies in the middle of the central Apennines surrounded by mountain ranges sometimes higher than 2000 m (Mt. Velino, 2486 m a.s.l.), which are shaped essentially from Meso-Cenozoic carbonate shelf sediments. The closed basin is not connected
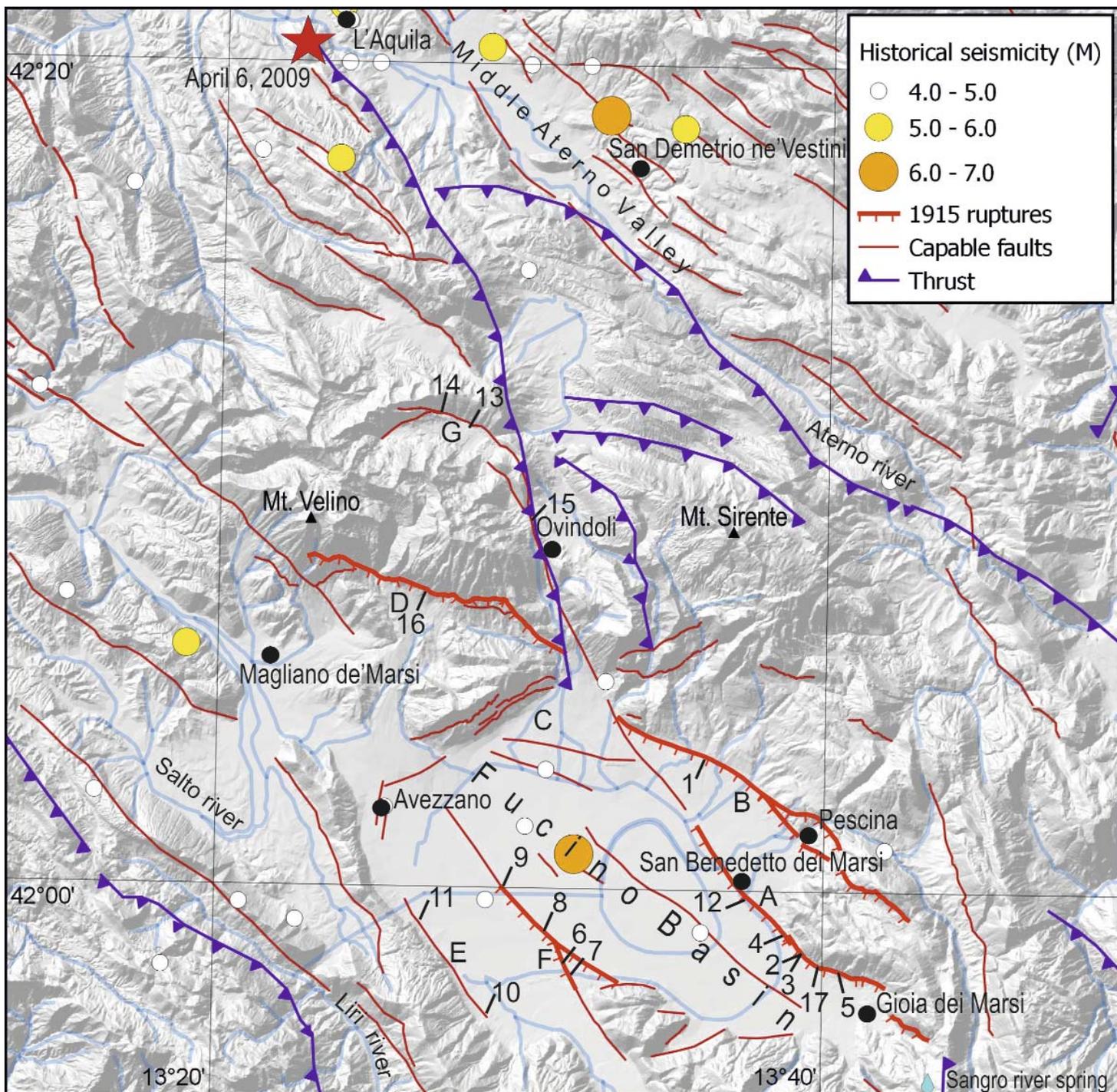
to important rivers. Instead, around it the upper courses of several rivers flow: the Salto river runs to the NW, the Liri river runs south and then SW, the Sangro runs south and then east (Fig. 9).

The central part of the hydrologically closed basin, a wide roughly round-shaped plain between about 650 and 700 m high, during the Late Glacial and Holocene was

Fig. 9 - Tectonic map showing the system of capable normal faults in the Abruzzi Apennines. The distribution of historical seismicity since 1000 A.D. (Rovida et al., 2011) is also represented. Note the absence of earthquakes in the Fucino area before the 1915 event and compare with paleoseismic data in Table 1. Legend: **A)** San Benedetto-Gioia dei Marsi fault; **B)** Cerchio-Pescina-Parasano fault; **C)** Tre Monti fault; **D)** Magnola fault; **E)** Luco dei Marsi fault; **F)** Trasacco fault; **G)** Ovindoli–Piani di Pezza fault. Numbers locate paleoseismological sites and are the same of Table 1.

occupied by the third largest lake in Italy (ca 150 km²). In the II century A.D. the emperor Claudius prompted the drainage of Fucino Lake. This was accomplished through the excavation of a 6 km long tunnel mostly in Mesozoic limestone, one of the most remarkable engineering projects in the Roman history. The final drainage of this area was performed in the second half of the XIX century by Alessandro Torlonia. In 1875, Fucino Lake disappeared from maps.

The range fronts bounding the Fucino basin are fault-controlled. In particular, the Quaternary activity of the master normal fault zone at its NE border generated several flights of lacustrine terraces. Over the Quaternary, these were progressively uplifted, tilted and faulted and younger terraces repeatedly

Fig. 10 - Geologic cross section of the Fucino basin interpreted from seismic reflection profiles. **A)** and **B)** locate respectively the San Benedetto-Gioia dei Marsi and Cerchio-Pescina-Parasano faults. Modified after Cavinato et al. (2002).

developed in the down-thrown block. Therefore, tectonics has left a clear imprint on the sedimentary setting. In Fig. 11, the Quaternary terraces are grouped into three major orders, namely «upper», «intermediate» and «lower terraces», separated by prominent fault scarps.

The «upper terraces», include two main terrace surfaces of Late Pliocene (?) - Early Pleistocene age. The highest one culminates at 1050 m a.s.l. and represents the top of the most ancient lacustrine cycle, as demonstrated also by wave-cut terraces in the bedrock. The second one is faulted and reworked by a depositional surface of the Alto di Cacchia unit, culminating at 950 m a.s.l. (Blumetti et al., 1993; Bosi et al., 1995; Bosi et al., 2003). Two intersecting NW-SE and SE-NW trending normal faults border the «upper terraces» and generate fault scarps up to 100 meters high (Fig. 11; Raffy, 1981-1982; Blumetti et al., 1993).

The «intermediate terraces» include two main Middle Pleistocene terrace surfaces. According to Bosi et al. (1995) and Messina (1996), the higher one can be divided in three orders «developed at base levels not very different from each other». We will consider them as a single terrace culminating at 850-870 m a.s.l. (Fig. 11).
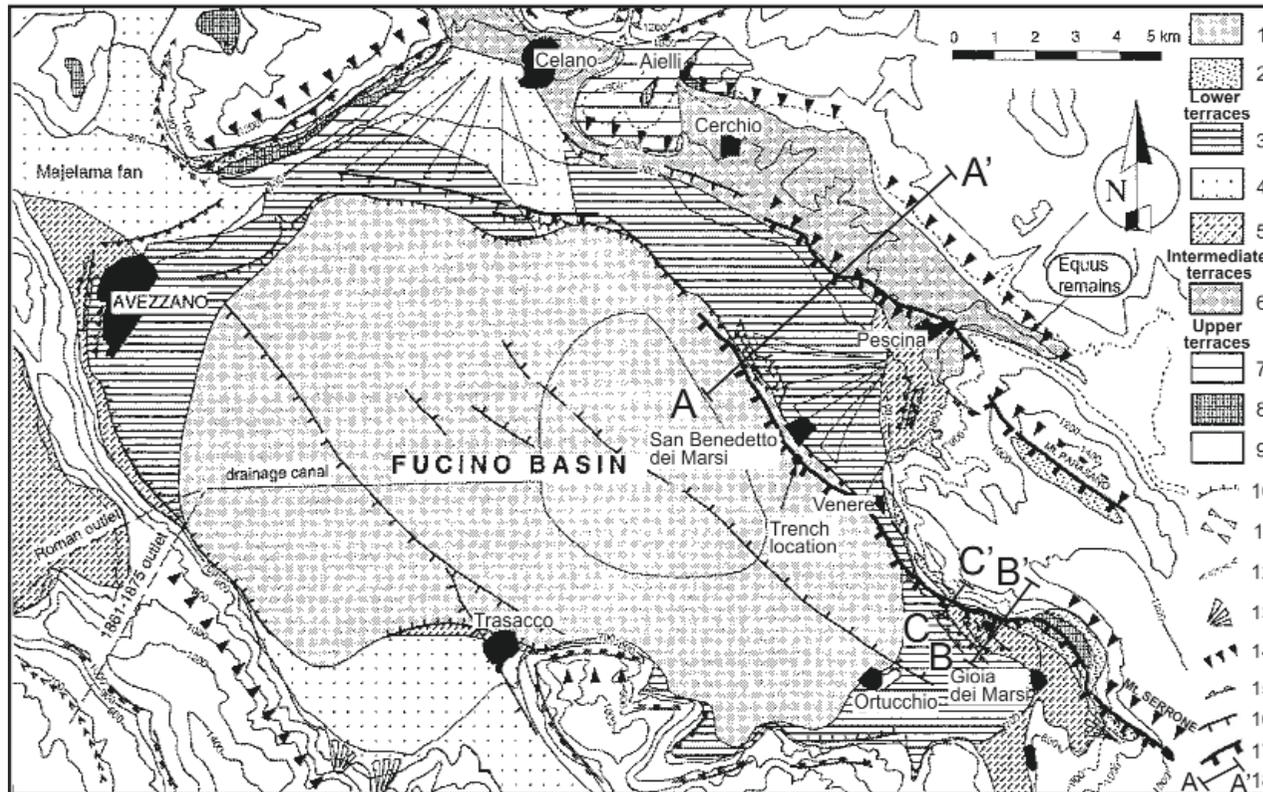
Fig. 11 - Geologic map of the Fucino basin, displaying the surface faulting associated with the 1915 earthquake. Site is marked where remains of *Equus cf. altidens* were found. Legend: **1)** Historical lake; **2)** talus deposits (Late Glacial to Holocene); **3)** alluvial deposits (Holocene); **4)** alluvial fan deposits (Late Glacial); **5)** fluvio-lacustrine deposits (Late Glacial); **6)** fluvio-lacustrine deposits (Middle Pleistocene); **7)** fluvio-lacustrine deposits (Late Pliocene?-Lower Pleistocene); **8)** breccias (Late Pliocene-Middle Pleistocene); **9)** sedimentary bedrock (Meso-Cenozoic); **10)** fluvio-lacustrine terrace edge; **11)** trough; **12)** V-shaped valley; **13)** alluvial fan; **14)** fault scarp; **15)** fault scarp within the lower terraces; **16)** Holocene normal fault; **17)** 1915 coseismic rupture; **18)** Trace of cross section. Modified after Michetti et al. (1996).

Slightly entrenched in this terrace, there is a second surface that, in the Giovenco River valley and in the surroundings of Cerchio, is about 800-830 m a.s.l. Both these terraces are limited to the SW by a major fault scarp up to 100 m high.The «lower terraces» constitute the part of the basin at elevations ranging from 660 m to ca. 720 m a.s.l., where Upper Pleistocene to Holocene lacustrine and fluvio-glacial deposits crop out. These are both depositional and erosional surfaces (Raffy, 1981-1982; Giraudi, 1988; Blumetti et al., 1993). The central part of the basin between 649 and 660 m a.s.l. is the bottom of the historic lake.

The following chronological constraints allow estimating the age of the above mentioned lacustrine terrace: the latest Pleistocene to Holocene evolution is very well defined by a wealth of archaeological, radiocarbon and tephrachronological data (Radmilli, 1981; Narcisi, 1993). The works by Giraudi (1988) and Frezzotti & Giraudi (1992; 1995) provide an extensive review of these data, building up a detailed paleoenvironmental reconstruction for this time interval. During this period, the maximum high-stand of the lake is dated ca. 20 to 18 ka BP It produced a prominent wave-cut terrace, well preserved at several sites along the basin margins (Raffy, 1970; see cross section B-B, Fig. 40, and description in Stop 1.5; trace of cross section in Fig. 11).
Information on the 20 to 40 ka BP time interval mostly comes from radiocarbon dating of the Majelama fan stratigraphic units. This shows (1) a fluvial sedimentary environment since ca. 30 ka BP, (2) the formation of a thick paleosoil developed from volcanic parent materials at 33 to 31 ka BP. In the center of the basin, volcanic horizons originating from the Alban Hills district, ca. 40 to 50 ka old, are found 10 to 15 m below the ground surface (Narcisi, 1994). Pollen data show that in the same area the lake sediments deposited during the Eemian period are ca. 60 to 65 m deep (Magri & Follieri, 1989).

Chronological data before the Late Pleistocene are very poor. The only available age is ca. 540 ka (^{39}Ar/^{40}Ar dating) of for a tephra found 100 m deep in the center of the basin (Fig. 29; Follieri et al., 1991).
The «intermediate terraces» have provided the first Middle Pleistocene mammal remains of the Fucino basin: a fragmentary maxillary bone with teeth of an equid (*Equus cf. altidens*) at the Ponte della Mandra site (830 m a.s.l.; Fig. 29), in a complex alluvial sequence of the Giovenco valley. This species characterizes the Italian fauna from the end of the Early Pleistocene and is no longer documented during the Late-Middle Pleistocene. In particular, the biochronological distribution of this equid spans c.a. 1 to 0.45 Ma (latest Villafranchian to latest Galerian, in terms of Mammal Age). This finding definitely confirms the Middle Pleistocene age of the Cerchio-Collarmele-Pescina sequence («intermediate terraces» in Fig. 11).
Regarding the chronology of the «upper terraces», two different interpretations are found in the literature. Bosi et al. (1995; 2003) attribute the Aielli formation to the Pliocene, based on regional stratigraphic correlations. According to Raffy (1979), the Aielli formation is late Early Pleistocene in age, based on the amount of volcanic minerals in the Aielli lake deposits and regional geomorphology.

Paleoseismic data

In this section, we summarize the data coming from the many paleoseismic analyses carried out in and around the Fucino basin. This will lead to some considerations on the growth of the Fucino tectonic structure by repeated strong earthquakes.

Along the eastern border of the Fucino basin and its NW extension in the Ovindoli and Piano di Pezza area (Salvi & Nardi, 1995; Pantosti et al., 1996), the Holocene paleoseismology and deformation rates have been investigated at several sites along the traces of the San Benedetto - Gioia dei Marsi (sites 2, 3, 4, 5, 12 and 17 in Fig. 9; Michetti et al., 1996; Galadini et al., 1995; Galadini et al., 1997b; Saroli et al., 2008), Cerchio-Pescina-Parasano (site 1 in Fig. 9; Galadini et al., 1995; Galadini et al., 1997b) and Ovindoli-Pezza (sites 13, 14 and 15 in Fig. 9; Pantosti et al., 1996) faults, as described in Table 1. Recently, paleoseismological investigations on the Magnola fault (site 16 in Fig. 9 and Table 1) have testified the reactivation of this fault during the 1915 event.

It is possible to view these paleoseismological results in terms of variation in deformation rates and earthquake recurrence along a single tectonic structure. For instance, the extension rates vary with distance from the center of the Fucino basin. In fact, as already pointed out, most of the eastern part of the basin is bounded by two parallel normal faults, the Parasano - Cerchio fault (or Marsicana fault of Galadini et al., 1997b) and the San Benedetto-Gioia dei Marsi fault, both reactivated during the 1915 earthquake (Oddone, 1915; Serva et al., 1988; Galadini et al., 1995) and carrying evidence of Holocene displacement. If the extension rates observed along these two traces using the San Benedetto trenches (1.0 to 1.6 mm/yr; site 12 in Fig. 9; Michetti et al., 1996) and the Marsicana trenches (0.4 to 0.5 mm/yr; site 1 in Fig. 9; Galadini et al., 1997b) are summed up, the cumulative value near the center of the segment is 1.4 to 2.1 mm/yr for a 45° dipping fault. This is significantly higher than the value at the NW termination of the Fucino structure, i.e along the Magnola fault, that have a Holocene slip rate of about 0.9 mm/yr, and in the Ovindoli - Piano di Pezza area, where a maximum extension rate of 1.0 to 1.2 mm/yr can be derived for a 45° dipping fault plane, interpreted as a secondary listric splay of the master fault (Nijman, 1971).

Data in Table 1 also indicate that the variation in extension rates is probably due to a higher frequency of earthquakes per unit time at the center of the fault system compared to its NW termination. Other capable faults have also been ruptured by Holocene earthquakes in the Fucino basin. Galadini et al. (1997b) have trenched 2 other faults in addition to the San Benedetto-Gioia dei Marsi and Cerchio-Pescina-Parasano faults and, assuming that the faults dip at 45°, the implied rates of horizontal extension
are ca. 0.4 - 0.5 mm/yr across the Trasacco and Luco dei Marsi faults. Therefore, the overall extension rate in the Fucino tectonic structure during the Holocene might be in the order of 3 to 3.5 mm/yr.

Evolutionary model of the Fucino basin

The Fucino basin is a half graben, with the master fault represented by the Celano-San Benedetto-Gioia dei Marsi fault. High continental terraces are stranded in the footwall of this normal fault at elevations up to 1050 m a.s.l.. Most likely, lacustrine sediments of the same age are buried below the modern deposits in the hanging-wall of this fault. Seismic reflection data from Cavinato et al. (2002) clearly show that continental deposits are several hundreds of meters thick toward the master fault. On the southern and western borders of Fucino basin we observe only the main younger terrace (at ca. 720 m a.s.l.), which forms a narrow banquette at the foot of the mountain slopes; instead, the edges of the ancient Fucino Lake before the Last Glacial Maximum (LGM) are not well defined. Since all the available data indicate that the Fucino basin was an endoreic, closed depression over the whole Quaternary, very hardly erosional processes could have obliterated any trace of the previous terraces. We can conclude that the Fucino basin extended progressively to the west and to the south following the continuing Quaternary hanging-wall subsidence of the Celano-San Benedetto-Gioia dei Marsi normal fault. The geomorphic changes observed during the January 13, 1915, earthquake are the last and most spectacular evidence of this long-lasting process.

Table 1 – Synopsis of paleoseismological analyses in the Fucino basin and nearby areas (site numbers as in Fig. 9); data from the ITHACA - Italy Hazards from Capable Faults, available at the webpage http://sgi.isprambiente.it. Data sources are Michetti et al., 1996; Pantosti et al., 1996; Galadini et al., 1995; 1997a; 1997b; Galadini & Galli, 1999; Saroli et al., 2008; Galli et al., 2012.

Trench Site	Locality	Strike	Dip	Holocene Vertical Offset (m)	Holocene Horizontal Offset (m)	Vertical Slip-Rate (mm/yr) and time-window(yr)	Recurrence Time and Time window (yr)	Total Events	Paleoearthquake Ages	Vertical Slip per Event (m)
1	Strada Statale Marsicana	NW-SE	SW	> 5	none	0.4-0.5 (last 20000)	4500-5000 (20000)	5	1915 AD; 6500-3700 BP; 7300-6100 BP; 13600-12300 BP; 19100-18500 BP	Event 1: 0.8
2	Colle delle Cerese	N50W	SW	>3	none	0.35-0.40 (last 7000)	1000-1800	3	1915 AD; 1100-1500 AD; 7200-6540 BP	Event 1: 0.7
3	Colle delle Cerese (Cave)	NW-SE	SW	10-15	none	0.35-0.40 (last 4200)	1400-2100	3	1915 AD; 150-1349 AD; 3760 BP-150 AD	Event 1: 0.7
4	Molini di Venere	NW-SE	SW	>3	none	0.35-0.40 (last 10000)	1200-1500 (2000)	4	1915 AD; 1300-1500 AD; 7120-5340 BP; 10400-7120 BP	Event 1: 0.7
5	Casali D'Aschi	NW-SE	SW	5	none	0.35-0.40 (last 20000)	800-1000 (3000); 3300-5500 (33000)	7	1915 AD; 1200-1400 AD; 2783 BP-1300 AD; 4700-2800 BP; 10400-7120 BP; 20000-10000 BP; 32520-20000 BP	Event 4: 2
6	Trasacco (Fosso 41)	N22W	WSW	>3	none	0.3-0.4 (last 7000)	1500-1800 (2000)	2	1915 AD; 1000-1349 AD	0.5; 0.6
7	Trasacco (Strada 37)	NW-SE	SW	>3	none	0.3-0.4 (last 7000)	1800 -2000 (7000)	5	1915 AD; 1000-1349 AD; 3700-3500 BP; 7120-5000 BP;10790-7120 BP	Event 1: 0.5
8	Trasacco (Strada 38)	N60W	SW	>3	none	0.3-0.4 (last 7000)	1600-1800 (10800)	7	1915 AD; 1000-1349 AD; 3700-3500 BP; 7120-5000 BP; 10790-7120 BP (2 events); >12000 BP	Events 1,2,3,4: 0.55; Events 5,6,7: 0.15;
9	Trasacco (Strada 10)	NW-SE	SW	>3	none	0.3-0.4 (last 7000)	1800-2000 (12000)	8	1915 AD; 1000-1349 AD; 3700-3500 BP; 7000-5000 BP;10790-7120 BP (3 events); >10790 BP	Event 1: 0.1
10	Luco dei Marsi (Strada 42)	NW-SE	NE	>3	none	0.8 (last 1500)	1000-1800 (1500)	2	1915 AD; 500-1500 AD	0.1; 0.15
11	Luco dei Marsi (Strada 45)	NW-SE	NE	>3	none	0.8 (last 1500)	(s.a.a.)	2	1915 AD; 500-1500 AD	0.1; 0.15
12	San Benedetto dei Marsi	NW-SE	SW	>3	none	1.0-1.6 (last 2000)	500-800	3	1915 AD; 885-1349 AD; 550-885 AD	ca.0.5; ca.0.5; >1
13	Piano di Pezza	N120E	SW	3.5	none	0.7-1.2 (Holocene)	800-3300 (5000)	2	860-1300 AD; 1900 BC	2-3.4; 1.2-2.5
14	Vado di Pezza	N135E	SW	12-16	none	(s.a.a.)	(s.a.a.)	3	860-1300 AD; 1900 BC; 3300-5000 BC	2-3.4; 1.2-2.5; 2.0
15	Campo Porcaro	N165E	W	6.5-11	5.5-8.5	(s.a.a.)	(s.a.a.)	2	860-1300 AD; 1900 BC	2-3.4; 1.2-2.5
16	Magnola fault	N115E	SW	>7	none	0.9 (last 8000)	1500-5000 (5500)	3	1915 AD; 508 AD; 45000 BP -508 AD	
17	Cave Santilli	WNW-ESE	SW	>3	none	0.14-0.35 (last 14000-15000)	(s.a.a.)	3	1915 AD? or 1500-1300 BC?; after 14000-15000 BP (2 events)	

3. The middle Aterno Valley and L'Aquila city

The 2009 earthquake

On April 6, 2009, a Mw 6.1 earthquake (Herrmann et al., 2011) struck a densely populated region in the Abruzzi Apennines, caused ca. 300 fatalities and was felt in a wide area of central Italy (Fig. 12). Due to its location and relatively shallow hypocentral depth (~10 km), the earthquake caused heavy damage in the town of L'Aquila and surrounding villages. Soon after the earthquake, the Paganica - San Demetrio Fault System (PSDFS), bounding to the east the middle Aterno Valley, was interpreted as the surface expression of the 6 April 2009 earthquake

Fig. 12 - Modified after Civico et al., 2015. Coseismic seismological and geodetic data converge in modelling the seismic source as a NW-striking, SW-dipping, 12 to 19 km-long normal fault (yellow box - for details: Chiaraluce, 2012; Vannoli et al., 2012). The inset shows the direction of extension across the central Apennines (black arrows) and the felt area for the 6 April mainshock (colored area).
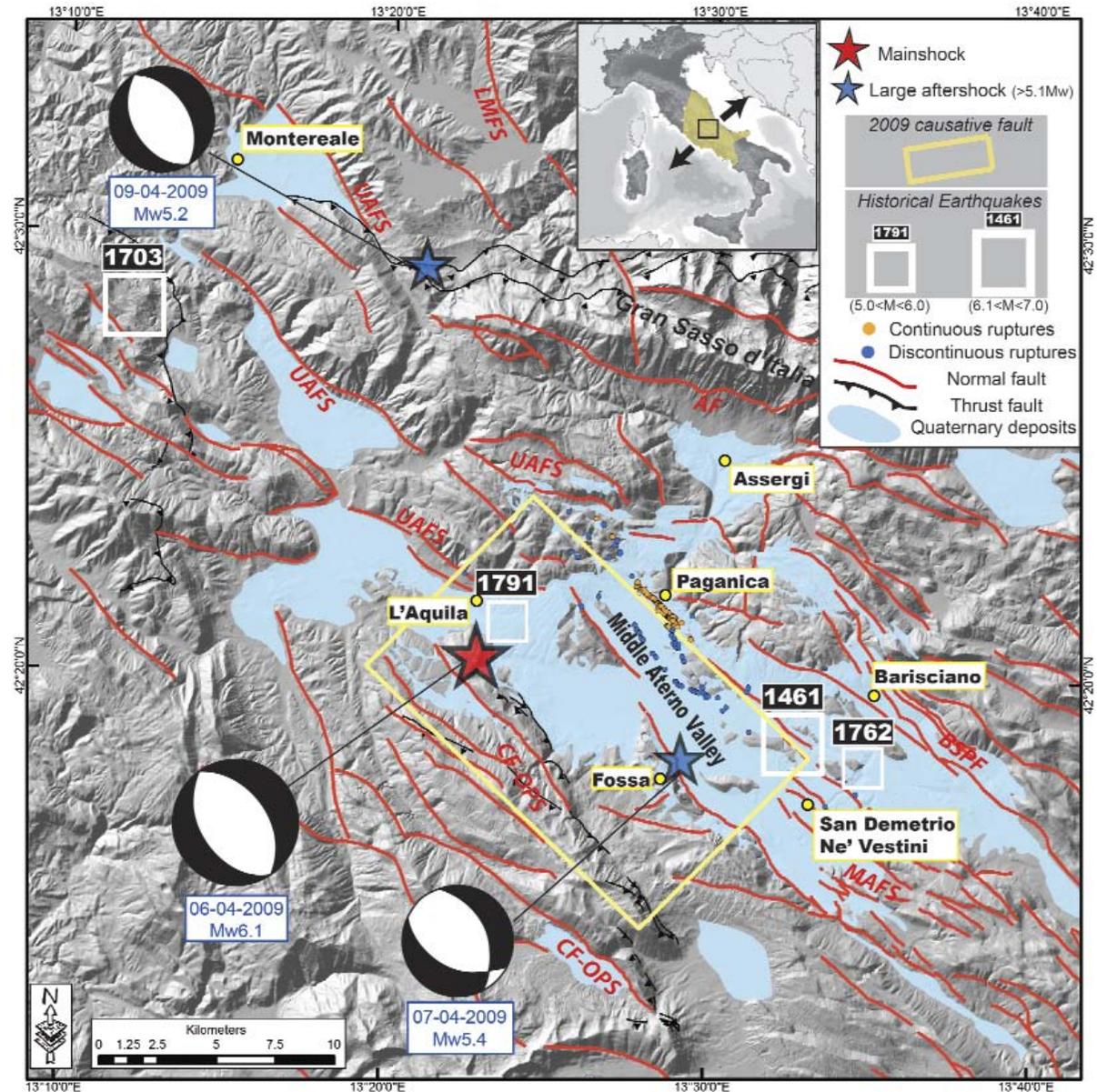
Fig. 13 - Surface rupture along the Paganica fault. The breaks consist of open cracks (av. 10 cm) with vertical dislocations (max 15 cm), SW-side down. The ruptures occurred with a persistent orientation of N130°–140°, regardless of slope angle, type of deposits crossed and the presence of man-made features (EMERGEO W.G., 2010).
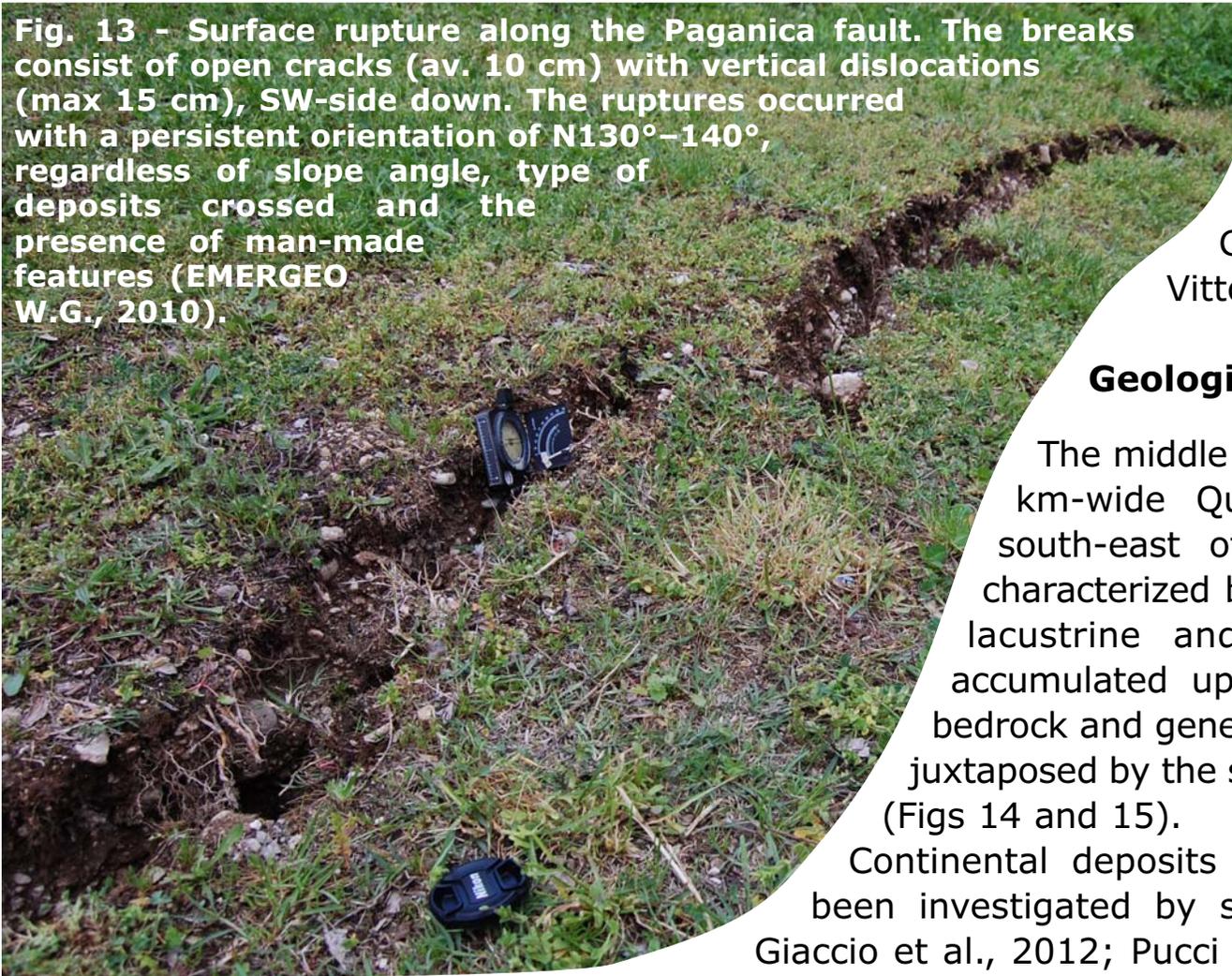
causative fault, and along its NW sector ~3-13 km of primary coseismic ruptures were observed (Fig. 13; Falcucci et al., 2009; Boncio et al., 2010; EMERGEO Working Group, 2010; Galli et al., 2010; Lavecchia et al., 2010; Vittori et al., 2011).

Geological setting – middle Aterno Valley

The middle Aterno Valley is a ca. 18 km-long, 3 to 6 km-wide Quaternary intramontane basin located south-east of the town of L'Aquila. The basin is characterized by the presence of an extensive cover of lacustrine and fluvial/alluvial Quaternary deposits accumulated upon a Meso-Cenozoic mainly carbonatic bedrock and generally separated by unconformities and/or juxtaposed by the several fault splays detectable in the area (Figs 14 and 15).

Continental deposits overlying the bedrock sequence have been investigated by several authors (Bertini & Bosi, 1993; Giaccio et al., 2012; Pucci et al., 2015) and can be referred to six main depositional cycles: (1) Early Pleistocene slope-derived carbonatic breccias (L'Aquila megabreccias and Valle Valiano fms. – MBR, VVB, VVC); (2) Early Pleistocene lacustrine and fluvio-lacustrine sequence (Limi di San Nicandro fm. - SNL), composed of whitish silts and clayey silts with gravel lenses, up to 100 m thick; (3) Early Pleistocene alluvial sequence (Vall'Orsa fm. - VOC), partially heteropic with the Limi di San Nicandro fm., and consisting of deltaic carbonatic conglomerates showing foreset and bottomset beds (100 m thick); (4) Early-Middle Pleistocene alluvial fan sequence (Valle Inferno fm. - VIC), consisting of well-bedded carbonatic conglomerates showing topset beds, with sparse silty layers and palaeosoils and (5) Middle-Late Pleistocene fluvial and alluvial sequence, made of silts, sands and gravels,

interbedded with volcanoclastic layers (San Mauro fm. – SMF, SMA). All these deposits are covered by (6) Late Pleistocene-Holocene fluvial/alluvial sediments, mainly related to the Aterno River, and by slope debris and colluvial deposits.

The 2009 L'Aquila earthquake triggered several studies aimed at defining the subsurface geometry of the middle Aterno basin (among the others: MS-AQ Working Group, 2010; Balasco et al., 2011; Improta et al., 2012; Santo et al., 2013).

Balasco et al., (2011) investigated the large-scale structure of the northeast part of the basin by means of a ~8 km-long ERT and a magnetotelluric profile. They suggested the existence of complex lateral and vertical resistivity changes in the NE sector (between Mt. Bazzano and Paganica), that can be related to the presence of a shallow conductive alluvial filling (~200 m-thick) above a rugged carbonate substratum. In the same area, Improta et al., (2012) performed a high-resolution seismic survey over an 8 km long section. Their tomographic images highlighted the presence of a complex

Fluvial unit (SMF)
Middle-Late Pleistocene

Conglomeratic alluvial fan (VIC)
Early-Middle Pleistocene

Gilbert fan delta (VOC)
Early Pleistocene

Lacustrine unit (SNL)
Early Pleistocene

Megabreccias (MBR)
Early Pleistocene
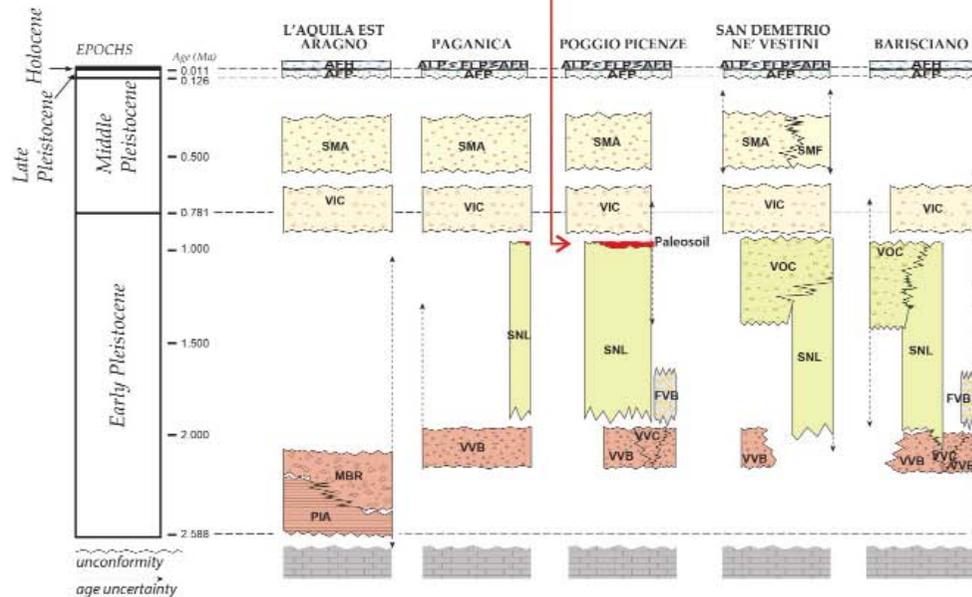
Fig. 14 – Scheme of the stratigraphic relationship of the Quaternary deposits (modified after Pucci et al., 2015). Pictures show a selection of the stratigraphic units and one of the identified unconformities (red arrow).

topography of the pre-Quaternary substratum, with a ~350 m deep depocenter in the Bazzano sub-basin. Moreover, they evidenced strong lateral heterogeneities and steps in the substratum (NE of Mt. Bazzano), suggesting the presence of buried synthetic and antithetic fault splays involving bedrock and basin infill deposits within the Paganica sub-basin.

Fig. 15 - Quaternary geology of the middle Aterno Valley (modified after Pucci et al., 2015). Geological section C-C' is shown in Fig. 61.

Structural setting - middle Aterno Valley

Several studies (Galli et al., 2010; Cinti et al., 2011; Giaccio et al., 2012; Blumetti et al., 2013) highlighted that the fault responsible for the 2009 earthquake is only a small segment of the PSDFS, which extends well beyond the Paganica sector and shows different potential rupture length, ranging between 12 and 30 km. Moreover, they pointed out that the PSDFS cumulative scarps have been built up by surface rupturing earthquakes affecting either its whole length or smaller sections (2009-like). Such outcome indicates a complex behaviour of the seismic source which may be better described by a variable-slip model (Schwartz & Coppersmith, 1984). More recent works (Pucci et al., 2015; Civico et al., 2015) highlighted the existence of a complex structural setting of the PSDFS at the surface, characterized by several parallel fault splays, 1-5 km long, frequently arranged in synthetic and antithetic pairs of variable size, where the net extension is mostly accommodated by SW-dipping structures. This style is found from the outcrop scale (a few meters) up to the entire basin scale (some km-scale) and it is therefore said "quasi-fractal" by Civico et al., (2015). The PSDFS comprises: (1) the Paganica sector to the NW, characterized by a narrow deformation zone and a small hangingwall Quaternary basin; (2) the San Demetrio sector to the SE, with a set of kilometer-spaced splays that exhume and dissect a wider Quaternary basin (Fig 16). The longest fault segments are NW-trending, whereas some minor E- and N-trending faults are present. These latter faults partly belong to an older system active during Early Pleistocene with complex kinematics, whereas the NW-trending faults mostly activated under the NE-extensional regime still affecting the chain. Notwithstanding this internal complexity, Civico et al., (2015) on the basis of the morphological throw distribution, defined the PSDFS as a ~19 km-long structure which behaves in the long-term as a single individual normal fault.
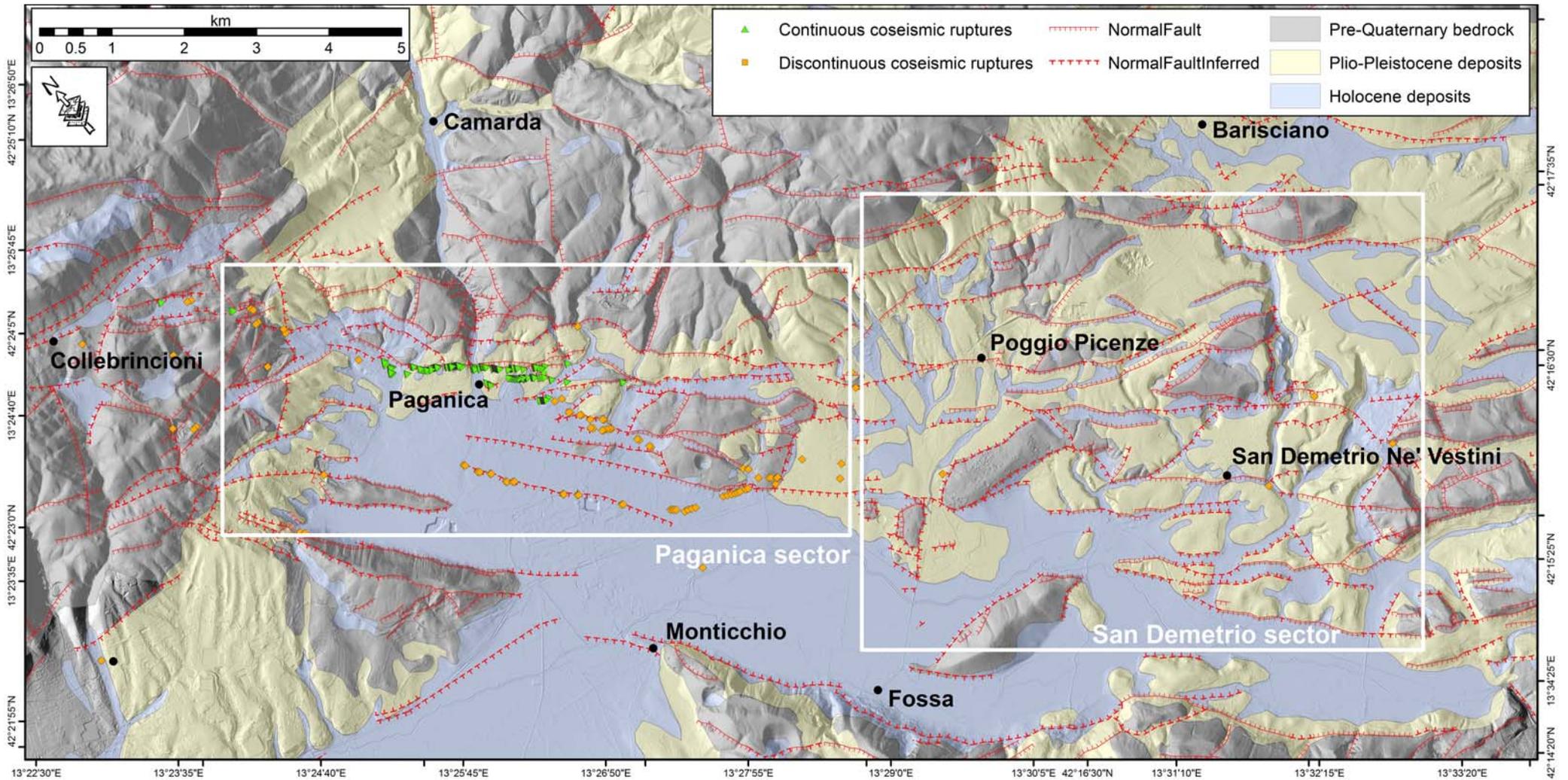
Fig. 16 – Map of the Paganica-San Demetrio Fault System (PSDFS) showing its geometrical arrangement at the surface and the extent and age of outcropping pre-Quaternary basement, and Plio-Pleistocene and Holocene deposits (modified after Civico et al., 2015).

Geological setting – L'Aquila city

L'Aquila is a moderate-sized city (about 70,000 inhabitants), settled in a tectonic basin delimited by prominent mountain ranges. It was founded at the half of the XIII century, becoming soon the most important centre of the area characterized by a large and valuable historic heritage.

Quaternary geology and paleoseismology in the Fucino and L'Aquila basins

S. Amoroso-F. Bernardini-A.M. Blumetti-R. Civico-C. Doglioni-F. Galadini-P. Galli-L. Graziani-L. Guerrieri-P. Messina-A.M. Michetti-F. Potenza-S. Pucci-G. Roberts-L. Serva-A. Smedile-L. Smeraglia-A. Tertulliani-G. Tironi-F. Villani-E. Vittori

The city centre is placed on a flat terraced hill whose schematic geological setting consists, from the top to the bottom, of Middle Pleistocene 80-100 m-thick calcareous breccias, ("brecce dell'Aquila" - MBR), which lay onto a 250-270 m-thick homogeneous Early Pleistocene fluvial-lacustrine pelites and sands, as shown in Figs 17 and 18. In particular, the "brecce dell'Aquila" are composed of fine to coarse calcareous fragments of variable size (mostly of some cm) embedded in sandy or silty matrix, characterized by highly variable cementation degree and mechanical properties (Monaco et al., 2013), while the fluvial-lacustrine deposits consist of fine- to medium-grained silts. The latter ones are placed onto the Meso-Cenozoic carbonate bedrock, whose depth decreases toward the NE, as testified by deep boreholes, gravimetric and seismic reflection investigations (Amoroso et al., 2010; Del Monaco et al., 2013; MS–AQ Working Group, 2010; Tallini et al., 2011). The "brecce dell'Aquila" thickness decreases from about 100 m in the central sector of the historical centre (i.e. Piazza Duomo) to 0-10 m in the southern slope of L'Aquila hill, where they are laterally replaced by sands, pelites and
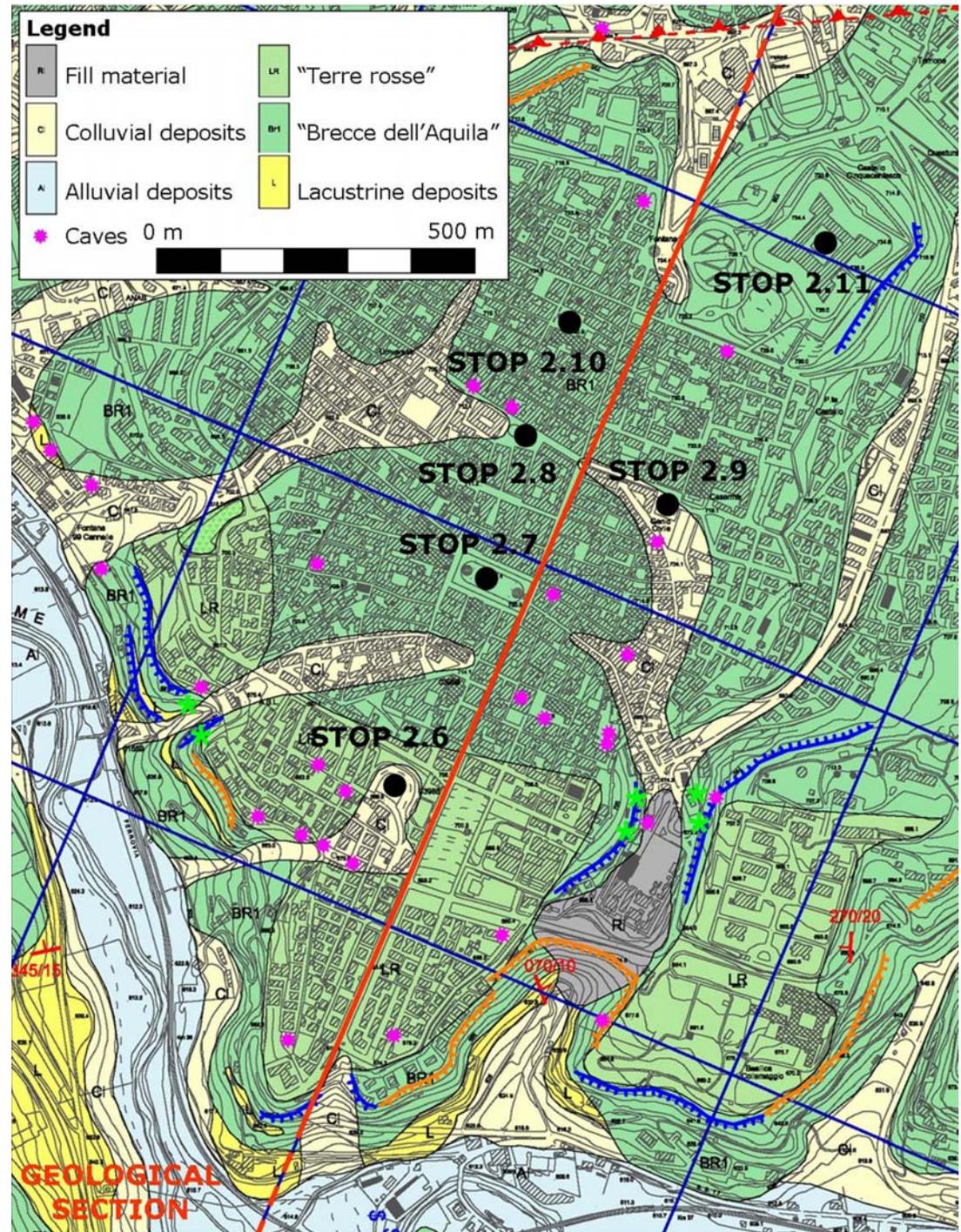
Fig. 17 - Geological map of L'Aquila city centre (MS–AQ WORKING GROUP, 2010).
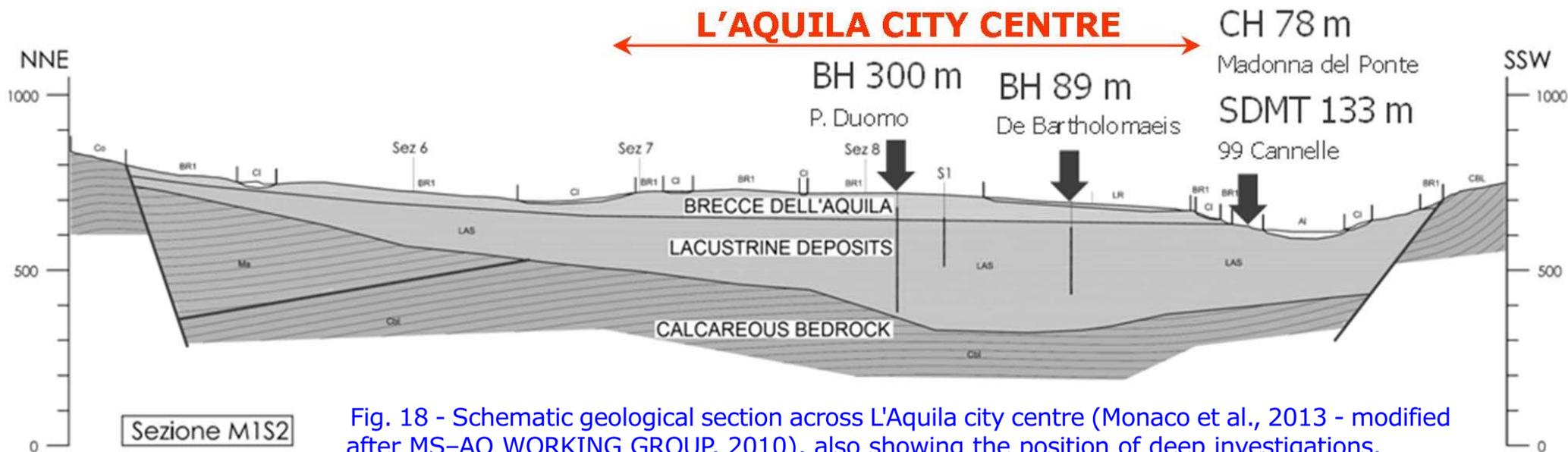
Fig. 18 - Schematic geological section across L'Aquila city centre (Monaco et al., 2013 - modified after MS–AQ WORKING GROUP, 2010), also showing the position of deep investigations.
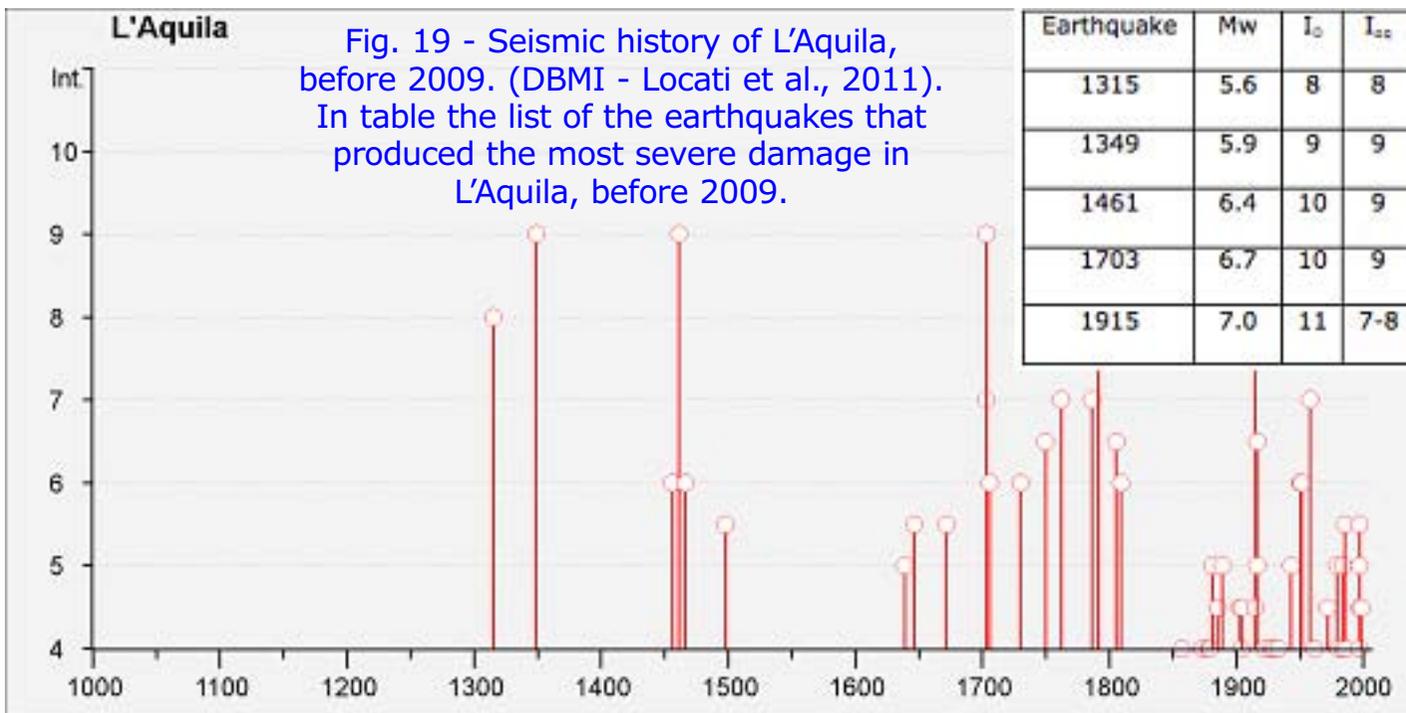
Fig. 19 - Seismic history of L'Aquila, before 2009. (DBMI - Locati et al., 2011). In table the list of the earthquakes that produced the most severe damage in L'Aquila, before 2009.

Earthquake	Mw	I₀	I₀₀
1315	5.6	8	8
1349	5.9	9	9
1461	6.4	10	9
1703	6.7	10	9
1915	7.0	11	7-8

calcareous gravels and breccia layers (Del Monaco et al., 2013). Further, at places, some underground caves (empty or filled with 1-10 m thick epikarst fine-grained residual soils named "terre rosse") are present in the "brecce dell'Aquila" (Del Monaco et al., 2013).

Unfortunately, the city is located within a highly seismic region (Fig. 19), whose activity is well documented by old historical sources since the

31

excursion notes

early XIV century. The first event that was reported to cause damage in L'Aquila occurred on 1315. Since then, L'Aquila has experienced several strong earthquakes. The city, which was heavily destroyed after all these events, has been restored each time. In particular, the 1461 event is considered, by historians and city planners, responsible of the disappearing of the medieval housing in L'Aquila (Clementi and Piroddi, 1986), while the 1703 earthquake marked the birth of the present urban plan (Fig. 20). This event was a major disaster in the history of L'Aquila and occurred during a long period of political and economic decline, in which further minor earthquakes (occurred in 1639, 1646, and 1672) damaged the city. After the 1703 earthquake

Fig. 20 - Map of the distribution of the damage due to the 1703 earthquake (modified after Colapietra, 1978).

collapses and very heavy damage.

partial collapses; large and extensive cracks.

light or no damage

a new building planning was established, in search of "antiseismic" techniques such as wooden beams to improve the connection of the walls and connections between roofs and walls, buttresses and reduction of floor height. However, the reconstruction of the city was very difficult and took many years: almost ten years after the earthquake, less than 15% of buildings had been rebuilt (De Matteis, 1973).

After the 1915 Avezzano earthquake and in the period between the two World Wars, the area inside the ancient walls was further urbanized, expanding into the open spaces that during ancient times had been reserved for vegetable gardens, pastures and cattle fairs.

The present building stock is very variable: buildings located downtown are mainly two to four storeys, built in simple stone masonry, often with tie-rod connections among walls, corresponding respectively to vulnerability class A and B, according to EMS98 (Grunthal, 1998). Massive stones or bricks were used only for some strategic and important edifices: among them there are more recent buildings, built during the last century, in brick masonry and reinforced concrete (RC) (vulnerability class C). In the suburban area, recently developed, most buildings are relatively modern reinforced concrete frame structures with masonry infill (vulnerability class C and D) (see for details: Tertulliani et al., 2011; 2012).

The 2009 earthquake in L'Aquila city

On 6 April 2009, at 01:32 GMT, a Mw=6.1 earthquake hit L'Aquila with devastating effects and causing very severe damage also in tens of villages nearby with a grievous social impact: 309 casualties (2/3 of them in L'Aquila city), 47% of the housing partially damaged, 20% of the housing heavily damaged and more than 40,000 people left homeless. The impact on religious and monumental heritage was disastrous. The assessed macroseismic intensity for L'Aquila was 8-9 EMS98. The damage in L'Aquila downtown has been subject of many studies after the earthquake, because it was the first time in Italy that, after the 1908 Messina-Reggio Calabria earthquake, a city was severely struck by a seismic event. The macroseismic survey performed soon after the earthquake (Fig. 21) highlighted that about 70% of the buildings, mainly represented in classes B and C, suffered substantial to very heavy damage. In particular:

· the most vulnerable buildings (class A) were all damaged; about 50% of them suffered very heavy destruction;

· classes B and C suffered a high rate of severe damage, from large and extensive cracks to partial structure failure in masonry buildings and damage to structural elements in RC buildings;

· more than 90% of the monumental buildings suffered damage from severe to total collapse;

The spatial distribution of the damage was quite distinct within the city:

· the heaviest damage was mainly concentrated in the western sector of the city (red circle in Fig. 21), in particular the 39% of total collapses were observed in San Pietro a Coppito quarter;

· about 80% of collapses in RC buildings occurred along the south-western border of the historical centre.

Fig. 21 - Distribution of the damage grades in L'Aquila downtown, after the 6 April 2009 earthquake (Tertulliani et al., 2011).
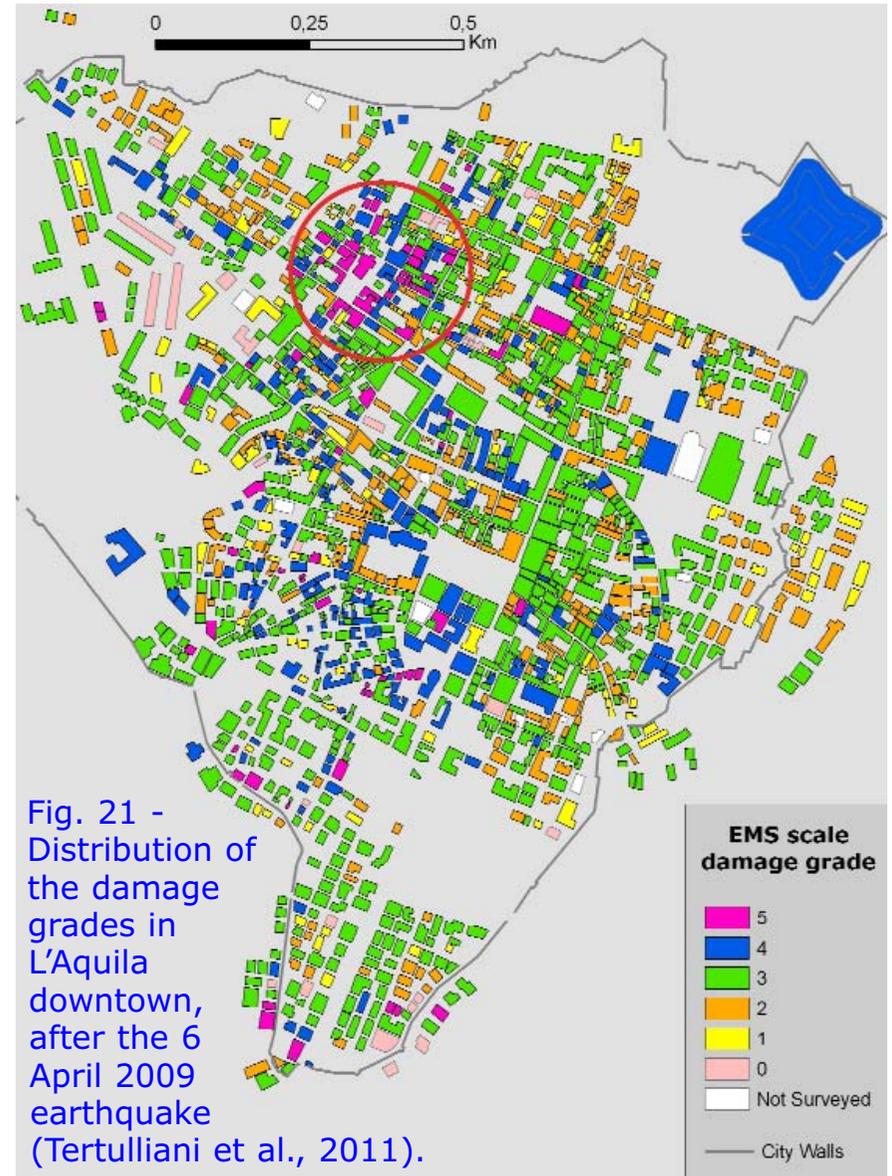
South L'Aquila

As introduced in the previous paragraph, in South L'Aquila several RC buildings collapsed or suffered severe damage due to the main shock causing 135 victims. Differently from the ancient part of L'Aquila centre (including most of the historical heritage and several old masonry buildings), the southern part (marked with red line in Fig. 22) features reinforced concrete frame buildings, mostly 5-7 storey high, built between 1950 and 1965. It was mainly dedicated to vegetable gardens and green areas until the end of the XIX century (Stokel, 1981; Centofanti, 1984; Piroddi et al., 1984; Figs 22a and 22b), except few buildings detected in Via Campo di Fossa since 1753 (Fig. 22a).

At the end of 1800s, this part of the city acquired building interests (Fig. 22c) due to the construction of Via XX Settembre to connect the city to the railway station, and because of the 1915 Avezzano earthquake, after which a parcelling plan was introduced (and never realized) that caused a chaotic construction (Stokel, 1981). During the years the urban expansion continued until the saturation was reached (Figs 22d and 22e).
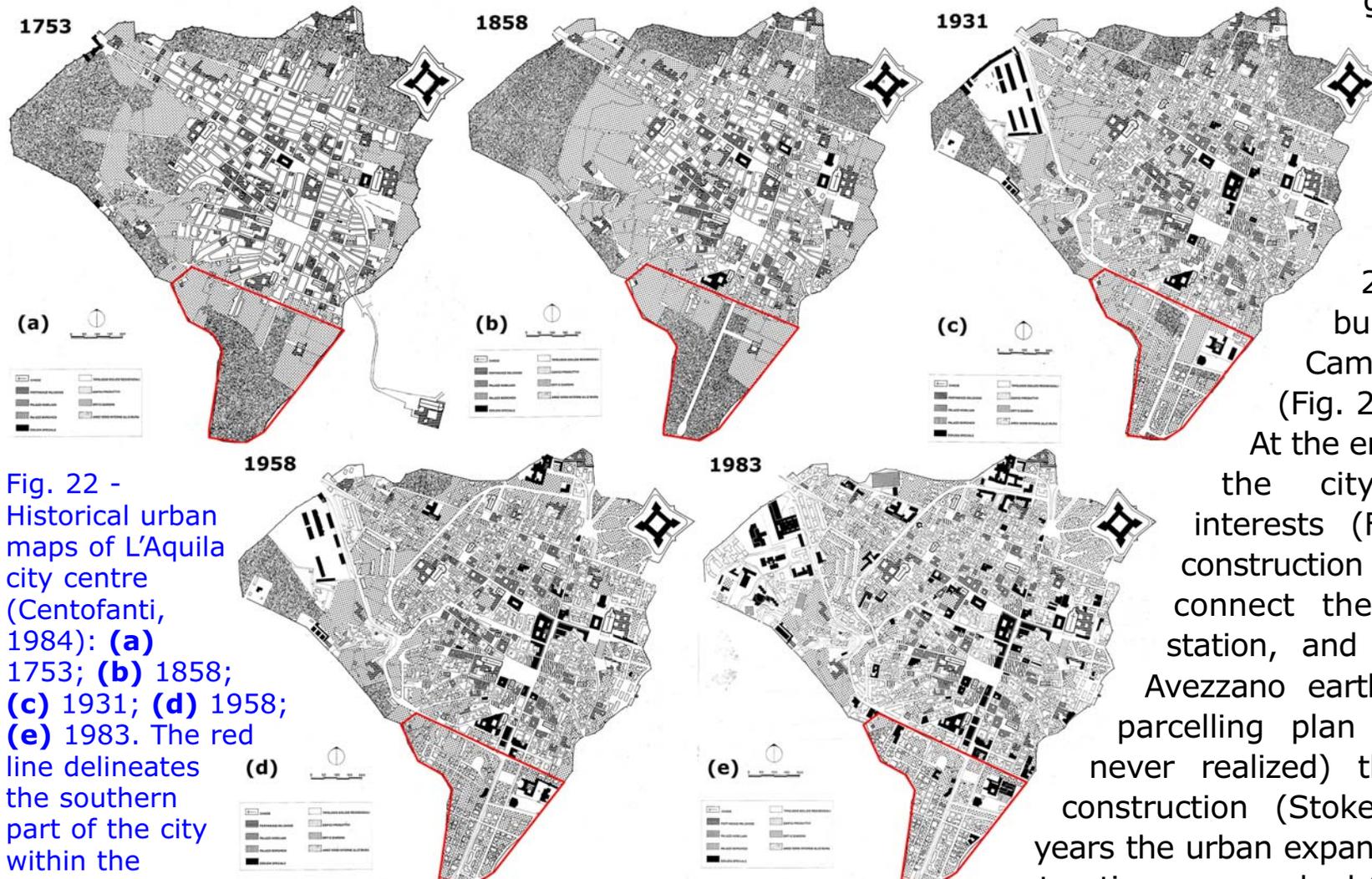
Fig. 22 - Historical urban maps of L'Aquila city centre (Centofanti, 1984): **(a)** 1753; **(b)** 1858; **(c)** 1931; **(d)** 1958; **(e)** 1983. The red line delineates the southern part of the city within the anciet walls.

DAY 1
Quaternary geology and palaeosismology in the Fucino basin
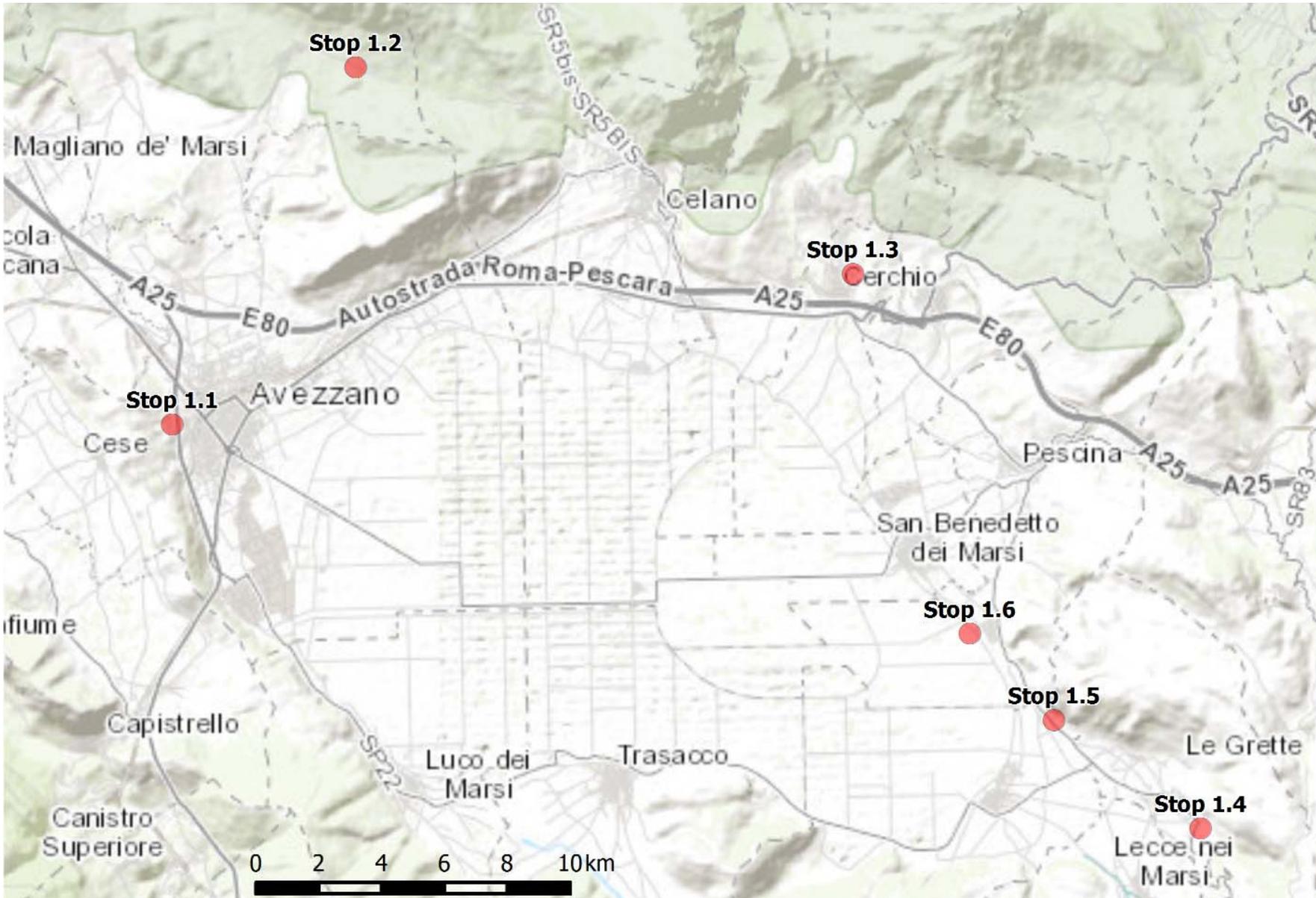
STOP 1.1 – Landscape view of the Fucino basin from Mt. Salviano and general introduction

From Mt. Salviano, looking north, it is possible to have a panoramic view on the fault escarpment of the Velino - Magnola Massif, with a spectacular Holocene normal fault scarp at its base. From the Majelama Valley, a typical "wine glass valley" (*sensu* Wallace, 1978) that divides Mt. Magnola from Mt. Velino, the Late-Glacial
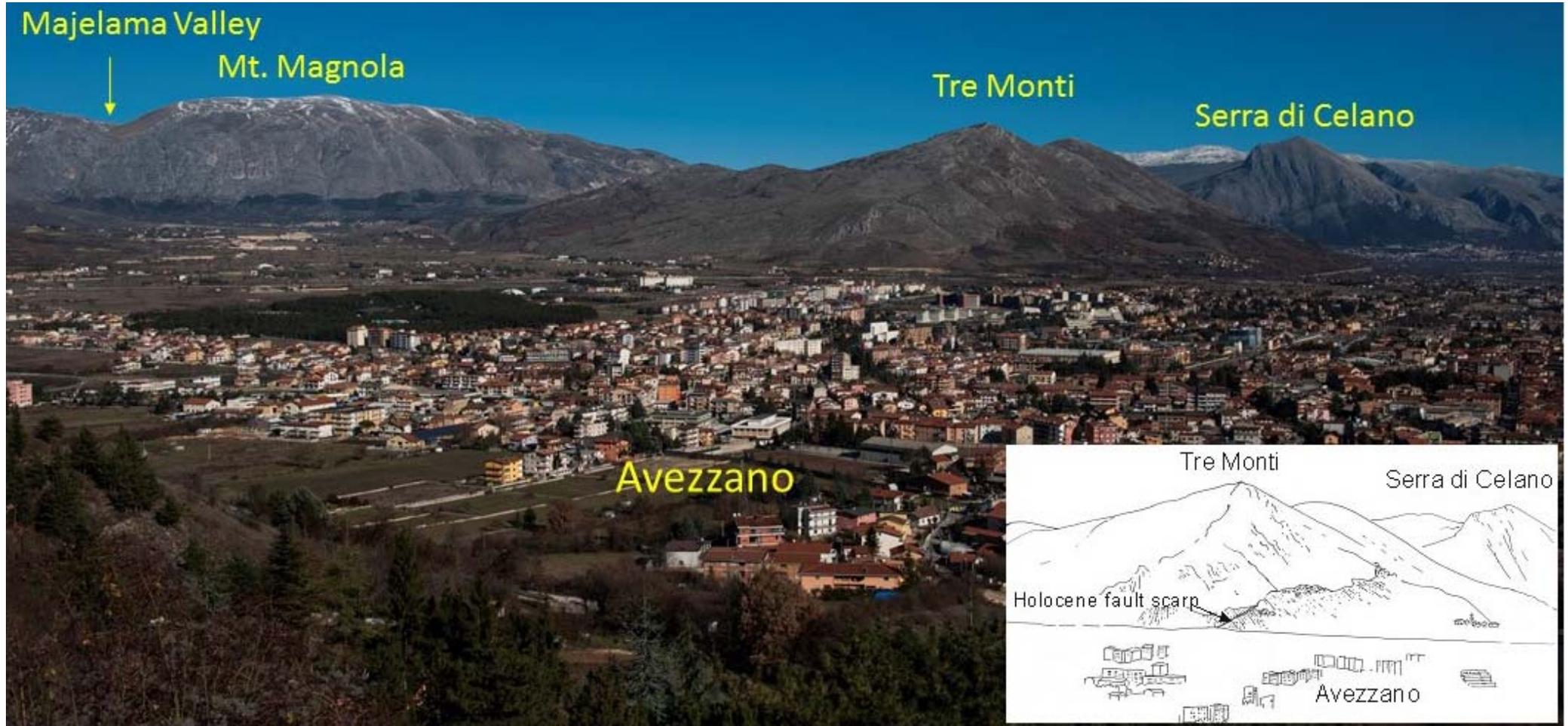
Fig. 23 - In the background the panoramic view of Mt Magnola, Tre Monti and Serra di Celano fault escarpments. The Majelama "wine glass valley" is also indicated. The inset drawing locates the "scarplet" (fault scarp) in Late Glacial slope-waste deposits, at the base of the Tre Monti fault escarpment. In the foreground the city of Avezzano.

Majelama alluvial fan gently slopes toward the Fucino basin. The city of Avezzano, partly built on the edge of the alluvial fan, was totally destroyed on January 13, 1915. Only one building was seen standing after the main shock; most of the 30,000 casualties due to the earthquake occurred in this town (94,9 % of the population). Looking NE, the Tre Monti fault escarpment also shows a prominent bedrock fault scarp ("nastrino" or fault ribbon); it is to notice that the SW termination of the Tre Monti fault cuts the Late Glacial stratified slope deposits, where it shows an about 2 m high fault scarp.

To the east, in the background, are the Quaternary continental terraces uplifted along the Cerchio-Pescina fault. The «upper terraces» include two main terrace surfaces of Late Pliocene (?) - Early Pleistocene age. The highest one culminates at 1050 m a.s.l. and represents the top of the most ancient lacustrine cycle, as demonstrated also by wave-cut terraces in the bedrock. The second one is faulted and reworked by a depositional surface of the Alto di Cacchia unit culminating at 950 m a.s.l. (Fig. 11). Two intersecting NW-SE and SE-NW trending normal faults border the «upper terraces» and generate fault scarps up to 100 m high.

In the middle, the Fucino Lake was filling the wide basin until the year 1870. Except for the artificial drainage of the lake in Roman times first and eventually by Alessandro Torlonia, the Fucino basin was hydrologically closed (endorheic) throughout the whole Quaternary.

STOP 1.2 – Paleoseismology and long-term activity along the Magnola fault (Fonte Capo La Maina, Forme)

The Stop allows a panorama view of the Magnola fault (MF, Figs 24-26), a prominent westnorthwest-eastsoutheast normal fault on the southern slopes of the Magnola-Velino mountain range front. The fault appears to represent the reactivation with reversed sense of slip of a thrust ramp of Late Miocene age, possibly reflected in the relatively moderate dip angle (30-50°). The MF length is estimated by Galli et al. (2012) in excess of 13 km, bounded to the west by the northwest-southeast trending Velino fault, while to the east, despite its trace disappears rather abruptly, it has a natural continuation in the Fucino fault system (the Marsicana Highway fault of Galli et al., 2012).

Recent studies have confirmed this fault is capable of major earthquakes (Galli et al., 2012).

In addition to the latter, key studies documenting the recent activity of the MF are those of Piccardi et al. (1999), Palumbo et al. (2004), Gori et al. (2007), Schlagenhauf (2010, 2011). The works of Piccardi et al. (1999) and Gori et al. (2007) focus on the major geomorphological and stratigraphic features of the fault zone and range front, assessing slip rates respectively of 0.7 mm/a after the Last Glacial Maximum (LGM) and 0.54-

Quaternary geology and paleoseismology in the Fucino and L'Aquila basins

S. Amoroso-F. Bernardini-A.M. Blumetti-R. Civico-C. Doglioni-F. Galadini-P. Galli-L. Graziani-L. Guerrieri-P. Messina-A.M. Michetti-F. Potenza-S. Pucci-G. Roberts-L. Serva-A. Smedile-L. Smeraglia-A. Tertulliani-G. Tironi-F. Villani-E. Vittori
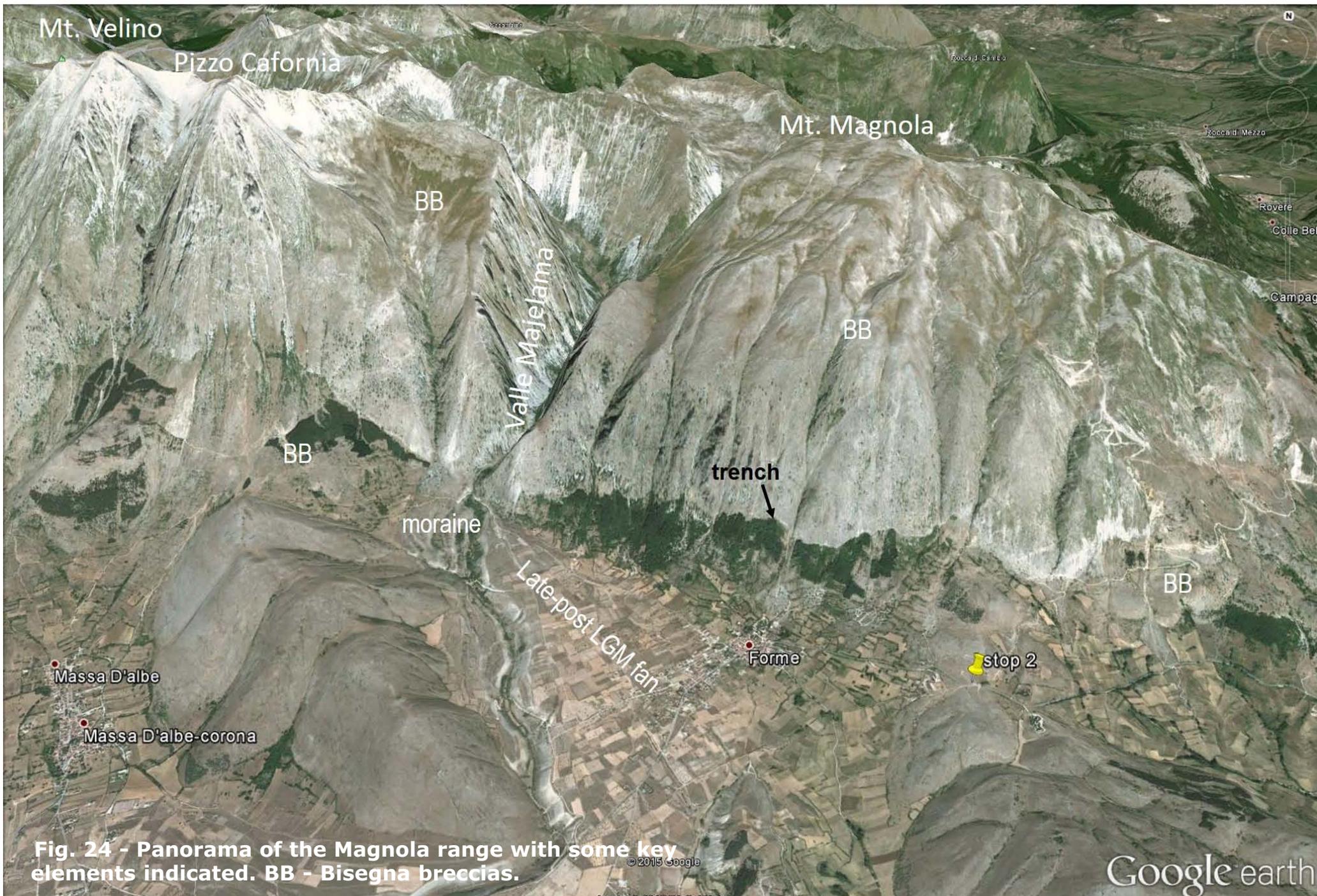
Fig. 24 - Panorama of the Magnola range with some key elements indicated. BB - Bisegna breccias.

0.81 mm/a for the last million years. Cosmogenic (^{36}Cl) dating of the exposed limestone fault slickenside has evidenced a number of rejuvenation events after the LGM (5 according to Palumbo et al., 2007, and 9 according to Schlagenhauf et al., 2010, 2011). If the rejuvenation events in the latter paper were all to be attributed to coseismic slip, then the average recurrence interval would be 1.5 ka, but largely uneven between events, possibly representing *earthquake supercycles*. Galli et al. (2012) have recalculated the Holocene vertical slip-rate, obtaining 0.9 ± 0.1 mm/a. They have inferred an event occurred during the so-called *Neoglacial* period (started ca. 4.5 ka ago) before the Roman period, followed by two historical earthquakes, an early Middle Age event documented in most of their trenches in the Fucino basin, which they interpret as the 508 CE earthquake (see discussion in Stop 1.6), and the 1915 event.

Fig. 25 - Panorama of the Magnola range-front fault escarpment. **Above**: view from west (Stop 1.2 is at the far right edge of the photograph). The Bisegna breccias crop out to the left of Valle Majelama; **below**: view from Stop 1.2. The Bisegna breccias crop out on the right side of the photograph.

Fig. 26 - **Left**: general aspect of the fault scarp around the location of the studies cited in the text. **Right**: detail of the fault slickenside (looking east from near the trench site).

The fault slickenside can be approached with a hike of at least 30 minutes. Standing near the fountain on the pass, the fault trace is seen marked by a line separating the denudated slope carved in Mesozoic shelf limestone from late Quaternary scree deposits and Early Pleistocene cemented breccias (Bisegna fm.). The presence of Holocene soil developed on these sediments allows the growth of vegetation that often marks the fault contact (Fig. 25). Figures 26 and 27 provide details of the fault scarp, here several meters high (vertical separation ca. 7 m).

At the Stop, the Bisegna breccias (after Bosi & Messina, 1991; named brecce Mortadella in Demangeot, 1965) can be seen on the right side of the slope (Fig. 25, below). With a typical light reddish color, they are a rather well cemented alluvial fan deposit dated at around 1 million year (early Pleistocene). Cropping out both on the footwall (on the upper flat surface carved in the limestone bedrock at ca. 1900 m a.s.l.) and the hangingwall, they represent a reference marker to estimate the long-term slip rate of the fault. In origin, they had to slope
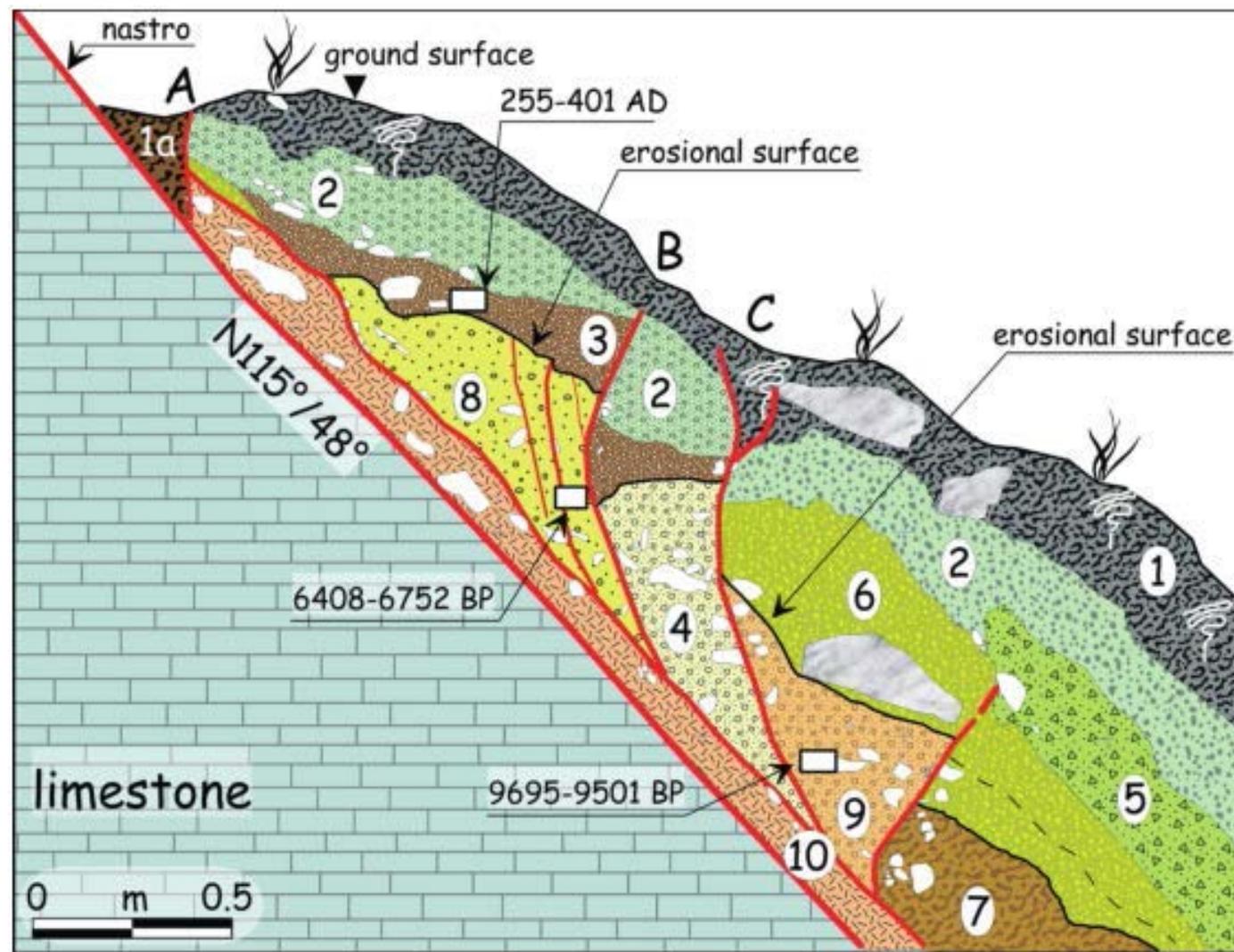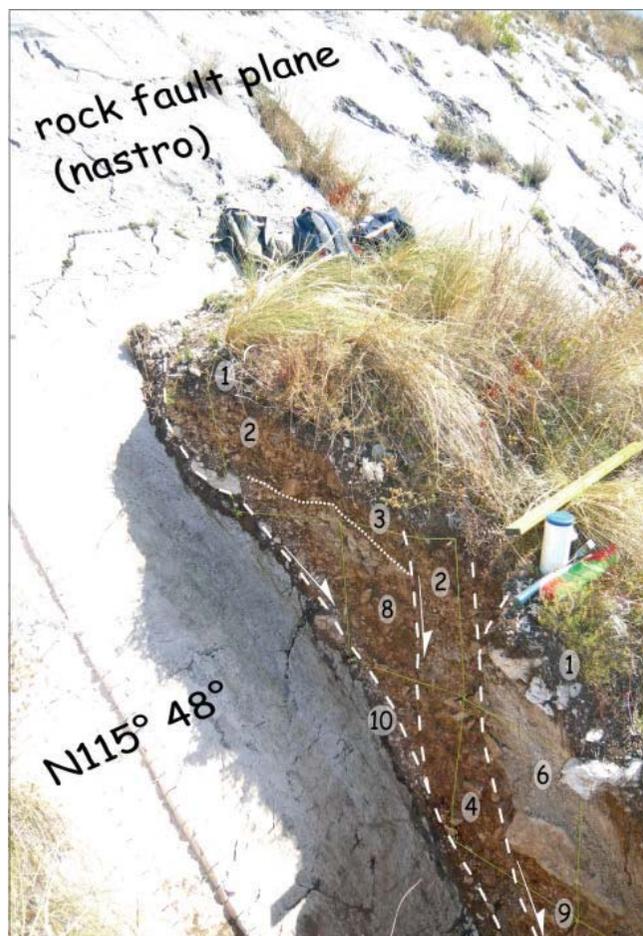
Fig. 27 - Oblique view lookink east and log of the Montagnola paleoseismological trench (after Galli et al., 2012).

several degrees southward, i.e. conformably to the slope, while they are found now to dip up to 10° counter-slope in the hangingwall. Their thickness is much higher in the hangingwall, reflecting either the natural downward thickening and the stronger erosion higher in the slope. Taking all this into account, Galli et al. (2012) have measured a net vertical offset of 550 m.

STOP 1.3 – Cerchio-Collarmele tectonic terraces: long-term activity along the Cerchio-Pescina fault

From this panoramic viewpoint (Fig. 28) it is possible to observe the landscape of the «intermediate terraces» that culminate with a well preserved top surface at about 850-870 m a.s.l.. They are mostly carved in the Pescina formation (Messina, 1996), made up of fluvial gravel, belonging to a river that used the same course of the present Giovenco River. This formation is about 40 meter thick.
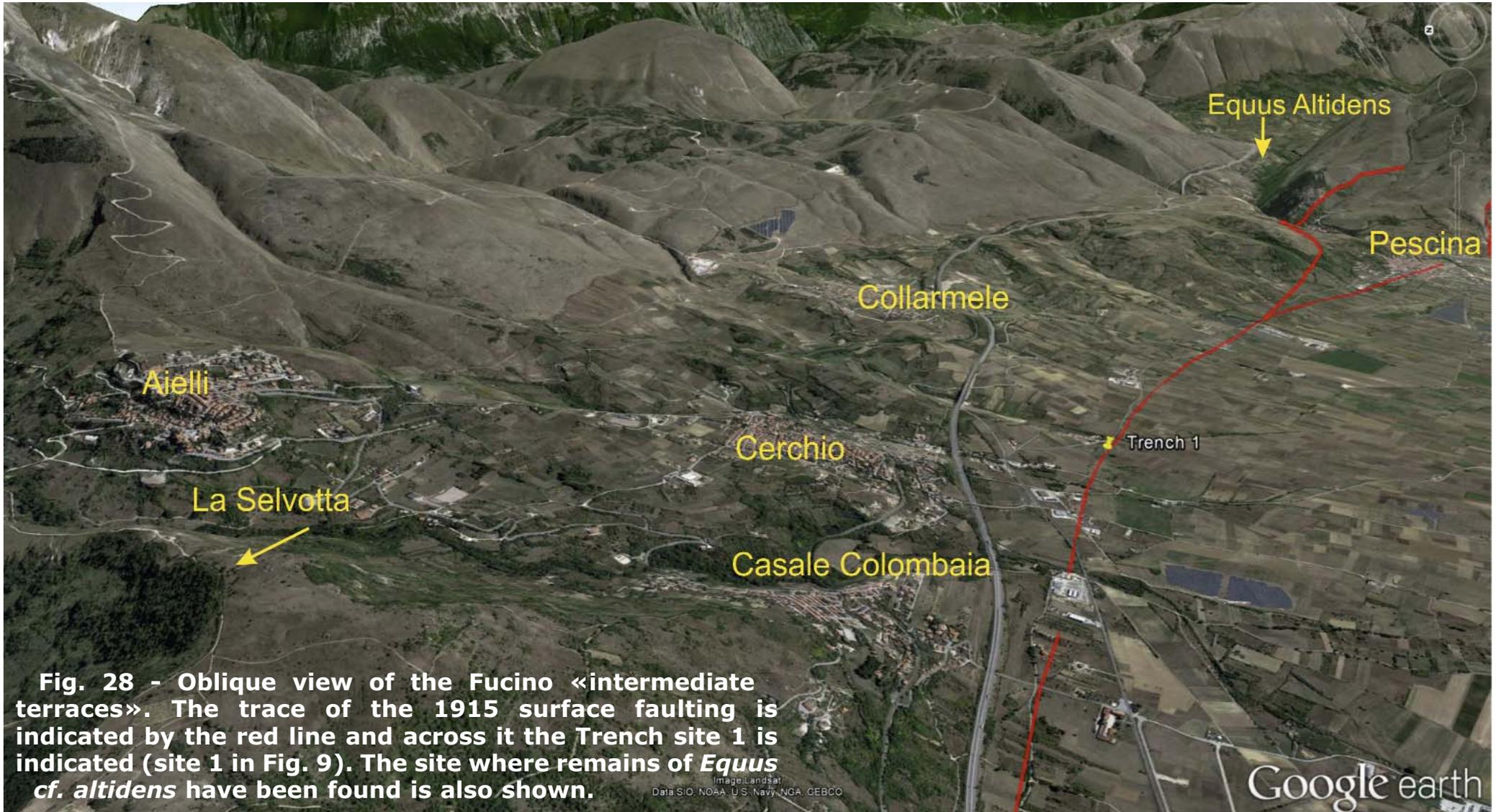
Fig. 28 - Oblique view of the Fucino «intermediate terraces». The trace of the 1915 surface faulting is indicated by the red line and across it the Trench site 1 is indicated (site 1 in Fig. 9). The site where remains of *Equus cf. altidens* have been found is also shown.

itinerary

Slightly entrenched in this terrace, in the Giovenco River valley and in the surrounding of the villages of Pescina and Cerchio, there is a terrace that culminates at about 800-830 m a.s.l.. This is also made up of fluvial gravel belonging to a paleo-Giovenco river. In a reddish paleosoil outcropping inside the Giovenco Valley, about at the top of this sequence (at Ponte della Mandra site, 830 m a.s.l.; Fig. 28), it was found a fragmentary maxillary bone with a tooth of an equid. The paleontological determination ascribes this fossil remain to *Equus cf. altidens*. This species characterizes the Italian fauna from the end of the Early Pleistocene and is no longer documented during the Late-middle Pleistocene. Both these terraces are limited to the SW by a major fault scarp up to 100 m high (Fig. 29), related to the activity of the Cerchio-Pescina-Parasano fault (B in Fig. 9). The correlation of the top surface of these terraces, dated with the *Equus cf. altidens* remains back to c.a. 1 Ma to 0.45 Ma, together with the age of a tephra found at a depth of 100 m in the centre of the basin, dated to ca. 540 ka BP (^{39}Ar/^{40}Ar age; Follieri et al., 1991) constrains the long term slip rate across the section A-A' of Fig. 29 to 0.3 - 0.6 mm/yr.
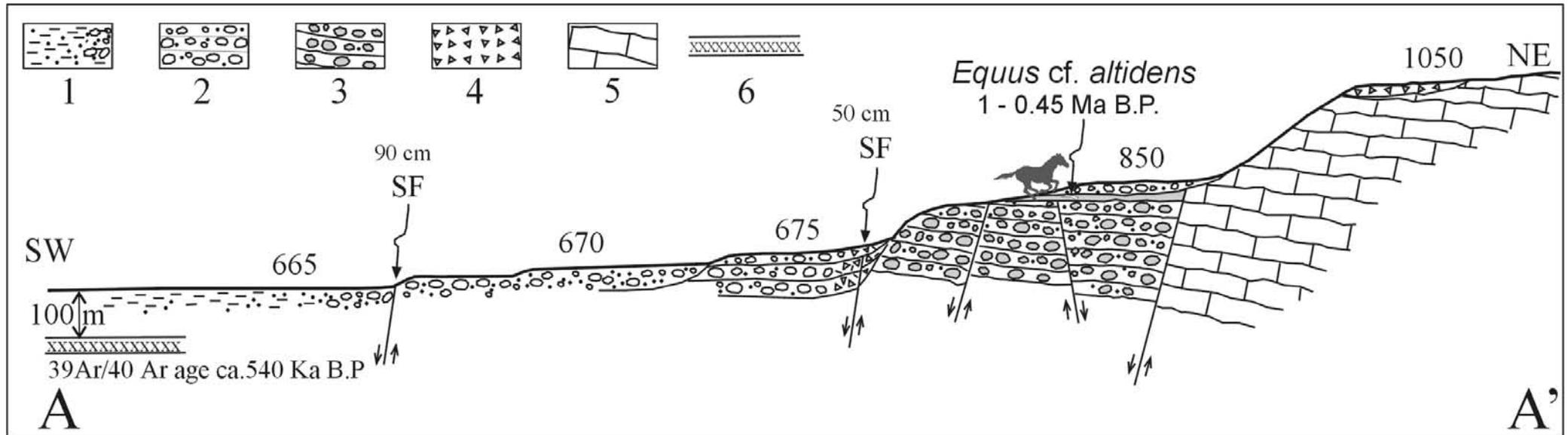
Fig. 29 - Schematic geologic profile across the Quaternary terraces at the NE border of the Fucino basin (location in Fig. 11). The «intermediate» and «lower terraces» deposits are shown, whereas the «upper terrace» is here represented by an erosional surface with only a thin layer of deposits. Legend: **1)** Holocene deposits of the Fucino Lake; **2)** Late Pleistocene to Holocene alluvial fan deposits; **3)** Middle Pleistocene fluvial and lake deposits; **4)** Pliocene?- Early Pleistocene? breccias; **5)** Meso-Cenozoic pelagic limestone sequence; **6)** Dated tephra layer; **SF)** Surface faulting occurred during the January 13, 1915 earthquake (modified after Serva et al., 2002).

Quaternary geology and paleoseismology in the Fucino and L'Aquila basins
S. Amoroso-F. Bernardini-A.M. Blumetti-R. Civico-C. Doglioni-F. Galadini-P. Galli-L. Graziani-L. Guerrieri-P. Messina-A.M. Michetti-F. Potenza-S. Pucci-G. Roberts-L. Serva-A. Smedile-L. Smeraglia-A. Tertulliani-G. Tironi-F. Villani-E. Vittori

In the '90s, the excavation of a long gas pipeline trench that crossed the Cerchio-Pescina fault (site 1 in Fig. 9 and Table 1), allowed to collect the paleoseismological data shown in Fig. 30 (Galadini & Galli, 1999).

Two fault planes, at a distance of about 35 m, were observed affecting Late Pleistocene–Holocene deposits up to the level of the ploughed soil (Fig. 30).

According to Galadini & Galli (1999), the trench stratigraphy revealed at least four displacement events (Table 1); the latest, occurred after 2500 B.C., was most likely the 1915 event; it had a vertical offset of about 1 m.

Legend:

1	Colluvial gravel with blackish matrix; soil in the upper part
2	Alternating sandy gravel and gravelly sand levels
3	Silt (fracture-filling)
4	Colluvial silt
5	Gravel with a sandy matrix
6	Partially layered volcanic sand with large biotite crystals (colluvium of 7)
7	Volcanic sand (calcareous sand in the upper part) with large biotite crystals (max. 1 cm)
8	Yellowish-grey clay (colluvium of 1)
9	Massive yellowish-grey clay (colluvium of 1? top of 1?)
10	Laminated yellowish-grey clay
11	Colluvial clay and gravel deformed by fault movement
12	Colluvial clayey silt, with fragments of level 10 clay

Fig. 30 - Geological cross-sections of the gas pipeline trench at site 1 (southern wall). Section **(b)** is located 35 m to the west of section **(a)**. Small stars indicate the event horizons; the triangle represents the sampling site for radiocarbon dating; unit 1 is a colluvium that buries an archaeological settlement close to this area, dated back to 2500 B.C. (after Galadini & Galli, 1999).

Quaternary geology and paleoseismology in the Fucino and L'Aquila basins

S. Amoroso-F. Bernardini-A.M. Blumetti-R. Civico-C. Doglioni-F. Galadini-P. Galli-L. Graziani-L. Guerrieri-P. Messina-A.M. Michetti-F. Potenza-S. Pucci-G. Roberts-L. Serva-A. Smedile-L. Smeraglia-A. Tertulliani-G. Tironi-F. Villani-E. Vittori

STOP 1.4 – The Serrone fault escarpment

Overview: The Filippone Hotel is located at the base of the Serrone Mt. normal fault scarp (Fig. 31). We have the opportunity to have a close-up view of a landscape feature that is nearly identical to the Magnola, Velino and Tre Monti fault scarps observed during the previous stops. From the swimming pool it is possible to see one of the most spectacular fault planes belonging to the San Benedetto-Gioia dei Marsi fault. This bedrock fault mirror is thought to have been reactivated during the 1915 earthquake, according to eye-witnesses. Therefore, the geomorphic characters of the Serrone Mt. fault scarp can be used as a model for understanding the evolution of similar landforms throughout the Apennines, which appear to be controlled by the repeated occurrence of strong recent earthquakes.

Fig. 31 - Panoramic view of the southwestern flank of the Mt. serrone fault escarpment. The Holocene fault scarp is visible about half-way up the slope. This scarp was likely reactivated during the 1915 earthquake.

The Serrone fault scarp is close to the SE fault tip of the fault that controls the NE border of the Fucino Lake basin (Fig. 32). Compared to the centre of the fault we expect a relatively-low value for total throw, along-strike thinning of the basin-fill sediments, a reduction of the relief across the fault escarpment, low values of slip per earthquake and oblique-slip kinematics.

itinerary

Total throw and basin fill: The total throw across the fault is defined by geological cross-sections showing the offset of the base of the Miocene strata. The total throw is 250-300m (Roberts & Michetti, 2004), compared to a throw of 1600 m ~3km NW of San Benedetto dei Marsi near the centre of the fault (Fig. 32 from Cavinato et al., 2002). This difference reveals the displacement gradient along strike. Basin-filling lacustrine and alluvial sediments, dating from Pliocene and Pleistocene that thicken towards the fault in a classic half-graben geometry, decrease in thickness along strike from ~900 m where the throw is 1600 m to 100-200 m at Gioia dei Marsi (Cavinato et al., 2002).

Expected slip per event: The fault length is 35 km in length (modified from Roberts & Michetti 2004 and Faure Walker et al., 2010). Using empirical relationships in Wells & Coppersmith (1994) we expect ~1.5 m maximum slip at the centre of the fault, but only ~0.2 m slip at the site chosen for ^{36}Cl dating because we are within a few kilometres of the SE fault tip.

Kinematics: The slip vector across the fault plunges at 54° towards 222°, so the faulting is almost pure dip-slip with a small right-lateral component, as expected from the location near to the SE fault tip (Roberts & Michetti, 2004).
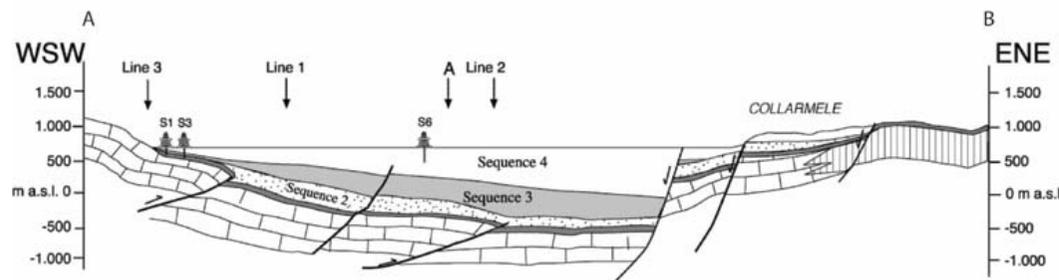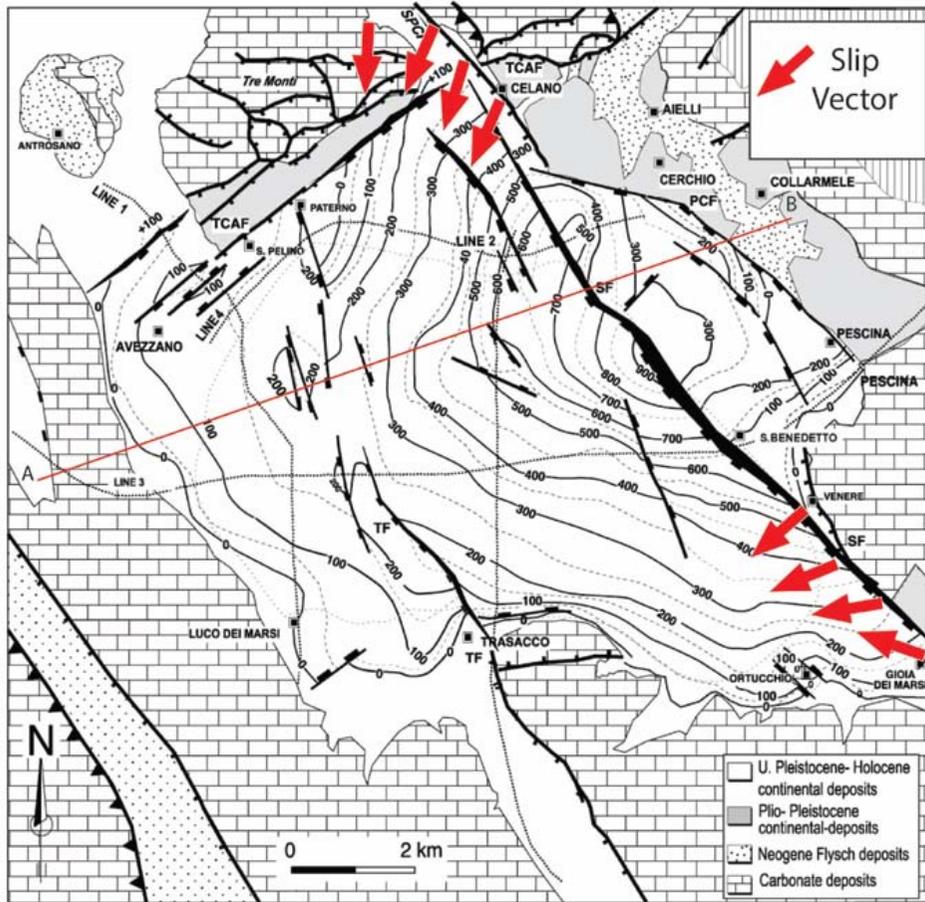
Fig. 32 - Map and cross-section along Line A-B showing the geometry of the basin-bounding fault on the NE side of the Fucino Lake basin (modified, from Cavinato et al., 2002). Slip-vectors on the fault are from Roberts & Michetti (2004). Sample site is SE of Gioia dei Marsi.

Quaternary geology and paleoseismology in the Fucino and L'Aquila basins
S. Amoroso-F. Bernardini-A.M. Blumetti-R. Civico-C. Doglioni-F. Galadini-P. Galli-L. Graziani-L. Guerrieri-P. Messina-A.M. Michetti-F. Potenza-S. Pucci-G. Roberts-L. Serva-A. Smedile-L. Smeraglia-A. Tertulliani-G. Tironi-F. Villani-E. Vittori

Geomorphology: The fault displays the classic geomorphology of upper slope, free-face and lower slope revealed by LiDAR data (Figs 33 and 34). This morphology forms when a preserved last glacial maximum (LGM) landscape is offset by Holocene surface slip across an active normal fault. During the LGM, faulting uplifted the bedrock limestone in meter-scale faulting events. The cold climate (-12°C mean temperature of the coldest month; Allen et al., 1999) promoted free-thaw action and high erosion rates that outpaced scarp growth through faulting. The emerging scarp was eroded, so no cumulative scarp could form. Sediments accumulated as scree sheets on the down-faulted hangingwall. The result was a smoothed landscape with continuous slopes across the active normal faults. When temperatures increased after the demise of the LGM (0 to 4°C mean temperature of the coldest month; Allen et al., 1999), erosion rates decreased. This allowed a cumulative scarp to accumulate through surface faulting. On the nearby Magnola fault, study of pitting of fault surfaces and upper slope versus fault plane angles imply Holocene erosion rates perpendicular to slopes of 0.001 mm/yr with LGM erosion rates of 0.2-0.4 mm/yr (Tucker et al., 2011). The timing of the demise of the LGM is 12-18 ka, defined by a number of climate proxies, most notably the change in dominance of coniferous to deciduous pollen in lake sediments (Allen et al., 1999). Thus, the change in climate provides a time marker for the faulting. The free-face formed in 12-18 kyrs.
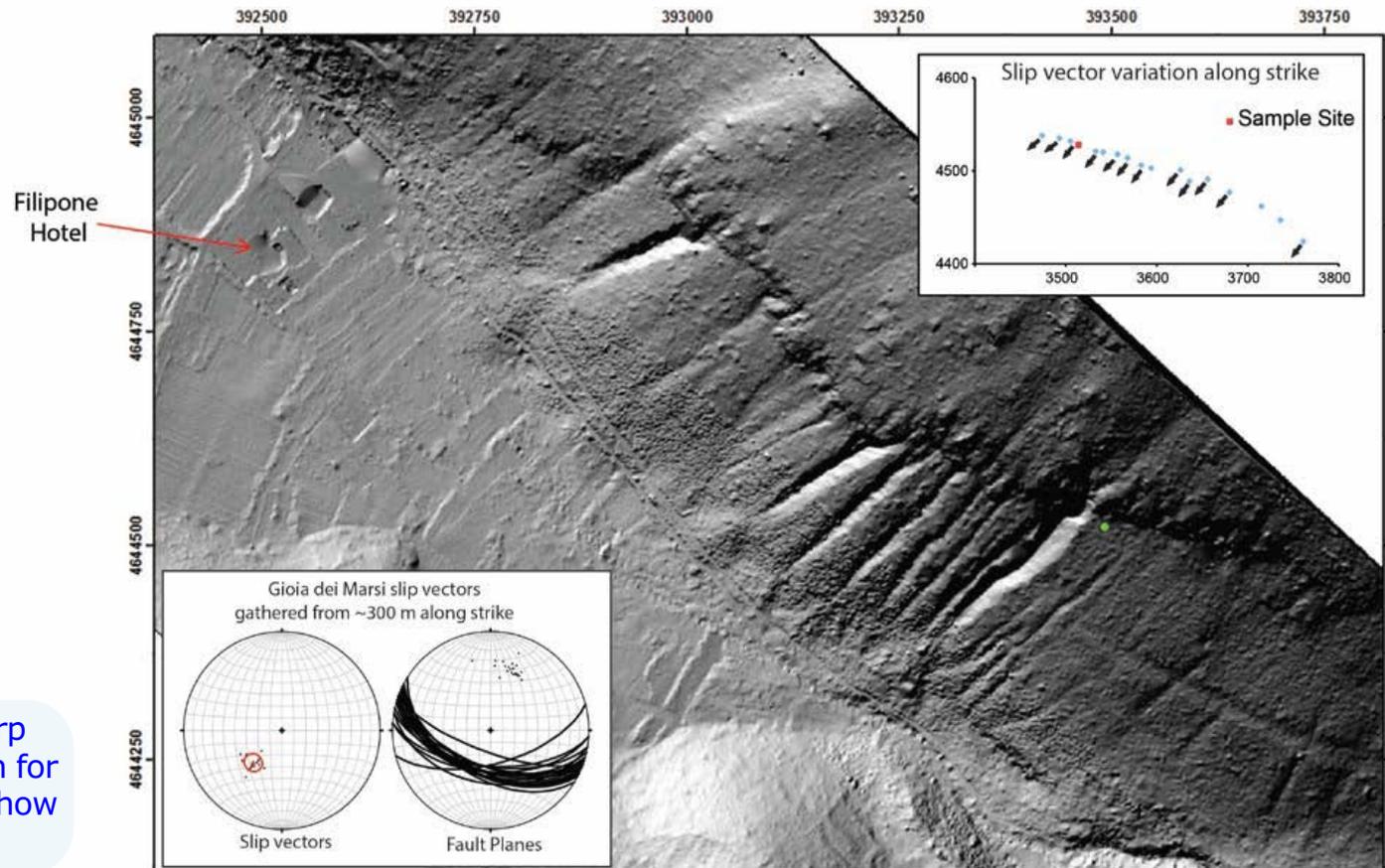
Fig. 33 - Hillshade of the Serrone scarp from terrestrial LiDAR data. The site chosen for ^{36}Cl dating is indicated in green. Insets show kinematic data from structural mapping.
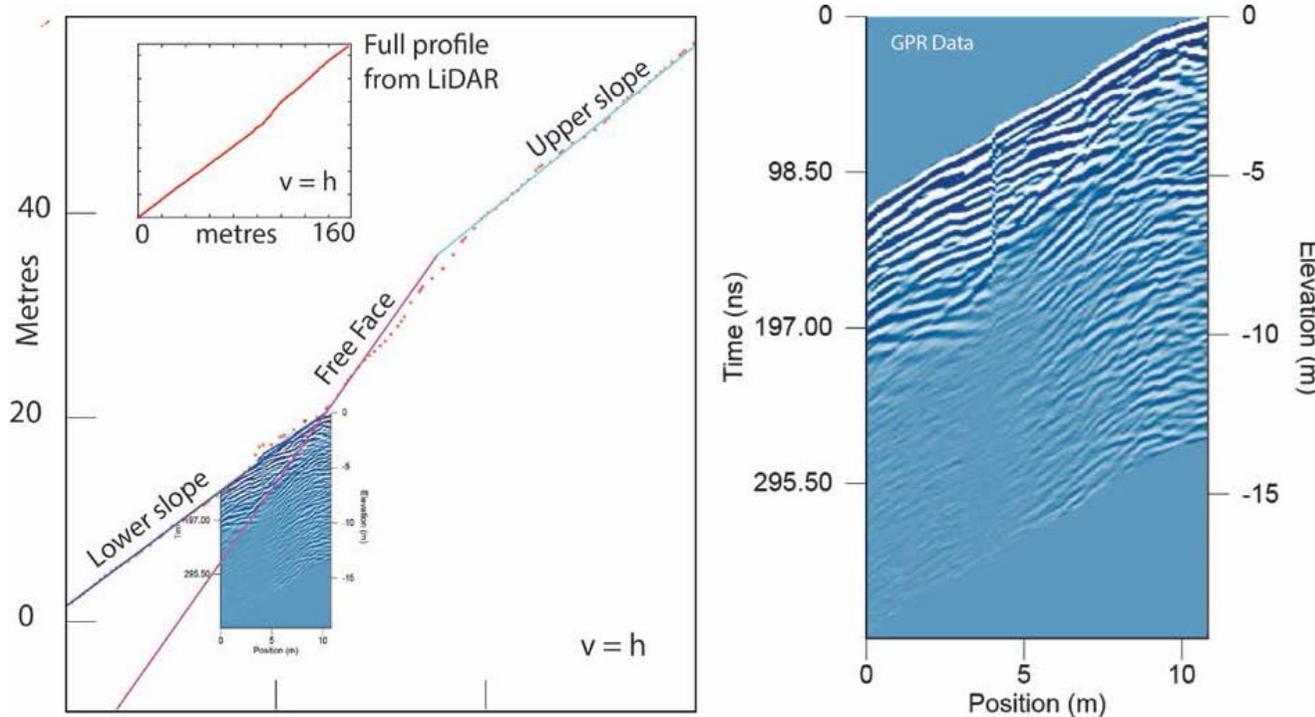
Fig. 34 - Scarp profile of the Serrone scarp from terrestrial LiDAR data, showing the classic geomorphology of upper slope, free-face and lower slope developed during the transition from cold to warmer climate across the demise of the Last Glacial Maximum (LGM). GPR data show the geometry of strata in the sub-surface, confirmed by exhumation of a trench.

LiDAR data set and detailed geomorphology of the chosen ^{36}Cl site: A tripod-based LiDAR data set has been processed to remove vegetation and to produce a hillshade map and scarp profiles (Figs 33 and 34). The scarp profiles are used to define the throw and slip after the LGM and define the dip values for the upper-slope, lower-slope and free-face. These values are needed to model the ^{36}Cl data.

We emphasise that geomorphology of the scarp differs along strike, so site selection is essential to exclude mass-wasting as a fault plane exhumation process. Along the NW portion of the Serrone scarp (Fig. 33), the lower slope has been modified by Holocene mass wasting to produce deeply-incised debris-flow channels cut into the formerly-planar lower slope. Along the SE portion of the Serrone scarp (Fig. 33), the lower slope is less-modified by incised debris-flow channels. In places the hangingwall cut-off at the time of the demise of the LGM is preserved. This hanging wall cut-off formed when sedimentation rates decreased as the climate warmed during the demise of the last glacial maximum (LGM), and the slope was offset by the first post LGM surface faulting event. The hangingwall cut-off is horizontal and continuous for tens of metres along strike where we have sampled for ^{36}Cl. The hangingwall cut-off must be preserved in this way at sites where ^{36}Cl dating is conducted otherwise part of the exhumation will be due to mass wasting and not slip in earthquakes.

48

Quaternary geology and paleoseismology in the Fucino and L'Aquila basins
S. Amoroso-F. Bernardini-A.M. Blumetti-R. Civico-C. Doglioni-F. Galadini-P. Galli-L. Graziani-L. Guerrieri-P. Messina-A.M. Michetti-F. Potenza-S. Pucci-G. Roberts-L. Serva-A. Smedile-L. Smeraglia-A. Tertulliani-G. Tironi-F. Villani-E. Vittori

Where the fault scarp has not been modified by Holocene mass wasting (SE portion), we have chosen a site to date with [36]Cl. The upper slope, which is cut into bedrock limestone, is relatively smooth and planar, dipping towards the basin at 39-40° (Fig. 34). The lower slope, formed of breccia/conglomerate colluvium derived from the upper slope (scree), is also very smooth and planar, dipping at 37-38° towards the basin. The similarity in dip between these slopes cut on different materials suggests they were formerly the same slope in the LGM that has become offset by surface fault slip. The free-face is a carbonate fault plane that is formed in indurated carbonate fault gouge that is 20-30 cm thick. The free-face slickenside is corrugated on a decimetre scale and over tens of metres, and is covered in millimetre-scale frictional-wear striae. The frictional wear striae plunge parallel to the crests of corrugations defining the slip vector. The free-face is almost free of erosion, with millimetres scale frictional wear striae preserved for the lowermost ~5 metres (measured in the plane of the fault).

We have sampled this fault plane for [36]Cl (Fig. 35). However, the upper ~10 metres of the fault plane (measured in the plane of the fault) have been eroded by a few decimetres to a few metres (termed the degraded free face; see Fig. 34). We have not sampled this for [36]Cl. This erosion has also removed the lowest portion of the upper slope (termed degraded upper slope). Thus, this erosion has removed the footwall cut-off, but we are able to reconstruct it by projecting the un-

Fig. 35 - **(a)** free-face and **(b)** trench along the Serrone scarp showing the site for [36]Cl dating.

eroded free-face upwards and the un-eroded upper slope downwards until they intersect. This line of intersection, the footwall cut-off, is horizontal for tens of metres along strike. A Holocene <1m thick colluvial wedge exists, but we have been able to project the lower slope beneath this to define the ground surface at the time of the demise of the last glacial maximum (hangingwall cut-off; Fig. 34).

Ground Penetrating Radar (GPR) and shallow trench excavation: To check that the lower slope has not been modified by mass-wasting or formation of channels before later re-surfacing we collected a ground-penetrating radar dataset and dug a shallow trench (1.95 m deep, measured in the plane of the fault; Fig. 34). The GPR achieved penetration of at least 5 metres through the hangingwall sediment. The data reveal reflectors that parallel the present-day ground surface. In the trench excavation we found ~10 cm of organic rich soil (probably Holocene) before entering light-coloured, indurated scree deposits that are free of organic material (probably LGM sediments). Layering in this LGM colluvium parallels the present-day ground surface, confirming the findings from GPR, and that the LGM lower slope(s) had similar dips to the upper slope cut into bedrock limestones. We interpret the layers to be former ground surfaces that became progressively offset by faulting during the LGM. This confirms we have correctly identified the hangingwall cut-off at the top of the LGM sediments, and that the site has not been disturbed by mass-wasting or formation of channels before later re-surfacing. We determine the density of the colluvial wedge as this also influences ^{36}Cl accumulation in the subsurface portion of the fault plane.

Throw after the Last Glacial Maximum and throw-rate: The throw measured between the footwall cut-off and the hangingwall cut-off, measured in the vertical plane defined by the slip-vector, is continuous for tens of metres along strike and is 15.5 ± 1 metre. This implies 20.9 – 18.4 metres slip in the plane of the fault since the demise of the last glacial maximum. If we assume the age of the slopes is between 12 and 18 ka, the known age of the demise of the LGM from climate data (Allen et al., 1999; 15 ± 3 ka), the implied throw-rate is 1.06 ± 0.3 mm/yr and the slip-rate is 1.35 ± 0.4 mm/yr.

^{36}Cl approach: We have sampled the lowermost 5 m of the free-face, plus the 1.95 m of fault plane exposed in the trench (all measured in the plane of the fault). We collected a continuous sample in 5 cm sections, and have analysed a subset of the samples collected. We have 56 determinations of ^{36}Cl concentration (Fig. 36a), with supporting elemental analyses with ICPMS and ICPOES, plus blanks and spiked samples. The surface

samples will have accumulated ^{36}Cl since exhumation above the ground by surface slip, and during their residence in the sub-surface. Thus, the rate of exhumation of the uppermost free-face that is now eroded and not amenable to sampling must be factored in to calculate the accumulation of ^{36}Cl in the 56 samples whilst they were in the sub-surface. We do this by including exhumation by faulting for the full extent of the free-face in the modelling, rather than specifying a so-called "pre-exposure" value. Our approach is possible because the scarp profile from LiDAR, with the reconstructed footwall and hangingwall cut-offs of the LGM slope (Fig. 35), defines the offset and the time-averaged rate of faulting since 12-18 ka. We can iterate the actual rate of faulting to model the 56 samples using the age of the LGM slope (12-18 ka) as extra information that would not be available if the entire extent of the free-face was not considered. This approach is similar to that termed "seismic pre-exposure" by Schlagenhauf et al., 2010.

^{36}Cl data and expected resolution of time versus slip: Concentrations of ^{36}Cl increase from ~0.5 x 10^5 atoms/gram in the trench to ~2 x 10^5 atoms/gram measured 5 metres above the hangingwall cut-off of the LGM slope. Error bars associated with accelerator mass spectrometry are ± ~0.1 x 10^5 atoms per gram. Thus, although we have rock samples from between the heights of our 56 analyses, we have not analysed these because analytical error bars would not allow further resolution of details of the height versus ^{36}Cl concentration profile. Furthermore, we have calculated a hypothetical ^{36}Cl profile from a hypothetical time versus slip dataset that includes slip magnitudes of <50 cm. We have found that it is not possible to recover < 50 cm slip events with certainty - that we know are in the input slip versus time data using model fitting unless samples spaced <~ 5 cm are analysed. However, as described above, analytical uncertainty shows that no increase in resolution can be achieved if samples spaced this closely are analysed. We conclude that it will be challenging to recover individual earthquakes like the 0.2 m slip events expected at our ^{36}Cl site. Instead, we have concentrated on resolving slip-rate variation through time.

^{36}Cl interpretation: We modelled the data (black points in Fig. 36a) using the code of Schlagenhauf et al., 2010 with the site geometry parameters (fault dip, upper and lower/hangingwall slope dips, total scarp height) obtained from our LiDAR survey of this site. The red dashed lines on Fig. 36b show the expected variation of ^{36}Cl as a function of height up the fault plane at this site if the fault has been slipping at a constant Holocene rate based on 15 ± 3 ka as the beginning of the Holocene. Clearly, the fault has not been slipping at a constant rate. Recent slip has been rapid, exhuming low ^{36}Cl concentrations above the hangingwall cut-off.

itinerary

To fit a model to the data we have used an optimisation approach that seeks to minimise misfit between measured and modelled ^{36}Cl concentrations (Fig. 36c) through multiple model runs. Two model runs are shown (blue and green circles) in which the recent slip rate on the fault has been higher than the Holocene average rate since ~1500 years ago. Although both of these models fit the data better than a model that assumes a Holocene-averaged rate, the lowest RMS is obtained when we include a long elapsed time since significant slip accumulated at this site (800 ± 200 years ago; green circles in Fig. 36d). Note that in the 1915 Fucino earthquake surface slip at this site was most likely much smaller (or even zero slip) compared to our sampling and thus is not resolved. The period of rapid slip that we infer from the ^{36}Cl data at this site would coincide with the timing of the earthquake of 801 A.D., which produced strong shaking in Rome, and an additional event between 1000 A.D. and 1349 A.D. that was inferred from trenching (see Michetti et al., 1996 for discussion of these events). This is the first time that cosmogenic dating of a bedrock fault scarp has been explicitly linked to paleoseismic trench results along strike along the same fault.
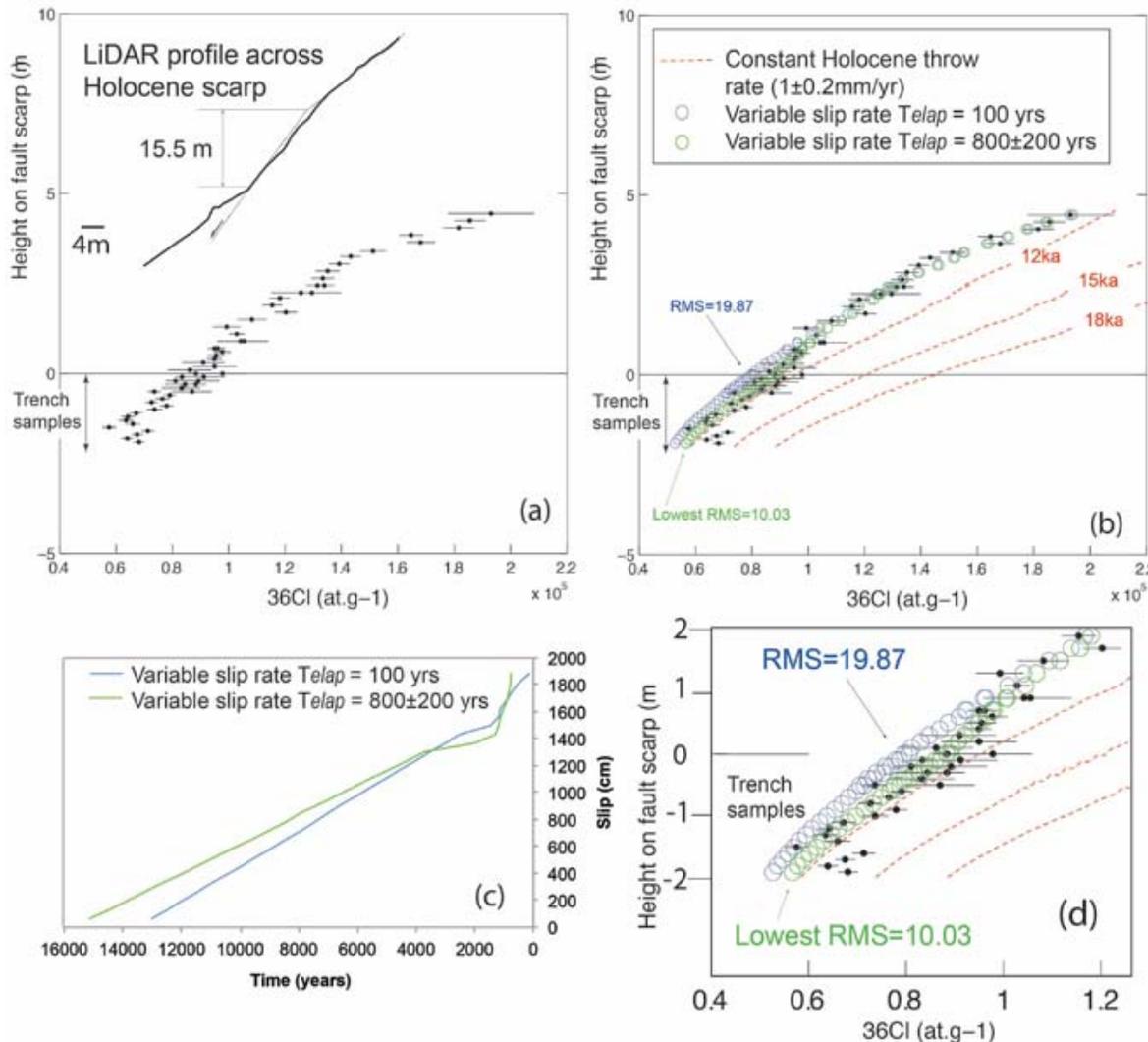
Fig. 36 - ^{36}Cl results for the Serrone scarp. **(a)** Data; **(b)** interpretation; **(c)** time versus slip. The best fit to the data shows a pulse of rapid slip that coincides with palaeo-earthquakes identified in trenches along strike (see Michetti et al., 1996). **(d)** close-up of **(b)**.

Quaternary geology and paleoseismology in the Fucino and L'Aquila basins

S. Amoroso-F. Bernardini-A.M. Blumetti-R. Civico-C. Doglioni-F. Galadini-P. Galli-L. Graziani-L. Guerrieri-P. Messina-A.M. Michetti-F. Potenza-S. Pucci-G. Roberts-L. Serva-A. Smedile-L. Smeraglia-A. Tertulliani-G. Tironi-F. Villani-E. Vittori

Conclusions from this site and implications: It is possible to use ^{36}Cl concentrations to resolve a history of fault slip despite concerns that climate changes and mass wasting might dominate exhumation of samples. However, we strongly-emphasise that this is only possible where the site is chosen very carefully to exclude mass wasting and to resolve exhumation purely through fault slip. We also emphasise that the geometry of the scarp and knowledge of age of the climate change that formed the geometry of the scarp (15 ± 3 ka) gives extra constraints that allow modelling to include so-called seismic pre-exposure rather than simple pre-exposure. Although we doubt that individual earthquakes can be resolved, we are able to test whether the slip-rate was constant through time. Our results show a phase of rapid slip that corresponds with the timing of palaeoearthquakes resolved in traditional palaeoseismic trenches a few kilometres along strike to the NW and the historical record. The rapid slip indicates that earthquake recurrence may be strongly clustered in time. Temporal clustering must be included in calculations that attempt to define earthquake probabilities that combine mean recurrence intervals, elapsed time since the last earthquake, and clock-advance produced by Coulomb stress transfer.

STOP 1.5 – The Venere quarries: surface faulting of the 1915 earthquake and paleoseismic evidence

The Stop focuses on the surface faulting of the 1915 Fucino earthquake along the San Benedetto-Gioia dei Marsi fault section (Figs 37 and 38) and on the post-LGM evolution of this sector of the Fucino basin.

Fig. 37 - Panoramic view of the Venere quarries nowadays. Red line shows the trace of the 1915 surface faulting along the San Benedetto-Gioia dei Marsi fault. Yellow stars locate pictures. Yellow lines indicate the trace of the geological profiles in Figs 39 and 40.

We follow a 500 m long segment of the 1915 fault, starting from Cave Santilli, at km 13.1 of SS 83 Marsicana (starting point; Fig. 38) up to a point where the fault reactivation was observed by eye-witnesses (Fig. 41). The quarry excavation allows a 3D observation of the geologic and geomorphic features that are the effect of repeated Late Quaternary coseismic surface faulting events.

Fig. 38 - Exposure in the Cave Santilli of the San Benedetto-Gioia dei Marsi fault ruptured in 1915. **Left**: picture taken in the '80s in the northern part of the present Cave Santilli (location in Fig. 37). **Right**: exposure of the fault inside the quarry and detail of faulted debris.

Particularly, one of the quarry walls (location in Fig. 37) exposes a limestone wave cut terrace (Fig. 39 left; WT in Fig. 39 right) buried by the Late Glacial and Holocene talus. Both the wave-cut terrace and the overlying debris are affected by a fault scarp several metres high. Just upon this erosional surface, LGM fan delta deposits were observed in other ancient quarries, some hundred meters to the east, near San Veneziano Village (Fig. 40 left), constraining the age of the lake abrasion platform to about 20 ka. Its present position indicates that it was uplifted by several metres along the San Benedetto-Gioia dei Marsi fault section (Radmilli, 1956; 1981; Raffy, 1970; Giraudi, 1995).
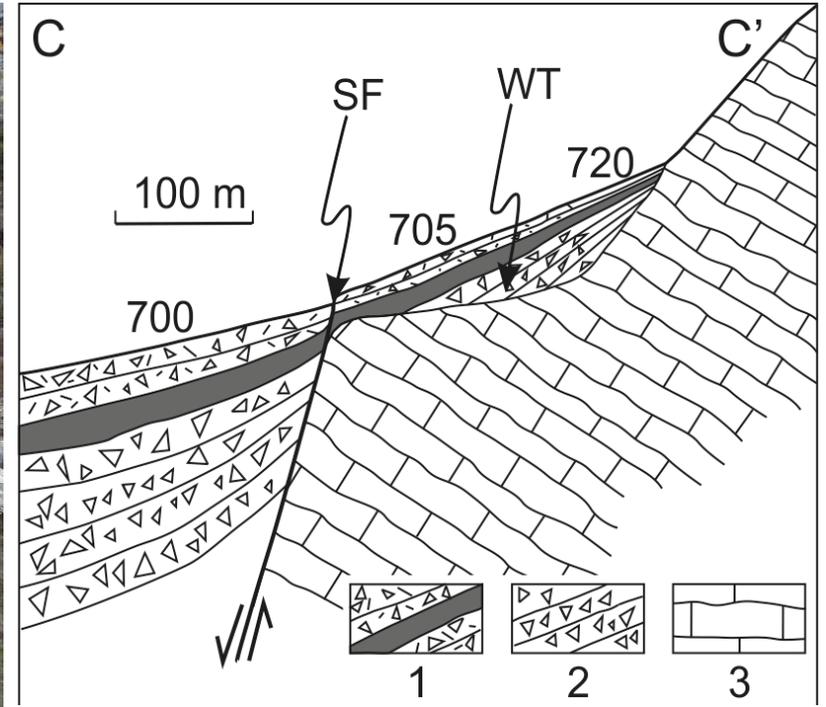
Fig. 39 - Left: Exposure of the limestone wave-cut terrace in the Cave Santilli quarry. Right: Geological profile showing a bedrock wave-cut terrace associated to the LGM high-stand of the Fucino Lake, displaced several times during the Holocene (after Blumetti et al., 1993). The 1915 offset was 50 to 100 cm. Legend: **1)** Holocene talus with a level containing Neolithic pottery; **2)** Late Glacial stratified slope-waste deposit; **3)** bedrock; **WT)** wave-cut terrace; **SF)** Surface faulting. The profile trace is shown as C-C' in Figs 11 and 37.

Some Paleolithic sites are located in the caves at the inner edge of the wave-cut terrace, at the base of the bedrock cliff, *e.g.*, the Riparo di Venere site (Radmilli, 1956), few hundreds of meters north of Cave Santilli (Fig. 37). The latter shows LGM high-stand lakeshore gravel deposits covered by fire places with charcoal and other archaeological remains dated at 19 to 12 ka BP. The caves and the wave-cut terrace are presently buried by the Late Glacial and Holocene talus. Both the wave-cut terrace and the overlying debris are affected by a fault scarp several metres high, locally subdivided into subsidiary segments. This scarp was clearly reactivated also during the 1915 earthquake with an average displacement of 50-100 cm.
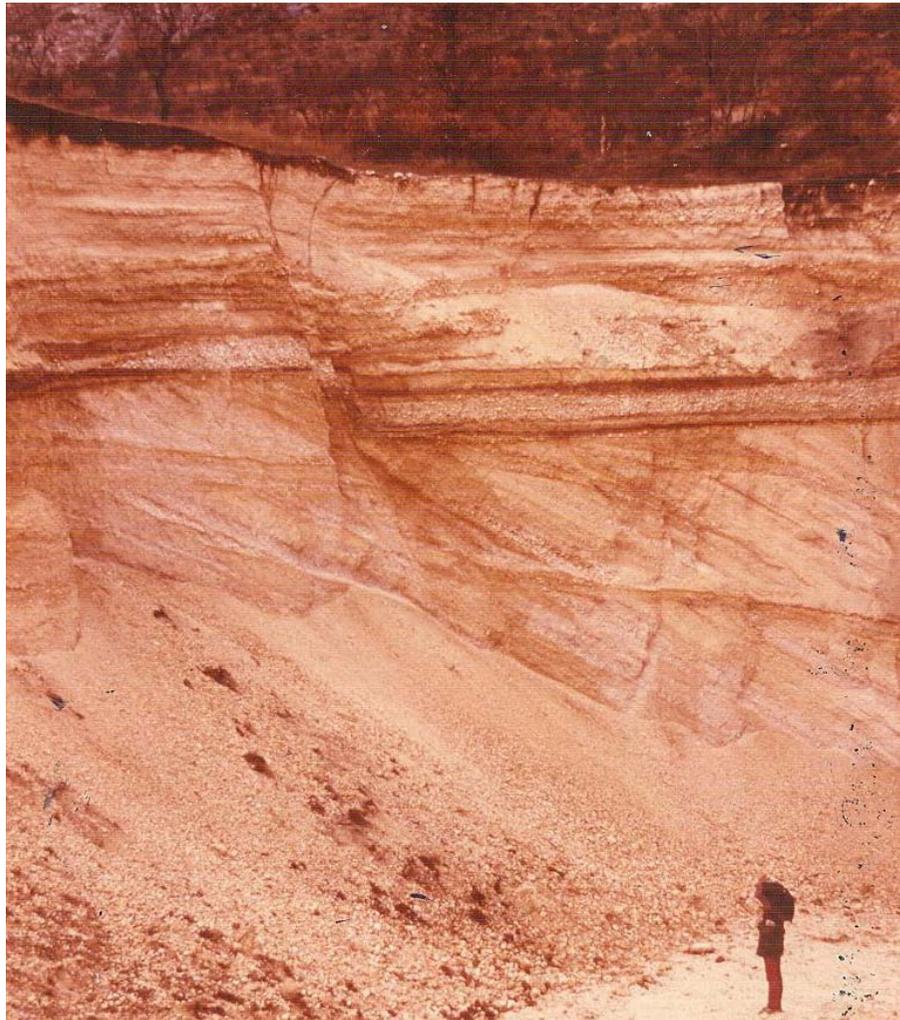
Inside the ancient quarries of San Veneziano, it was possible to detect several listric normal faults, defining a little graben parallel to the slope, c. 20 m wide and more than 100 m long, with an overall down-faulting of a few metres (Fig. 40). These faults do not displace the present-day soil. In fact, the structure is truncated by an erosion surface that levels the top of the alluvial sequence. Instead, a few metres downslope, the same erosion surface is affected by some fault scarps that produce a series of topographically depressed and uplifted belts, always running parallel to the slope. They have a maximum height of a few metres, a length of a few hundreds of meters and width of a few tens of metres, and were formed prior to the 1915 earthquake.

We leave Cave Santilli following the fault scarp to ESE. Another exposure of recent faulted deposits is preserved on the wall of an old quarry (Fig. 41). Here, a stratigraphic log was described by Saroli et al., 2008 (Fig. 41), allowing to identify at least three displacement events occurred after 14-15 ka BP.

56

itinerary
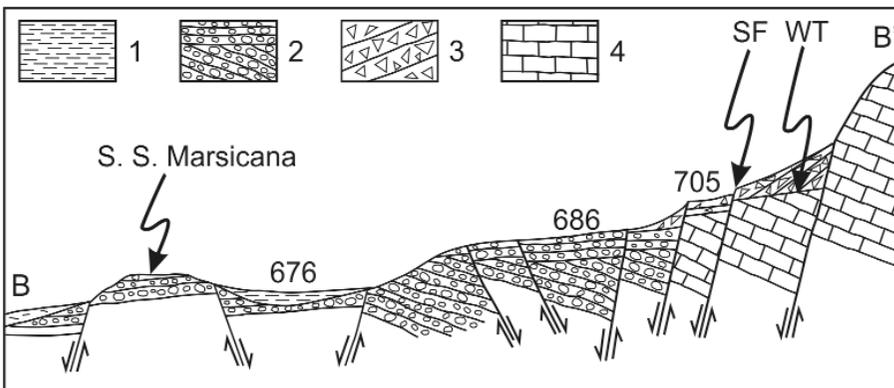
Fig. 40 - Up: fan delta deposits affected by a listric normal fault, antithetic to the Fucino master fault, in an ancient quarry located some hundred meters east of Cave Santilli, near San Veneziano. Based on this and other exposures in the surrounding of San Veneziano Village (near Gioia dei Marsi), the cross section down drawn showing the "lower terraces" (modified, after Blumetti et al., 1993; see location in Figs 11 and 37). It shows several listric normal faults, defining a little graben parallel to the slope, ca. 20 m wide and more than 100 m long, with an overall down-throw of a few metres. Legend: **1)** Lacustrine sediments; **2)** Fan delta deposits; **3)** Late Glacial to Holocene talus; **4)** bedrock; **WT)** Wave-cut terrace; **SF)** Surface faulting.

About 150 m towards east, the limestone fault plane is very well exposed at the edge of an abandoned vineyard. Here, two eye-witnesses of the 1915 earthquake (Fig. 42) reported that here the coseismic offset was about 70 cm.
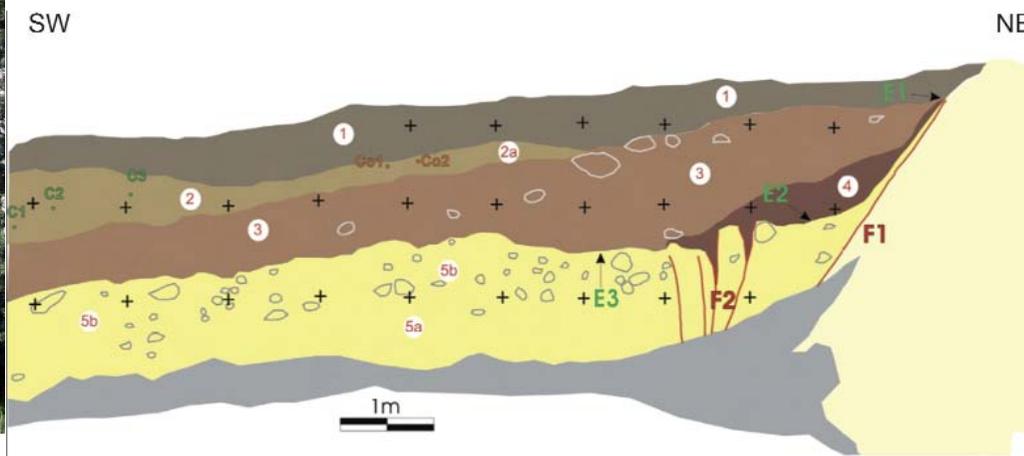
Fig. 41 - Recent faulted deposits on the wall of an inactive quarry. The stratigraphic log is described in Saroli et al., 2008. It shows a pit-fire containing fragments of Eneolithic (Copper Age) and Bronze Age pottery shards (3000-1500 B.C.) inside unit **2** (just below the present soil, unit **1**). The characteristics of unit **3** gravels indicate deposition along the shoreline, while unit **4** (gravels in sandy matrix) is interpreted as a colluvial wedge deposited from a coseismic scarp. Finally, unit **5** represents the result of the re-organisation of alluvial gravel along the lacustrine shoreline.

Fig. 42 - **Left**: The 1915 coseismic slip was observed by two eye-witnesses (Alfonso Di Salvatore and Antonio De Angelis) here with Leonello Serva (Serva et al., 1988). **Right**: The same outcrop 30 years later. The ageing is clearly visible on Leonello's hair.

itinerary

STOP 1.6 – 1915 coseismic rupture in the lake sediments and trench logs

West of San Benedetto and Venere dei Marsi, Oddone (1915) observed a ground rupture, directed toward the northern edge of the Fucino basin, dislocating the recent lake sediments with an offset of 30 to 90 cm (Oddone, 1915). The images in Fig. 43 (from Oddone's paper) indicate a complex scarp, similar to those commonly observed in ruptures involving soft sediments; actually, it must be recalled that the lake bed had been definitely reclaimed only a few decades before the earthquake (1875) and the water table is still very close to the surface, especially in winter.
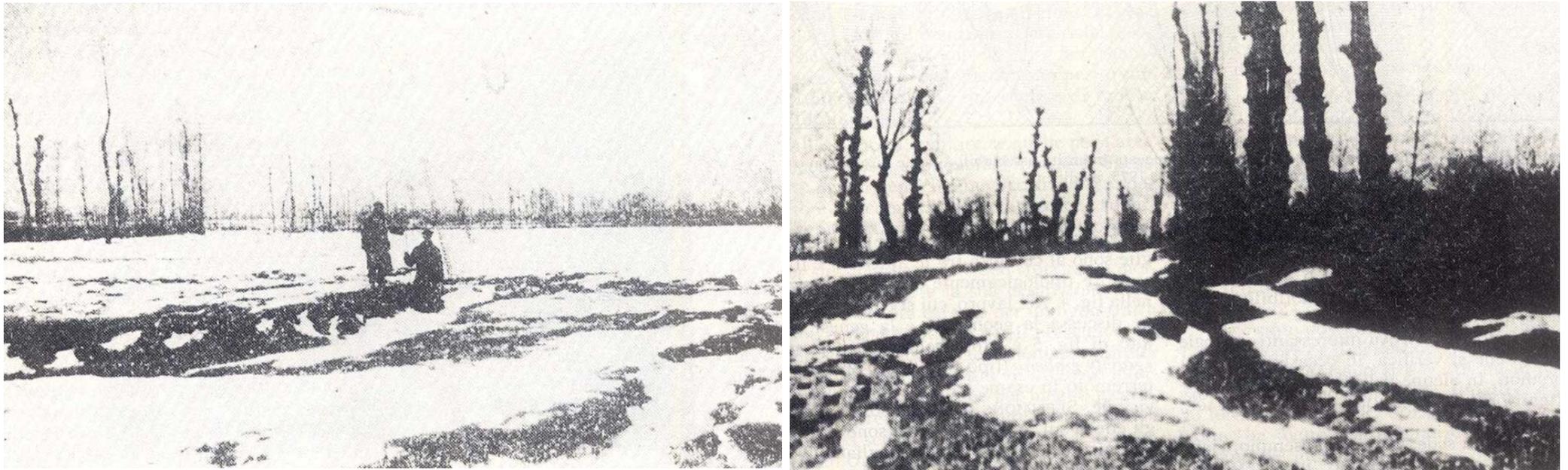
Fig. 43 - Reproduction of the original photographs in the paper of Oddone (1915).

Despite the intensive farming activities since then, a subdued scarp was still evident in the '90s (Fig. 44). After nearly 20 more years, the scarp is now almost vanished, but the fault can still be discerned and actually seen in vertical excavations, even very shallow as the water ditches bordering the farmed fields cutting across orthogonally to it. A clear example is shown in this Stop, located between the 1996 trenches of Michetti et al. (1996) and those of Galadini & Galli near Venere (summary in Galadini & Galli, 1999).

Fig. 44 - Scarp of the 1915 coseismic rupture in southern outskirts of San Benedetto dei Marsi, where the paleoseismological trenches of Michetti et al., 1996 were excavated (location and log in Fig. 48).
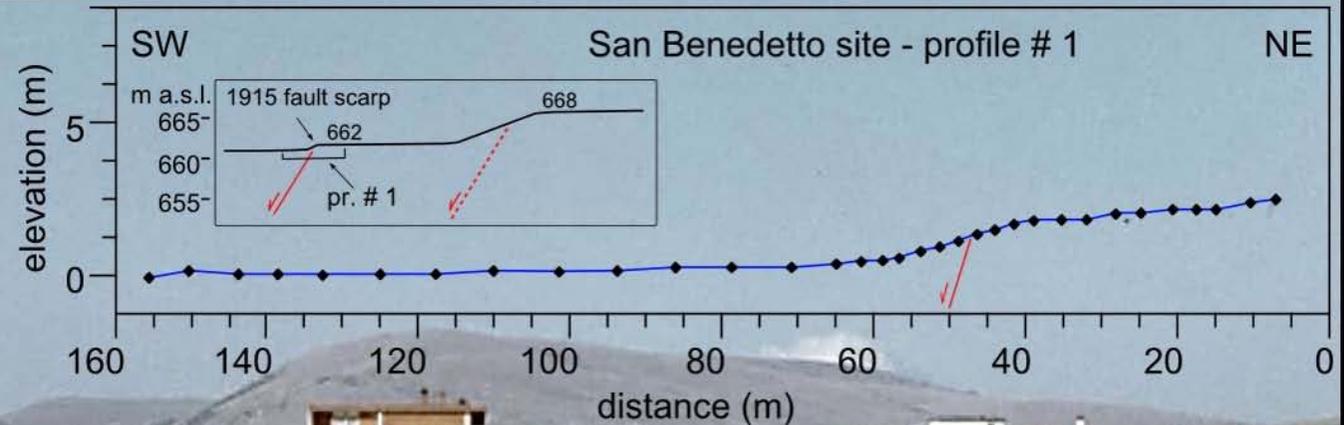
The first two paleoseismological trenches in the Fucino basin were dug across this scarp in 1996 (Michetti et al., 1996), just in the southwestern outskirts of San Benedetto (location in Fig. 48), soon followed by a number of trenches across different fault segments by Galadini & Galli (1999) (trenches near Venere dei Marsi in Fig. 48).

The planned Stop is located close to the trench site # 4 in Galadini & Galli (1999) and less than 2 kilometers from the trenches of Michetti et al. (1996) (Fig. 44). From the parking lot, a short walk takes to one of shallow ditches cutting across the fault (Fig. 45) where, on its western face, the fault can be clearly seen cutting the most recent lake sediments (Fig. 46). More details are reported in Galli et al., (2016).

itinerary

The exposed section is ca. 90 cm high and shows, below the ploughed level, light grey-blue lacustrine clayey silts (early Holocene; right side in Fig. 46) faulted against grey silts, and sandy gravels rich of Roman pottery shards. The latter are mantled by light-grey silt deposited during the last high-standing levels of the Fucino Lake (Middle Age-19th century). Beside the 1915 event, this section likely records the previous 508 AD earthquake.

The schematic logs in Fig. 48 give evidence of historical faulting events comparable to the 1915 earthquake, without being able to precisely constraining their occurrence time, because of the large uncertainties in radiocarbon ages.

Fig. 45 - The 1915 rupture at Stop 1.6 (see Fig. 46 for close-up view).

Based on stratigraphic and archaeological evidence, Michetti et al. (1996) have inferred two events since the VI century, i.e. after the obstruction of the Emperor Claudius' drainage system, likely for lack of maintenance, and the lake return to flood the area. An event (B) is constrained between 550 and 885 CE, possibly referable to the 801 or 847 earthquakes that caused damages in Rome (Galli & Molin, 2014).

Fig. 46 - Close-up view of the fault rupture at Stop 1.6.

A more recent event (A) might have occurred afterwards, still in the Middle Age but before the 1349 earthquake, because since then the historical seismic catalogue is deemed complete for events of such a magnitude. Instead, Galadini & Galli (1999) infer only one penultimate event in historical times occurred between the II and XV centuries (only in their trench # 5 the age is better constrained at 426-782 CE). They attribute this event to the 508 earthquake strongly felt in Rome, responsible of significant damages to the Colosseum (Galli & Molin, 2014). In summary, leaving aside the more obscure event A of Michetti et al., (1996), the paleoseismological evidence points to a post-Roman earthquake comparable to the 1915 one, most likely corresponding to the 508 or 801 – 847 events, which have left historical and archaeological traces of partial collapses in Rome. Actually, the 801 and 847 events are excluded by Galadini & Galli (1999) because tentatively attributed to other capable faults (L'Aquila basin, Aquae Juliae fault near Venafro), as summarized in Galli & Molin (2014).

61

itinerary

Fig. 47 - Panorama view of the 1915 ruptures between San Benedetto and Gioia. There is no general consensus regarding the rupture along the Parasano fault. **M96**: trenches of Michetti et al., (1996), **GG**: trenches described in Galadini & Galli (1999).
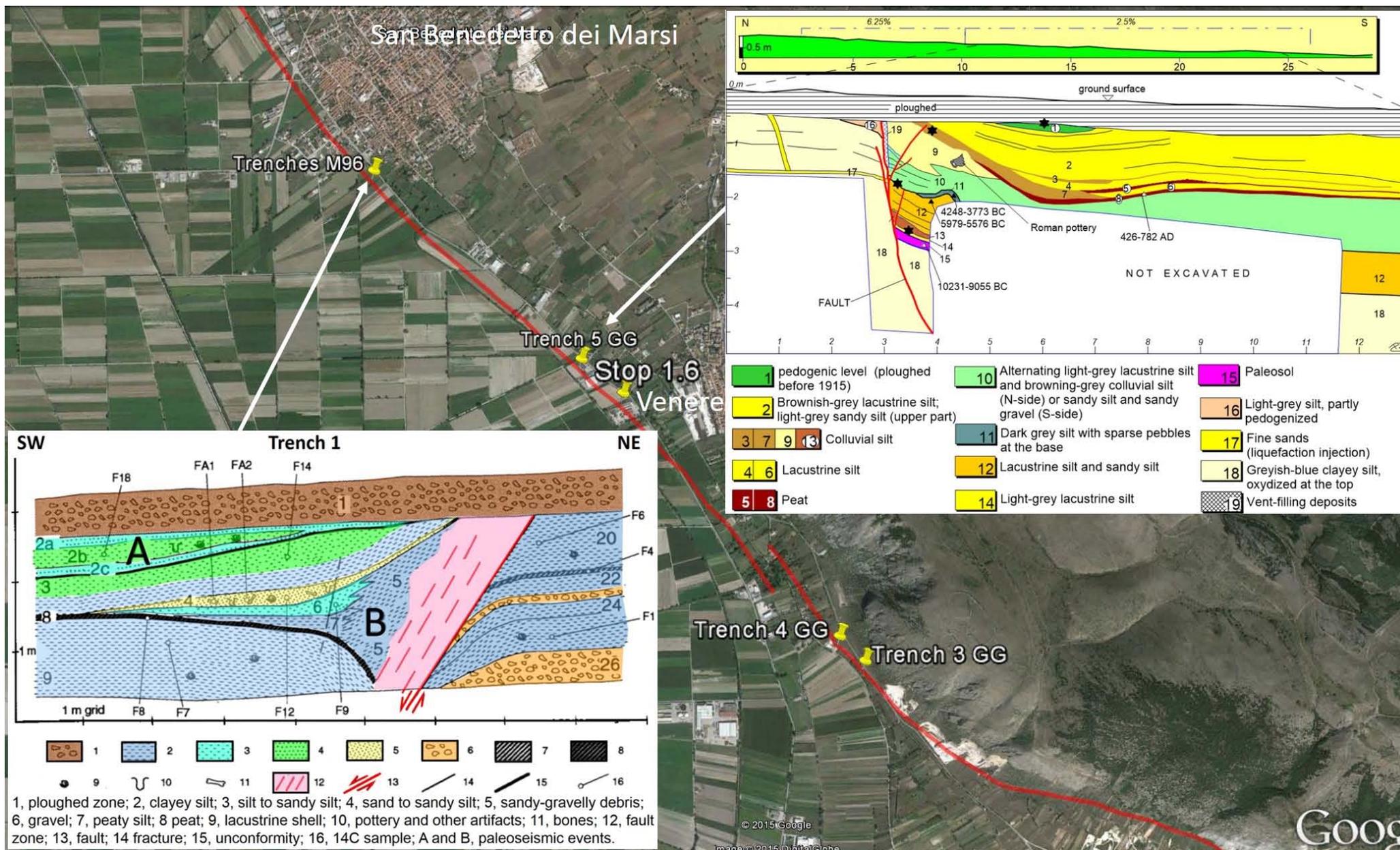
Fig. 48 - Location of Stop 1.6 and trench logs across the 1915 rupture in the San Benedetto-Venere dei Marsi area (**M96**: Michetti et al., 1996; **GG**: Galadini & Galli, 1999).

DAY 2
Quaternary geology and palaeosismology in the
L'Aquila basin
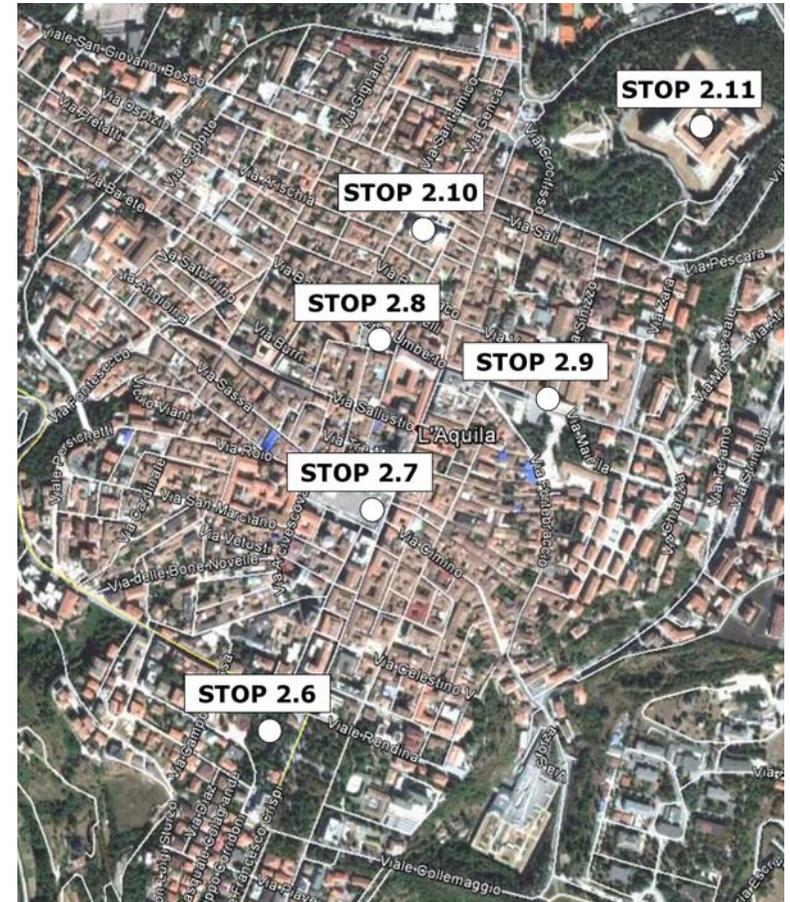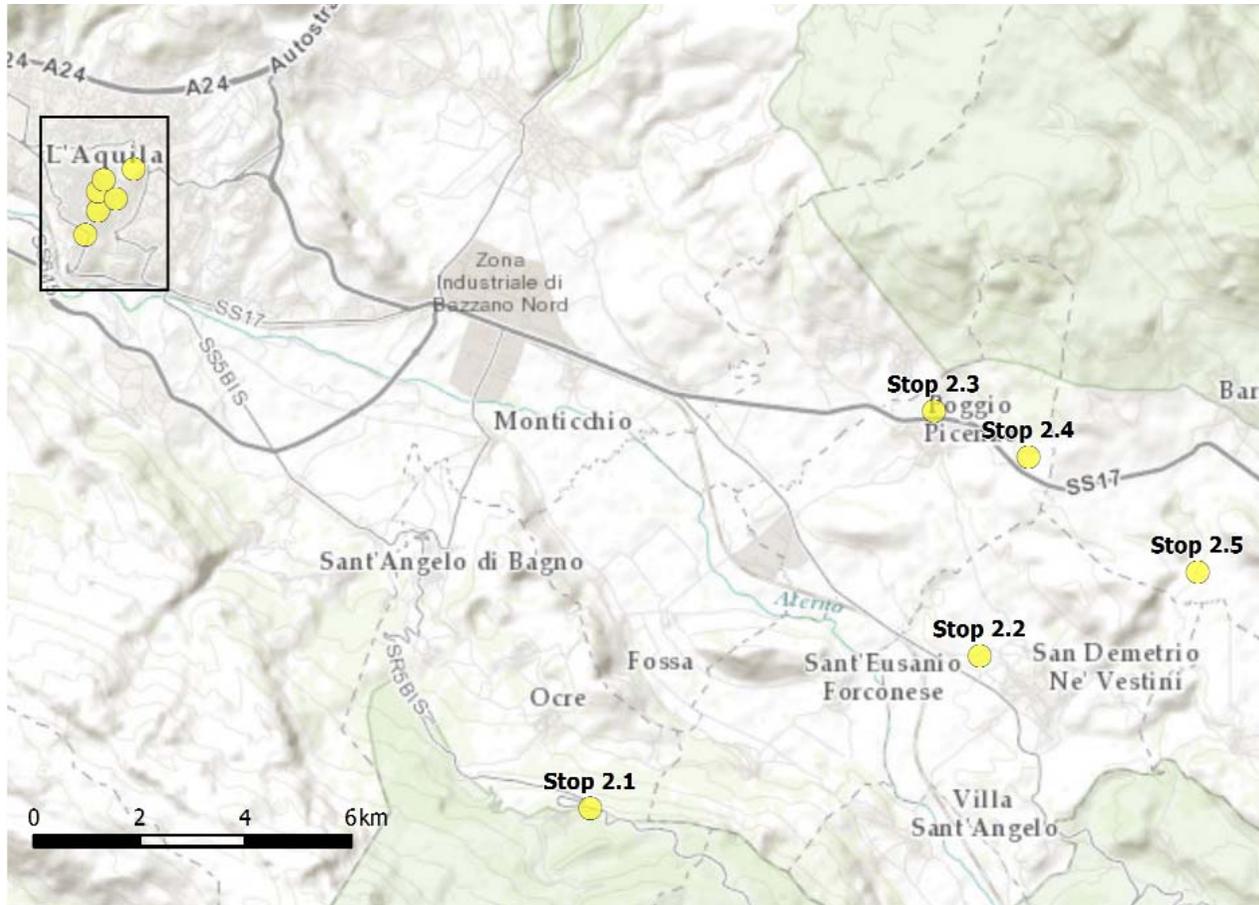
Field trip stops in the middle Aterno Valley. The black box encloses the area covered by Part 2 of the field trip (afternoon) inside L'Aquila city.

STOP 2.1 - Panoramic view from San Martino d'Ocre

The main topographic highs bounding the valley to the north and to the south correspond to some major Quaternary normal fault scarps belonging to the Paganica - San Demetrio Fault System (PSDFS). In the Paganica sector, it is possible to see the cumulative fault scarp of the 2009 L'Aquila earthquake source and the sites where continuous (red dots) and discontinuous (yellow dots) surface coseismc surface breaks were observed. In the San Demetrio sector another Quaternary cumulative fault scarp is visible (Stop 2.2).
The valley is filled with a complex sequence of continental deposits. Among the oldest sediments, Early Pleistocene lacustrine silts (Stop 2.3) and fan-delta conglomerates (Stop 2.4) are found. The south-eastern part of the basin was progressively exhumed and dissected by the long-term activity and footwall uplift of the PSDFS.
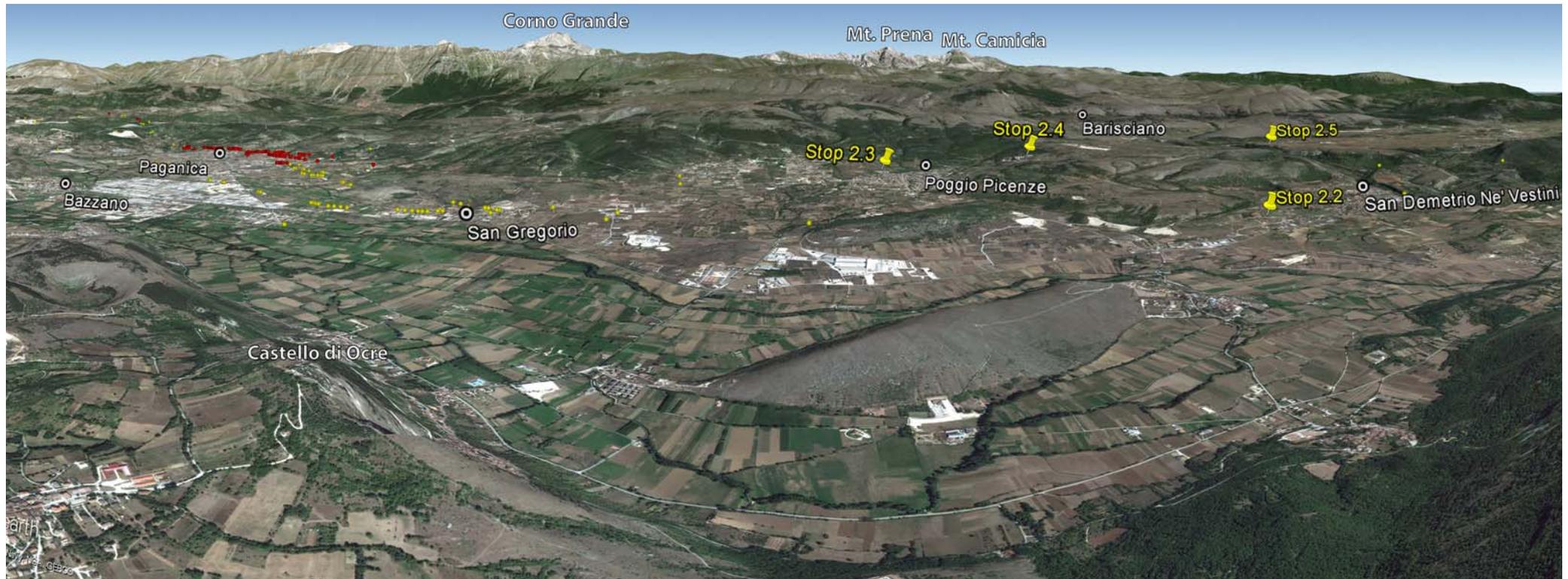
Fig. 49 - Panoramic view of the middle Aterno Valley from San Martino d'Ocre. From NW (to the left) to SE (to the right) the main villages close to L'Aquila town are clearly visible. The Gran Sasso range (with its main peaks) is in the background.

STOP 2.2 - San Demetrio Ne' Vestini - Quaternary composite fault scarps and paleoseismological investigations

Paleoseismological investigations along the PSDFS were performed in order to reconstruct its Late Pleistocene–Holocene rupture history.

Blumetti et al. (2015) investigated a splay of the San Demetrio Ne' Vestini sector. Here, the fault displaces Early-Middle Pleistocene alluvial fan deposits (VIC), Middle-Late Pleistocene alluvial sediments (SMA) and, in the fault zone, Holocene colluvial deposits and presents a ca. 25 m-high composite fault scarps (Fig. 50). Cinti et al., (2011), Galli et al., (2010; 2011) and Moro et al., (2013) excavated the 2009 earthquake causative fault at the Paganica sector. By interpreting the paleoearthquake record at four different sites, Cinti et al., (2011) conclude that 1) five distinct surface faulting earthquakes (including the 2009 event) occurred since 2900-760 B.C. and 2) there are indications for earthquakes in the past larger than the April 6, 2009 event, likely related to the rupture of the whole PSDFS. Moreover, Cinti et al., (2011) estimated that the late Holocene and late Pleistocene dip-slip rates for the investigated portion of the fault are consistent, and range between 0.2 and 0.4 mm/yr (Fig. 51).
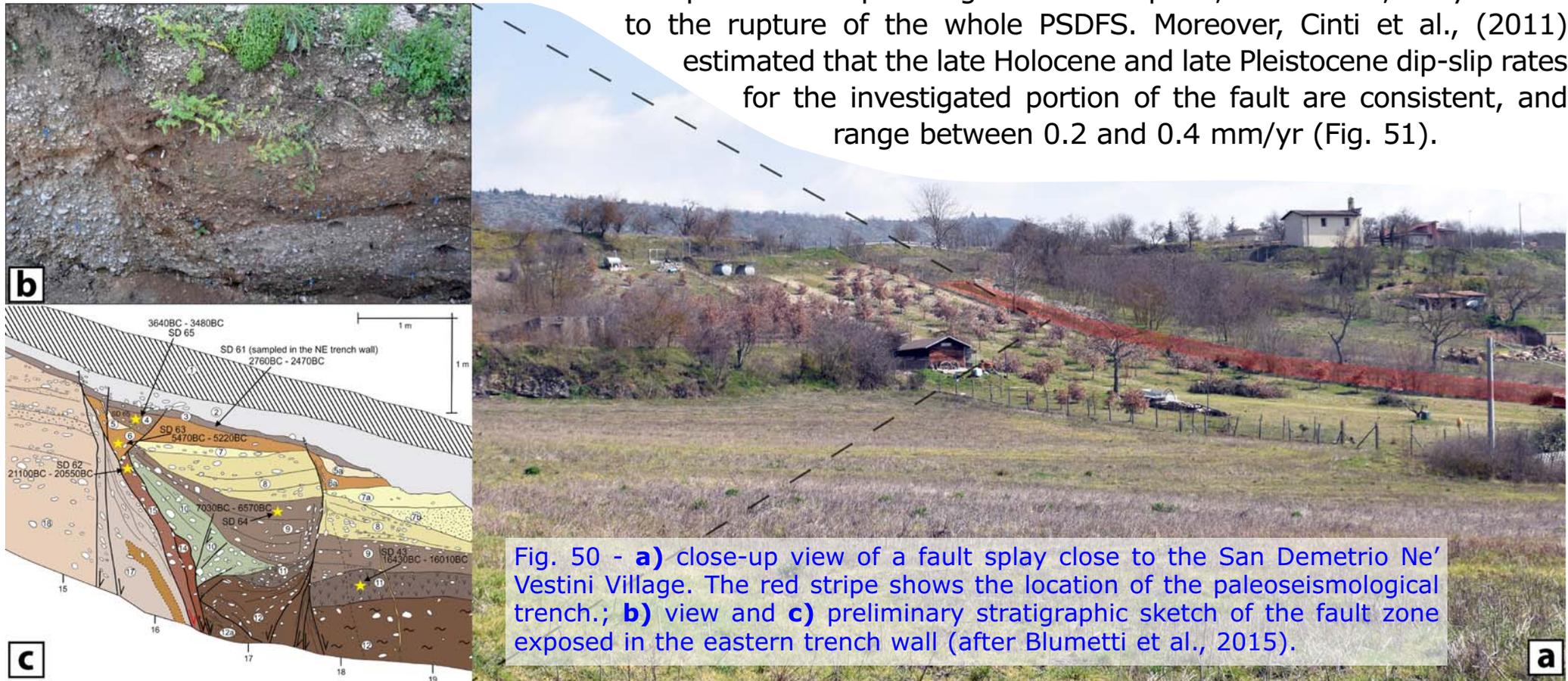
Fig. 50 - **a)** close-up view of a fault splay close to the San Demetrio Ne' Vestini Village. The red stripe shows the location of the paleoseismological trench.; **b)** view and **c)** preliminary stratigraphic sketch of the fault zone exposed in the eastern trench wall (after Blumetti et al., 2015).

itinerary
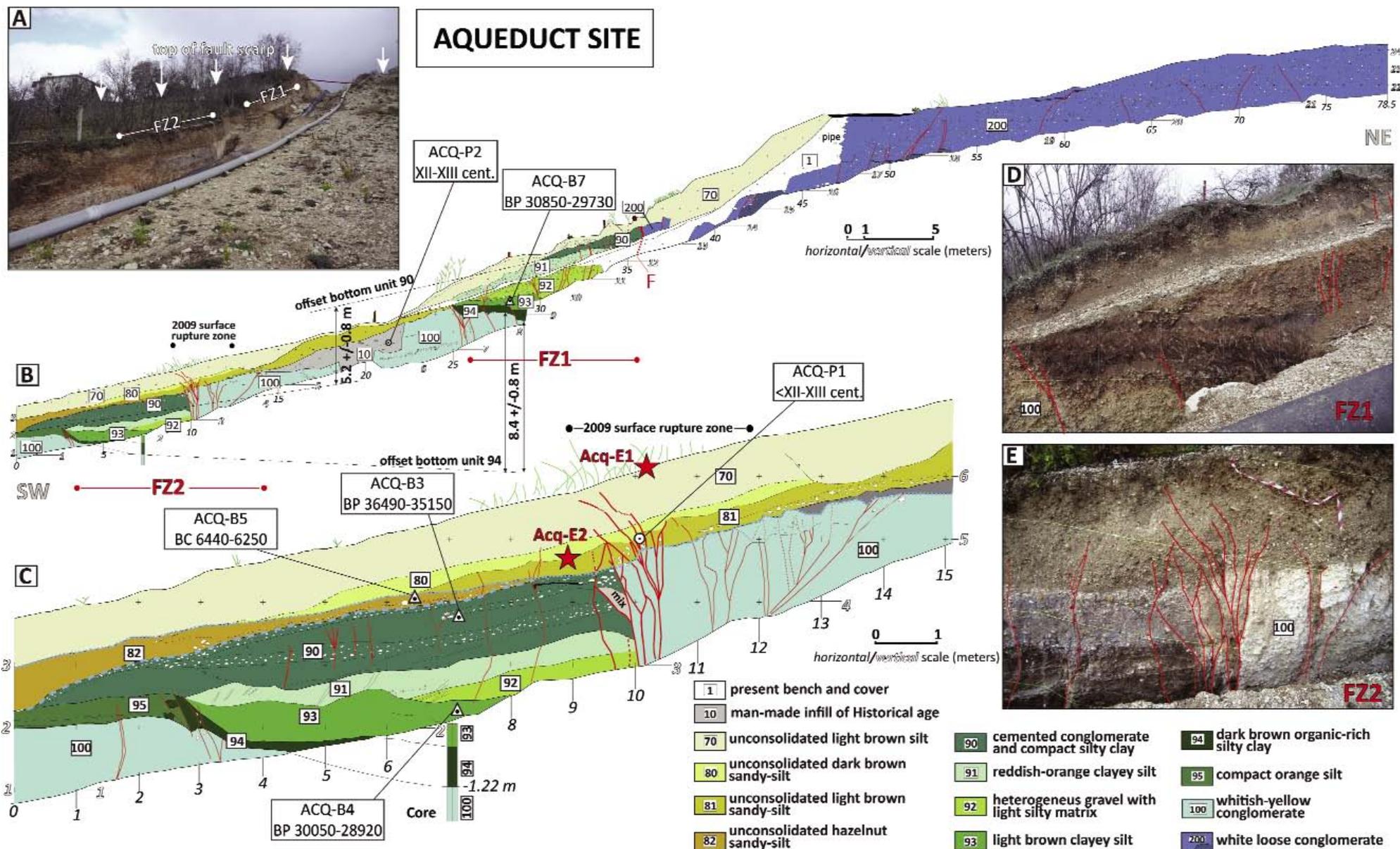
AQUEDUCT SITE

Fig. 51 - Aqueduct site trench (after Cinti et al., 2011). **a)** excavation along the Paganica sector crossing the 20 m-high cumulative scarp. **b)** and **c)** detailed log of the NW wall of the trench; **d)** and **e)** view of the main fault zones. At this site, the 2009 ruptures occurred at the base of the scarp on the fields and tarmac road adjacent to the pipeline. In coincidence of fault zone 2 (FZ2) the 2009 ruptures produced diffuse deformation accompanied both by cracking and warping.

Fig. 52 - Location map and geology of Stop 2.3 (after Pucci et al., 2015).
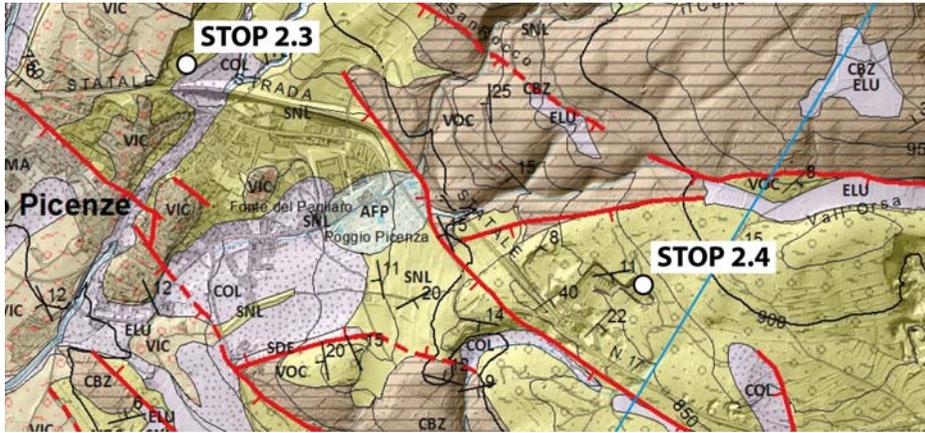
STOP 2.3 - Poggio Picenze - Early Pleistocene lacustrine deposits

This outcrop shows Early Pleistocene lacustrine deposits (limi di San Nicandro fm. - SNL), composed of laminated, whitish, fine-grained calcareous silts and sands with thin layers of clayey silts, containing at places small leaves fragments (Figs 52-54). This formation testifies the late stage of the middle Aterno basin opening when the depocenter probably reached its maximum depth. The formation has a maximum thickness > 100 m. In the more proximal facies it shows sparse gravelly intercalations due to the progradation of the fan-delta deposits (Stop 2.4).

67

Fig. 53 - outcrop of lacustrine deposits. The considerable dip of the bedding (~20° to the W) is mostly due to tectonic tilting.
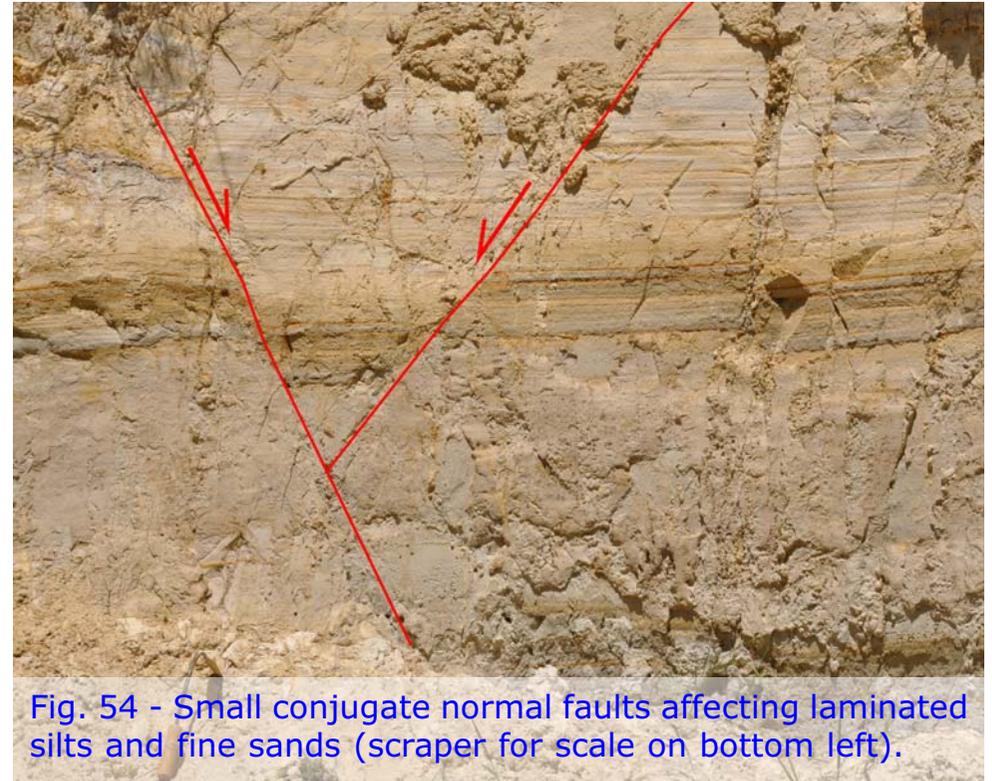
Fig. 54 - Small conjugate normal faults affecting laminated silts and fine sands (scraper for scale on bottom left).

itinerary
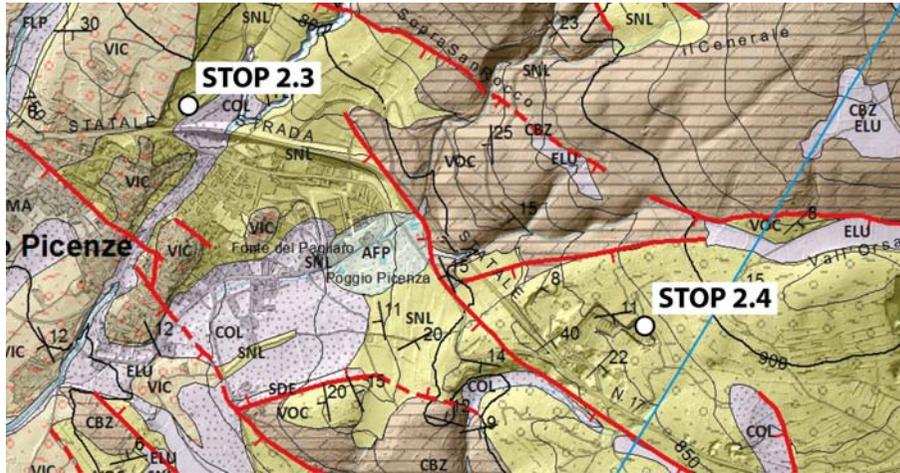
STOP 2.4 - Le Macchie - Early Pleistocene Gilbert fan delta conglomerates

This outcrop shows the Vall'Orsa fm. (VOC), which consists of Early Pleistocene thick and polygenic beds of carbonatic conglomerates with sandy matrix mixed with sparse, thin and whitish clayey-silt layers (Fig. 55). Clinoforms, cross-bedding and pinch-out structures are visible, together with some sets of conjugate normal faults (Figs 56, 57). This formation overlies the limi di San Nicandro fm. (SNL). The general dip to the SE of the foresets testifies the progradation of a huge fan-delta system and a consistent drainage flow towards an early south-eastern depocenter in the middle Aterno basin.

Fig. 55 - Location map and geology of Stop 2.4 (after Pucci et al., 2015).

Fig. 56 - Carbonatic conglomerates showing foreset beds related to a Gilbert fan delta. This unit is partially heteropic with the Limi di San Nicandro Fm.
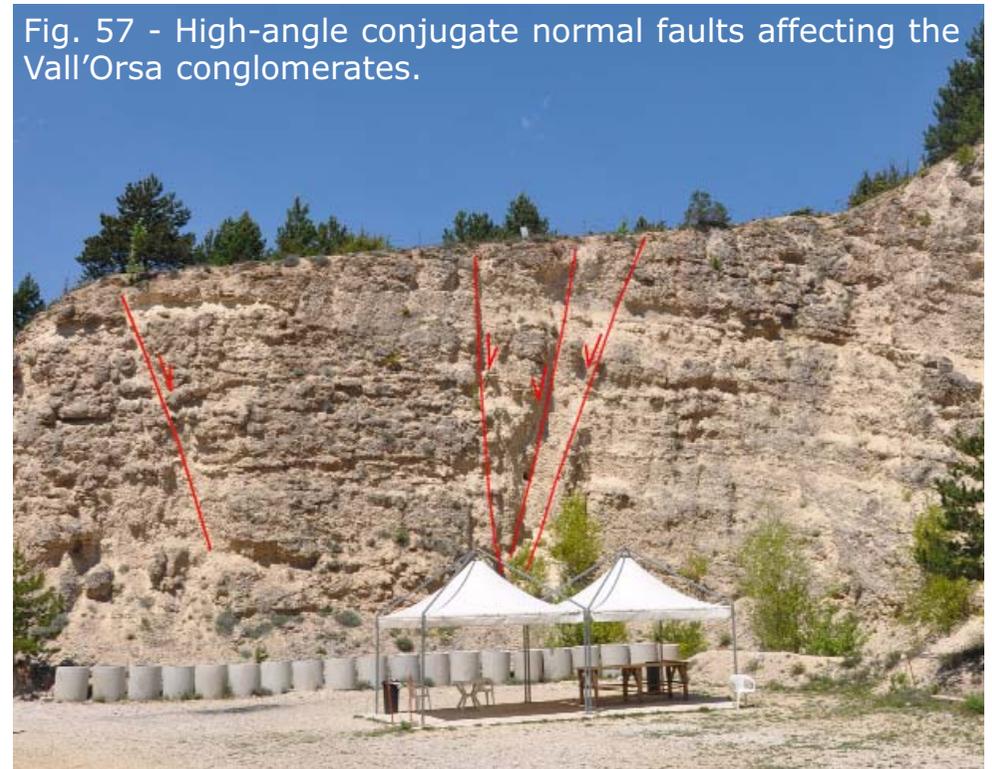
Fig. 57 - High-angle conjugate normal faults affecting the Vall'Orsa conglomerates.

Quaternary geology and paleoseismology in the Fucino and L'Aquila basins

S. Amoroso-F. Bernardini-A.M. Blumetti-R. Civico-C. Doglioni-F. Galadini-P. Galli-L. Graziani-L. Guerrieri-P. Messina-A.M. Michetti-F. Potenza-S. Pucci-G. Roberts-L. Serva-A. Smedile-L. Smeraglia-A. Tertulliani-G. Tironi-F. Villani-E. Vittori

STOP 2.5 - Valle dell'Inferno - The syntectonic deposition and drainage evolution
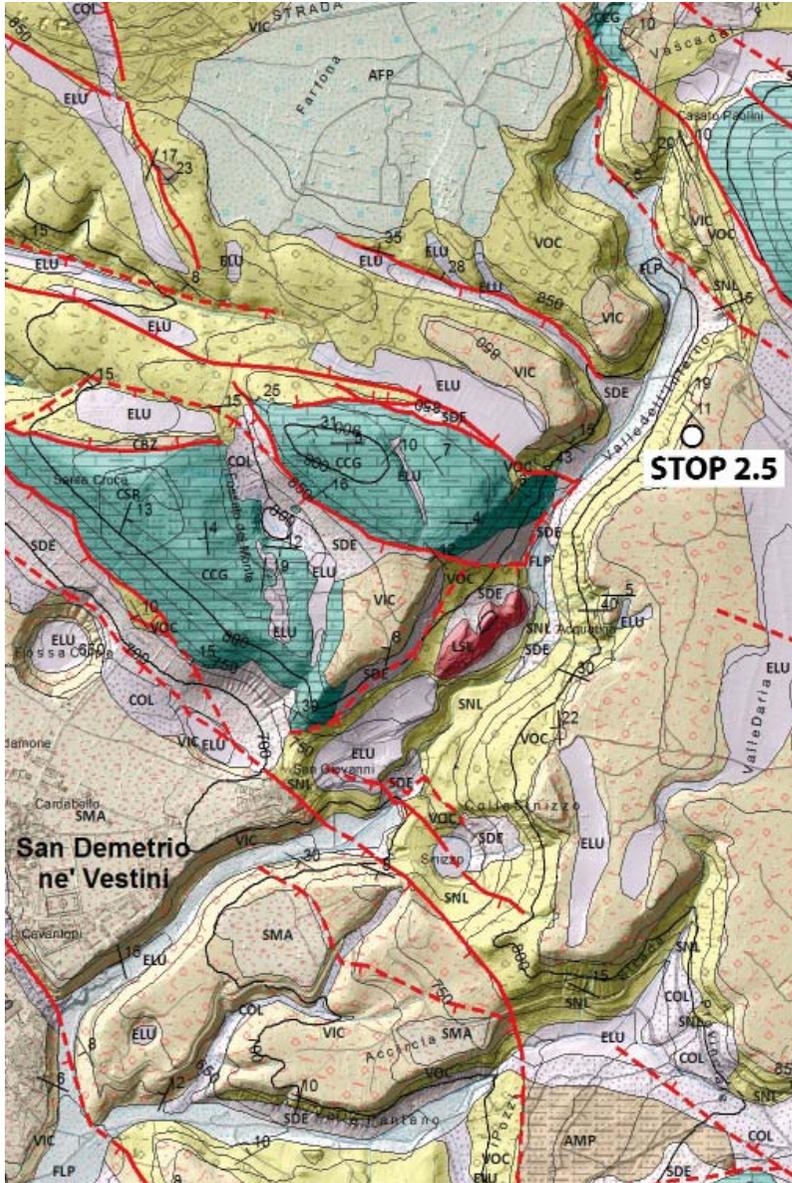
This Stop is a panoramic view of the Valle dell'Inferno showing the relationship between normal faults, continental deposits and drainage evolution (Fig. 58).

Here a fault scarp truncates two wide surfaces: a higher erosional surface carved on Cretaceous limestones and a lower depositional surface corresponding to the top of the Early Pleistocene alluvial fan conglomerate succession (Vall'Orsa fm. - VOC). This fault belongs to an E-trending system that acted mostly during Early Pleistocene times and was lately deactivated by the more recent NW-trending faults of the PSDFS. This kinematic change is testified by the Valle dell'Inferno gorge, which denotes a dramatic reorganization of the river network, with a new SW-flowing drainage, completely different from the Early Pleistocene SE-flowing one (Fig. 59).

69

itinerary
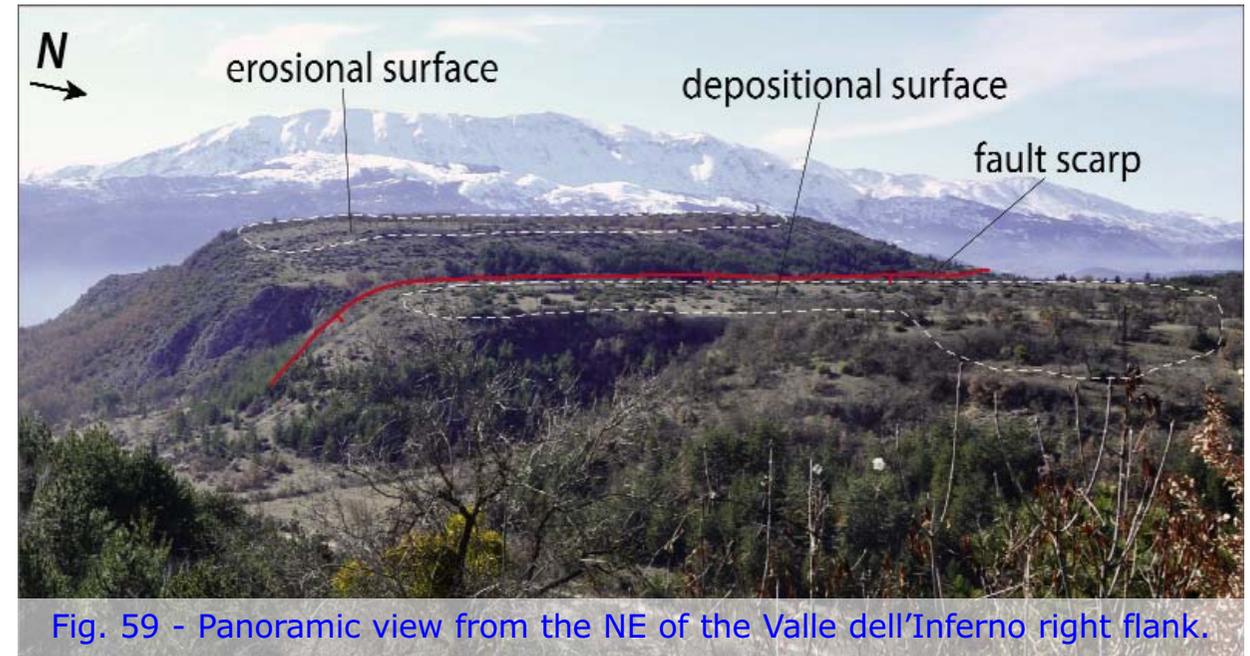
Fig. 58 - Geological map of the Valle Inferno area (after Pucci et al., 2015).

Fig. 59 - Panoramic view from the NE of the Valle dell'Inferno right flank.

Fig. 60 - View to the west showing details of the Valle dell'Inferno right flank with the top of the Early Pleistocene conglomerate succession (Vall'Orsa fm.) abutting against the N-dipping normal fault in Cretaceous limestones

Along the Valle dell'Inferno is visible the close alternance of synthetic and anthitetic fault splays, with the SW-dipping ones accommodating most of the displacement, that influence the thickness of the Quaternary depocenters (Figs 60 and 61).

Fig. 61 - Simplified NE-trending geological section showing the main Quaternary fault pattern and the continental depositional units (yellow, pale green and blue) over the undifferenitated carbonate pre-Quaternary bedrock (dark green) (after Pucci et al., 2015). The black rectangle encloses the area shown in Fig. 60. Trace location in Fig. 15.

Middle-Late Pleistocene fluvial deposits

Early Pleistocene alluvial fan deposits

Early Pleistocene fluvio-lacustrine deposits

Fig. 60

Pre-Quaternary Bedrock
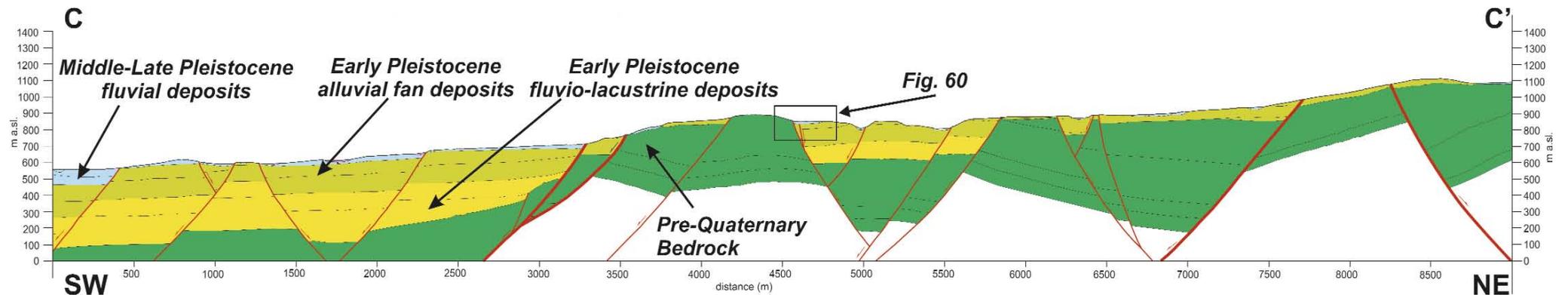
STOP 2.6 - South L'Aquila

In South L'Aquila, several RC buildings collapsed or suffered severe damage due to the main shock causing several tens of victims. Post-earthquake forensic surveys report that 135 victims were concentrated in the collapse of 11 buildings located in this area (i.e. about 44% of the total number of casualties). The huge concentration of damage within this area created speculation for both poor design and construction techniques, also related to inadequate evaluation of the seismic action provided by the Italian building code in use at the time of their construction. Indeed, the local subsoil condition is very complex and can cause significant amplification effects. In the area site effects can be related to: lithostratigraphic amplification due fine-grained soils ("terre rosse") interposed within, or placed above, the coarse-grained breccias ("brecce dell'Aquila"); man-made fills; underground caves; topographic effects (Milana et al., 2011; Tertulliani et al., 2012; Totani et al., 2012; Amoroso et al., 2014; 2015). In particular, underground caves, locally well known and commonly recognized in the "brecce dell'Aquila", are more frequent than in other parts of the city centre. Fig. 62a shows the location of the site investigations, underground caves and RC buildings collapsed due to the 2009 earthquake, within the area of the
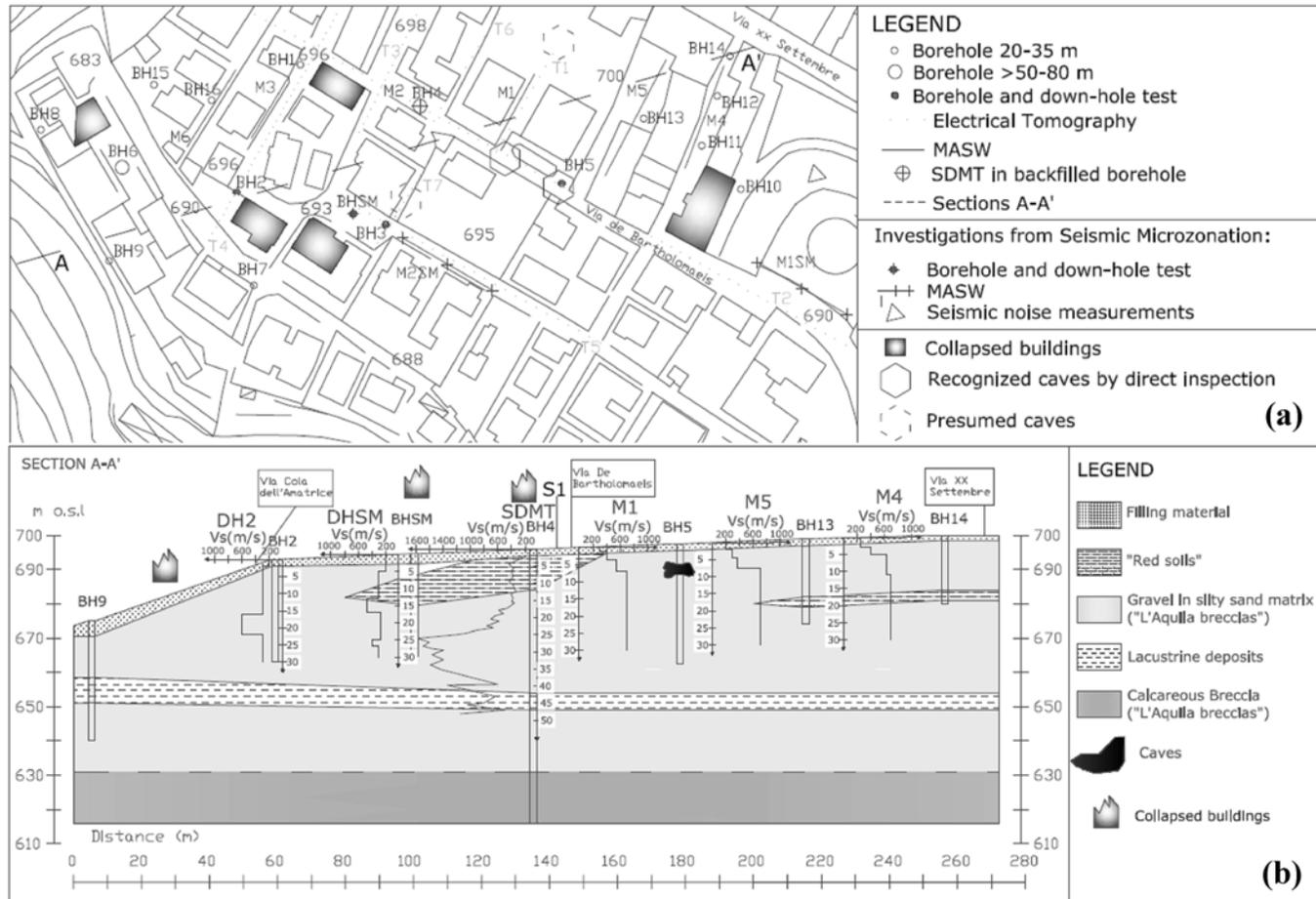
Fig. 62 - **a)** Location of site investigations in the area under study; **b)** Stratigraphic cross sections and V_s profiles from down-hole, surface wave and seismic dilatometer test (Amoroso et al., 2015).

field trip. In addition, Fig. 62a includes the line of the section named "A-A'", while Fig. 62b shows the topographic and stratigraphic profile of this cross section and the shear wave velocity V_S values of the subsoil layers. The upper portion of the subsoil is constituted by the "brecce dell'Aquila", with shear wave velocity V_S ≈ 600-1000 m/s or higher. The breccias are superimposed to lacustrine deposits, with V_S in the 400-700 m/s range, and laying on the bedrock. The upper portion of the subsoil is irregularly affected by peculiar local conditions (Fig. 62b): underground caves, "terre rosse" with V_S ≈ 400 m/s, man-made fills of maximum thickness ≈ 8-10 m with lower V_S (≈ 200-300 m/s). Examples of collapsed buildings are shown in Figs 63 and 64. Figs 65 and 66 shows two caves, located respectively in Via Campo di Fossa and Via De Bartholomaeis, that originated impressive sinkholes during the April 6, 2009 main shock. In this respect many geological, geophysical and geotechnical investigations were performed, and still ongoing, related to Seismic Microzonation studies and research activities and for supporting the reconstruction planning (Amoroso et al., 2014; 2015; Totani et al., 2012).

Fig. 63 - Example of RC building suffered severe damage in Via Cola dell'Amatrice during the April 6, 2009 main shock.

Fig. 64 - Example of RC building collapsed in Via Campo di Fossa during the April 6, 2009 main shock.

Fig. 65 - Example of cave originated in Via Campo di Fossa during the April 6, 2009 main shock.

Fig. 66 - Example of cave (areal extension ≈ 60 m originated with a maximum depth of 14 m) in Via De Bartholomaeis during the April 6, 2009 main shock (MS–AQ Working Group, 2010).

STOP 2.7 - Piazza Duomo

Piazza Duomo, is the biggest square of the city and the market place since 1303. The square has always represented the cultural centre of the city. The top surface of the bedrock in Piazza Duomo is located below 300 m depth, as shown in the 300 m deep borehole of Fig. 67.

The **Cathedral of Santi Massimo e Giorgio** was built in 1257 and repeatedly restored during times for damage causeed by earthquakes. Historical chronicles report that this church, reconstructed after the 1315 earthquake, totally collapsed during the destructive 1703 event. Also the 1915 damaged this church. During the 2009 earthquake the cathedral was severely damaged. In particular, the transept and part of the apse collapsed, and the vaulted ceiling was severely damaged.

itinerary

717 m a.s.l.

g.l.

3 m

8 m

FILL MATERIAL

RESIDUAL SOIL: CLAYEY SILT

CALCAREOUS BRECCIA

80 m

LACUSTRINE DEPOSITS: SILTY SAND AND CLAYEY-SANDY SILT
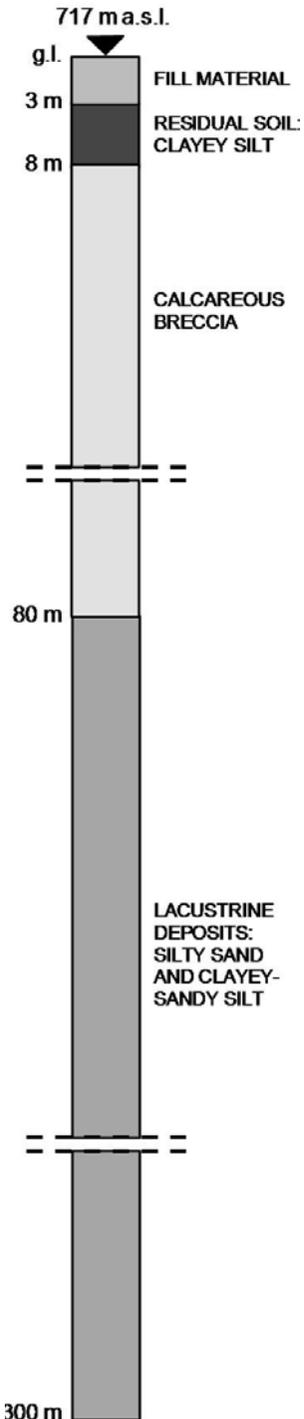
300 m

Fig. 67 - On the left a stratigraphic column reconstructed from a 300 m deep core-destructive borehole executed in Piazza Duomo, L'Aquila (Monaco et al., 2013, after Amoroso et al., 2010): the top surface of the bedrock in the city centre is located below 300 m depth. The upper portion of the subsoil, 80 m thick, is constituted by "brecce dell'Aquila" fine to coarse calcareous fragments of variable size (mostly of some centimetres) embedded in sandy or silty matrix, characterized by highly variable cementation and mechanical properties. Fine-grained residual soils, locally known as "terre rosse", are encountered in the upper 8 m, at the top of the breccias. The breccias are superimposed to fine-to medium-grained, mostly silty lacustrine deposits, more than 220 m thick.

The **S. Maria del Suffragio** church (better known as Anime Sante Church – Fig. 68) was starting to be built soon after the 1703 earthquake in place of a small church that was destroyed by the earthquake. The church was severely damaged by the 2009 earthquake, in particular the superb dome (attributed to G. Valadier), the lantern and the spires collapsed. The transept and roofing were in danger of collapse.

Fig. 68 - S. Maria del Suffragio church after L'Aquila earthquake.

74

itinerary

Quaternary geology and paleoseismology in the Fucino and L'Aquila basins
S. Amoroso-F. Bernardini-A.M. Blumetti-R. Civico-C. Doglioni-F. Galadini-P. Galli-L. Graziani-L. Guerrieri-P. Messina-A.M. Michetti-F. Potenza-S. Pucci-G. Roberts-L. Serva-A. Smedile-L. Smeraglia-A. Tertulliani-G. Tironi-F. Villani-E. Vittori

STOP 2.8 - Piazza Palazzo

This square has always represented the political centre of the city due to the presence of Palazzo Margherita (Fig. 69), seat of the municipality until the 6th April 2009. The Palace was built in 1294 for the establishment of the "Capitano" seat, the main local representative of the royal authority during the Middle Age. In 1572-1577 the Palace was deeply restored to become the set of Abruzzi Government held by Queen Margherita d'Austria, that gave the name to the building. The 1703 earthquake caused severe damage to Palazzo Margherita, as testified by the historical documentation on its restoration. In particular, the height of the tower, originally ≈ 70 m, was reduced as a consequence of the 1703 earthquake, and then modified in the upper part (Colapietra et al. 1997, Dander & Moretti 1974).

Fig. 69 - Upper panel: Palazzo Margherita after the 2009 earthquake. Lower panel: glimpse of the square.
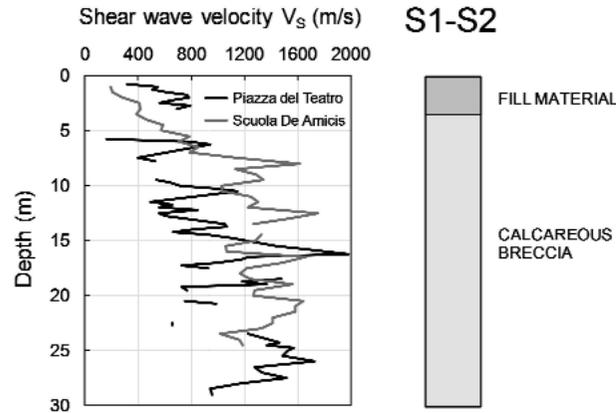
Fig. 70 - Profiles of shear wave velocity V_s measured by seismic dilatometer tests (SDMT) in 2 backfilled boreholes and stratigraphic column at the site of Palazzo Margherita, L'Aquila (Monaco et al., 2013). The upper portion of the subsoil belongs to the "brecce dell'Aquila" formation (V_s ≈ 600-1000 m/s or higher), and corresponds roughly to the upper 80 m deep. The dispersion of the V_s possibly reflects some variability in grain size, cementation and/or mechanical properties. Lower values (V_s ≈ 200-300 m/s) are found in shallow fill materials (0-2 m deep).

Fig. 71 - Particular of the Biblioteca Tommasi. The building was very severely damaged: the main facade was in danger of collapsing.

Quaternary geology and paleoseismology in the Fucino and L'Aquila basins

S. Amoroso-F. Bernardini-A.M. Blumetti-R. Civico-C. Doglioni-F. Galadini-P. Galli-L. Graziani-L. Guerrieri-P. Messina-A.M. Michetti-F. Potenza-S. Pucci-G. Roberts-L. Serva-A. Smedile-L. Smeraglia-A. Tertulliani-G. Tironi-F. Villani-E. Vittori

STOP 2.9 - Via San Bernardino

San Bernardino cathedral is one of the most important monument of L'Aquila. The church was built in XV century and the superb façade dates back to the first half of XVI century. The 1461 earthquake damaged the dome of the cathedral recently built. During the 1703 earthquake the cathedral collapsed almost entirely excluding the façade.

De Amicis primary school, strongly damaged by the 2009 earthquake, was one of the main school in the city centre until the 6th April 2009. It was built during the XV century for the establishment of San Salvatore Hospital and was damaged by the 1461 and the 1703 earthquakes. In 1875 the building became a military infirmary and finally in 1909 it turned in a school (Centofanti et al., 1992).

Fig. 72 - San Bernardino cathedral: the 2009 earthquake severely damaged the church especially the upper part of the bell tower that collapsed.
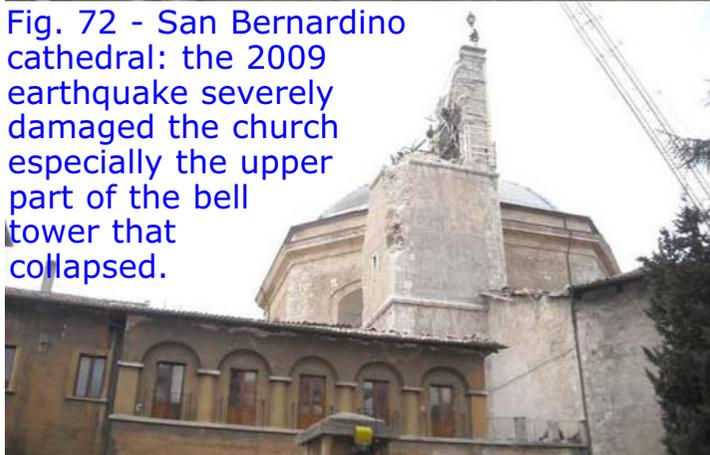
Fig. 73 - Scuola De Amicis after L'Aquila earthquake.
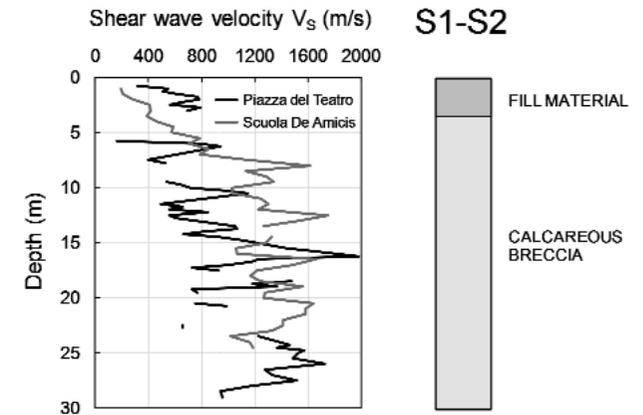
Fig. 74 - Profiles of V_s seismic dilatometer tests (SDMT) measured in 2 backfilled boreholes and schematic soil profile at the site of Piazza del Teatro - Scuola De Amicis (Monaco et al., 2013). The upper portion of the subsoil belongs to the "brecce dell'Aquila" formation, and corresponds roughly to the upper 80 m deep. The V_s measured in the breccias are mostly ≈ 600-1000 m/s or higher, generally increasing with depth. Lower values (V_s ≈ 200-300 m/s) have been locally measured in shallow fill materials (0-4 m deep).

Fig. 75 - Reconstruction of the wall completely collapsed in a room on the main floor.

STOP 2.10 - Palazzo Ardinghelli

Palazzo Ardinghelli is located in the heart of the historical center of L'Aquila. The building is on two main levels. The ground floor is dominated by the presence of passing entrance hall with the stairs on the left, and by a colonnaded courtyard. This floor reveals the various building phases that led its realization.

Conversely, the main floor, at least in the body facing the square, was completely rebuilt after the earthquake of 1703, with the creation of large vaulted halls and the insertion of a small chapel surmounted by a dome. Together with the facade, the courtyard is the element that characterizes the building. Its exedra termination differentiates it from almost all of the buildings in L'Aquila and gives coherence to the architectural complex. Under the

Fig. 76 - Main workings during the repair and consolidation of the damaged and collapsed masonry vaults.

Fig. 77 - Reconstruction of the wooden roofs conserving the original configuration.

stylistic unity provided to the palace by the eighteenth-century intervention, it is hidden an intense layering readable through the structure and character building of the factory.

The intervention is based on the traditional restoration principles and it is aimed to the restoration of the damage caused by the 2009 earthquake, to the seismic improvement and to the re-use of the building. The goal of the project is to equip the building with a structural plant that makes the Palace able to effectively respond to the seismic action. Moreover, it is provided the restoration of surfaces and decorations, finishing works and the building installations necessary for its future reuse. The earthquake damage was repaired with mixing traditional techniques and modern technologies. The damaged masonry vaults have been repaired and consolidated while the collapsed ones have been rebuilt with similar technology. The connections between walls have been realized with a systematic shackling at the height of the ceilings. A bead reinforced masonry has been realized on top of the walls, giving a better connection between the walls and the elements of the cover. The insertion of artificial diatones improved the textures masonry. The roofs were reconstructed with wooden warping, substantially preserving the original plant but regularizing the mesh of the main elements.

Quaternary geology and paleoseismology in the Fucino and L'Aquila basins

S. Amoroso-F. Bernardini-A.M. Blumetti-R. Civico-C. Doglioni-F. Galadini-P. Galli-L. Graziani-L. Guerrieri-P. Messina-A.M. Michetti-F. Potenza-S. Pucci-G. Roberts-L. Serva-A. Smedile-L. Smeraglia-A. Tertulliani-G. Tironi-F. Villani-E. Vittori

STOP 2.11 - Castello Cinquecentesco

This massive building is also known as Spanish Fortress. Located in the highest part of the city, was started to be built in 1534 under the Spanish domination. The fortress has a square plan with four massive bastions at the corners. The castle is surrounded by a moat that was not supposed to be filled with water. Historical accounts revealed that the castle was damaged during the 1703 and 1762 earthquakes.

The 2009 earthquake caused the partial collapse of the upper part of the walls and the roof, large and extensive cracks in the walls of the building. The historic and artistic heritage of the Museo Nazionale d'Abruzzo, inside the castle, were seriously damaged, as well as the offices of the INGV seated in the upper level of the castle.

Fig. 78 - Castello Cinquecentesco after the 2009 L'Aquila earthquake.

Fig. 79 - Castello Cinquecentesco after the 2009 L'Aquila earthquake.

References

Allen J., Brandte U., Brauer A., Hubbertens H-W., Huntley B., Keller J., Kraml M., Mackensen A., Mingram J., Negendank J., Nowaczyk N., Oberhansli H., Watts W., Wulf S. & Zolitschka B. (1999) - Rapid environmental changes in southern Europe during the last glacial period. Nature, 400, 740-743.

Amoroso S., Del Monaco F., Di Eusebio F., Monaco P., Taddei B., Tallini M., Totani F. & Totani G. (2010) - Campagna di indagini geologiche, geotecniche e geofisiche per lo studio della risposta sismica locale della città dell'Aquila: la stratigrafia dei sondaggi giugno-agosto 2010. Report CERFIS 1/10. University of L'Aquila. www.cerfis.it/en/download/cat_view/67-pubblicazioni-cerfis/68-reports.html (in Italian).

Amoroso S., Di Naccio D., Di Giulio G., Vassallo M. & Milana G. (2014) - Site effects along the southern flank of the L'Aquila terrace. Proceedings of 32nd Conference Gruppo Nazionale di Geofisica della Terra Solida (GNGTS), 25-27 November 2014, Bologna (Italy), Vol. 2, 122-128, ISBN: 978-88-940442-2-5 (volume), ISBN : 978-88-940442-0-1 (raccolta).

Amoroso S., Totani F., Totani G. & Monaco, P. (2015) - Local seismic response in the Southern part of the historic centre of L'Aquila. Engineering Geology for Society and Territory - Urban Geology, Sustainable Planning and Landscape Exploitation, Springer International Publishing, Vol. 5, Part XVIII, 1097-1100, DOI 10.1007/978-3-319-09048-1_208, Print ISBN 978-3-319-09047-4, Online ISBN 978-3-319-09048-1.

Balasco M.P. Galli A., Giocoli E., Gueguen V., Lapenna A., Perrone S., Piscitelli E., Rizzo G., Romano A., Siniscalchi & Votta M. (2011) - Deep geophysical electromagnetic section across the middle Aterno Valley (central Italy): preliminary results after the April 6, 2009 L'Aquila earthquake. Boll. Geofis. Teor. Appl., doi: 10.4430/bgta0028.

Bally A.W., Burbi L., Cooper C. & Ghelardoni R. (1986) - Balanced sections and seismic reflection profiles across the Central Italy. Mem. Soc. Geol. Ital., 35, 257–310.

Beneo E. (1939) - Le terrazze quaternarie della regione fucense ed i loro rapporti con i fenomeni orogenetici nella Marsica (Appennino abruzzese). Boll. Soc. Geol. It., 58, 77-104.

Bertini T. & Bosi C. (1993) - La tettonica quaternaria della conca di Fossa (L'Aquila). Il Quaternario, 6, 293-314.

Blumetti A.M., Dramis F. & Michetti A.M. (1993) - Fault-generated moun-tain fronts in Central Apennines (Central Italy); geomorphological features and seismotectonic implications. Earth Surface Processes and Landforms, 18, 203-223.

Blumetti A.M., Coltorti M., Ferreli L., Michetti A.M., Petronio C., Raffy J. & Sardella R. (1997) - Fucino Basin. In: B. Gentili & F. Dramis, Eds., "Geomorphology and Quaternary evolution of central Italy", Guide for the excursion, IV Int. Conf. on Geomorphology, Italy 1997, Supplementi di Geografia Fisica e Dinamica Quaternaria, suppl. III, 2, 1997, 79-103.

Blumetti A.M., Guerrieri L. & Vittori E. (2013) - The primary role of the Paganica–San Demetrio fault system in the seismic landscape of the Middle Aterno Valley basin (Central Apennines). Quat. Int., 288, 183–194. Doi: 10.1016/j.quaint.2012.04.040.

Blumetti A.M., Di Manna P., Vittori E., Comerci V. & Guerrieri L. (2015) - Paleoseismicity data on the San Demetrio ne' Vestini fault (L'Aquila Basin, Central Italy). Abstracts Volume 6th International INQUA Meeting on Paleoseismology, Active Tectonics and Archaeoseismology 19 - 24 April 2015, Pescina, Fucino Basin, Italy (Blumetti A.M., Cinti F.R., De Martini P.M., Galadini F., Guerrieri L., Michetti A.M., Pantosti D., Vittori E. Eds.), Miscellanea INGV, 27, 511-513, ISSN: 2039-6651.

Boccaletti M., Ciaranfi N., Cosentino D., Deiana D., Gelati R., Lentini F., Massari F., Moratti G., Pescatore T., Ricci Lucchi F., Tortorici L. (1990) - Palinspastic restoration and paleogeographic reconstruction of the peri-Tyrrhenian area during the Neogene. Paleogeogr. Paleoclimatol. Paleoecol., 77, 42–50. Doi: 10.1016/0031-0182(90)90097-Q

Boncio P., Pizzi A., Brozzetti F., Pomposo G., Lavecchia G., Di Naccio D. & Ferrarini F. (2010) - Coseismic ground deformation of the 6 April 2009 L'Aquila earthquake (Central Italy, Mw 6.3). Geophys. Res. Lett., 37, L06308. http://dx.doi.org/10. 1029/2010GL042807.

Bosi C., Galadini, F. & Messina, P. (1995) - Stratigrafia Plio-Pleistocenica della Conca del Fucino. Il Quaternario 8 (1). 83-94.

Bosi C., Galadini, F., Giaccio B., Messina P. & Sposato A. (2003) - Plio-Quaternary continental deposits in the Latium-Abruzzi Apennines: The correlation of geological events across different intermountane basins. Il Quaternario 16 (1bis), 55-76.

Bosi C. & Messina P. (1991) - Ipotesi di correlazione fra successioni morfolitostratigrafiche pliopleistoceniche nell'Appennino laziale-abruzzese. Studi Geol. Camerti, 1991, 257-263.

Carminati E. & Doglioni C. (2005) - Mediterranean Geodynamics: Encyclopedia of Geology. Elsevier, 135-146.

Carminati E., Corda L., Mariotti G. & Brandano M. (2007) - Tectonic control on the architecture of a Miocene carbonate ramp in the Central Apennines (Italy): Insights from facies and backstripping analyses. Sediment. Geol., 198, 233–253.

Carminati E., Lustrino M., Cuffaro M. & Doglioni, C. (2010) - Tectonics, magmatism and geodynamics of Italy: What we know and what we imagine. In: (Eds.) M. Beltrando, A. Peccerillo, M. Mattei, S. Conticelli & C. Doglioni, The Geology of Italy, Journal of the Virtual Explorer, Electronic Edition, ISSN 1441-8142, Vol. 36, paper 8, 2010.

Carminati E., Lustrino M. & Doglioni C. (2012) - Geodynamic evolution of the central and western mediterranean: Tectonics vs. igneous petrology constraints. Tectonophysics, 579, 173–192. Doi:10.1016/j.tecto.2012.01.026.

Cavinato G.P., Cosentino D., De Rita D., Funiciello R. & Parotto M. (1994) - Tectonic sedimentary evolution of intrapenninic basins and correlation with the volcanotectonic activity in Central Italy. Mem. Descr. Carta. Geol. d'It. 49, 63-76.

Cavinato G.P. & De Celles P. G. (1999) - Extensional basins in the tectonically bimodal central Apennines fold-thrust belt, Italy: Response to corner flow above a subducting slab in retrograde motion, Geology, 27, 955–958.

Cavinato G.P., Carusi C., Dall'Asta M., Miccadei E. & Piacentini T. (2002) - Sedimentary and tectonic evolution of Pio-Pleistocene lacustrine deposits of Fucino Basin (Central Italy). Sedimentary Geology 148, 29-59.

Cavinato G.P., Carusi C., Dall'Asta M., Miccadei E. & Piacentini, T. (2002) - Sedimentary and tectonic evolution of Plio-Pleistocene alluvial and lacustrine deposits of the Fucino Basin (central Italy). Sedimentary Geology 148, 29–59.

Centofanti M. (1984) – L'Aquila 1753 – 1983. Il restauro della città. Edizioni Libreria Colacchi, L'Aquila.

Centofanti M., Colapietra R., Conforti C., Properzi P. & Zordan L. (1992) – L'Aquila città di Piazze. CARSA Edizioni.

Chiarabba C., Amato A., Anselmi M., Baccheschi P., Bianchi I., Cattaneo M., Cecere G., Chiaraluce L., Ciaccio M.G., De Gori P., De Luca G., Di Bona M., Di Stefano R., Faenza L., Govoni A., Improta L., Lucente F.P., Marchetti A., Margheriti L., Mele F., Michelini A., Monachesi G., Moretti M., Pastori M., Piana Agostinetti N., Piccinini D., Roselli P., Seccia D. & Valoroso L. (2009) - The 2009 L'Aquila (central Italy) Mw 6.3 earthquake: main shock and aftershocks. *Geophys. Res. Lett.*, 36, L18308. Doi: 10.1029/2009GL039627

Chiaraluce L. (2012) - Unraveling the complexity of Apenninic extensional fault systems: a review of the 2009 L'Aquila earthquake (central Apennines, Italy). J. Struct. Geol., 42, 2–18. http://dx.doi.org/10.1016/j.jsg.2012.06.007.

Cinti F.R., Faenza L., Marzocchi W. and Montone P. (2004) - Probability map of the next M 5.5 earthquakes in Italy, Geochem. Geophys. Geosyst., 5, Q11003, doi:10.1029/2004GC000724.

Cinti F.R., Pantosti D., De Martini P.M., Pucci S., Civico R., Pierdominici S., Cucci L., Brunori C.A., Pinzi S. and Patera A. (2011) - Evidence for surface faulting events along the Paganica fault prior to the 6 April 2009 L'Aquila Earthquake Central Italy. J. Geophys. Res., 116, B07308. http://dx.doi.org/10.1029/2010jb007988.

Cipollari P. and Cosentino D. (1991) - La linea Olevano-Antrodoco: Contributo della biostratigrafia alla sua caratterizzazione cinematica. In: Studi Preliminari All'acquisizione Dati del Profilo CROP 11 Civitavecchia-Vasto, Stud. Geol. Camerti, Spec., vol. 1991/2, edited by M. Tozzi, G.P. Cavinato & M. Parotto, 143–149, Camerino, Italy.

Cipollari P., Cosentino D. and Parotto M. (1995) - Modello Cinematico-Strutturale dell'Italia Centrale, Stud. Geol. Camerti, Spec., vol. 1995/2, pp. 135–143, Camerino, Italy.

Civico R., Pucci S., Pantosti D. and De Martini P.M. (2015). Morphotectonic analysis of the long-term surface expression of the 2009 L'Aquila earthquake fault (Central Italy) using airborne LiDAR data. Tectonophysics, 644-645, 108-121, .

Civitelli G. and M. Brandano (2005) - Atlante delle litofacies e modello deposizionale dei Calcari a Briozoi e Litotamni nella piattaforma carbonatica Laziale-Abruzzese. Boll. Soc. Geol. Ital., 124, 611–643.

Clementi A. and Piroddi E. (1986). L'Aquila, Laterza, Bari, Italy, 214 pp.

Colapietra R. (1978) - L'Aquila dell'Antinori. Strutture sociali ed urbane della città nel Sei e Settecento, Antinoriana III: Studi per il bicentenario della morte di A.L. Antinori, L'Aquila. Nella Sede della Deputazione, Rome, Italy, 66–72.

Colapietra R., Centofanti M., Bartolomucci C. and Amedoro T. (1997) – L'Aquila: i Palazzi – Ediarte, L'Aquila.

Cosentino D., Cipollari P., Marsili P. and Scrocca D. (2010) - Geology of the Central Apennines: A regional review. J. Virtual Explor., 36, paper 12. doi:10.3809/jvirtex.2010.00223.

Critelli S., La Pera E., Galluzzo F., Milli S., Moscatelli M., Perrotta S. & Santantonio M. (2007) - Interpreting siliciclastic-carbonate detritalmodes in foreland basin system: An example from Upper Miocene arenites of the central Apennines, Italy. Geol. Soc. Am. Spec. Pap., 420, 107–133.

Dander M. & Moretti M. (1974) – Architettura civile Aquilana. Dal XIV al XIX secolo. Japadre Editore, L'Aquila.

De Matteis A. (1973) - L'Aquila e il contado: demografia e fiscalità (secoli XV-XVIII). Giannini ed., Napoli.

Del Monaco F., Tallini M., De Rose C. & Durante F. (2013) - HVNSR survey in historical downtown L'Aquila (central Italy): site resonance properties vs. subsoil model. Engineering Geology, 158, 34-47. doi: 10.1016/j.enggeo.2013.03.008.

Demangeot J. (1965) - Géomorphologie des Abruzzes adriatiques. Cartographiques Mémoires et Documents, Centre Recherche et Documentation, Paris, France, 403 pp.

Di Luzio E., Mele G., Cavinato G.P., Tiberti M.M. & Parotto M. (2009). Deepening of the Adriatic Moho beneath the central Apennines (Italy) along the CROP 11 seismic profile: indications from geologic, seismologic and gravity data and tectonic implications. Earth & Planet. Sci. Letters, 280, 1-12.

Doglioni C. (1991) – A proposal of kinematic modellig for W-dipping subductions – Possible applications to the Tyrrhenian – Apennines system. Terra Nova, 3 (4), 423-434.

Doglioni C. & Flores G. (1995) – An introduction to the Italian Geology. Ed. Il Salice, Potenza, 1-95.

Doglioni C., Mongelli F. & Pialli G.P. (1998) – Boudinage of the Alpine Belt in the Apenninic Back-arc. Mem. Soc. Geol. It., 52, 457-468.

EMERGEO Working Group (2010) - Evidence for surface rupture associated with the Mw 6.3 L'Aquila earthquake sequence of April 2009 (Central Italy). Terra Nova, 22/1, 43–51, http://dx.doi.org/10.1111/j.1365-3121.2009.00915.x.

Falcucci E., Gori S., Peronace E., Fubelli G., Moro M., Saroli M., Giaccio B., Messina P., Naso G., Scardia G., Sposato A., Voltaggio M., Galli P. & Galadini F. (2009) - The Paganica Fault and surface coseismic ruptures caused by the 6 April 2009 earthquake (L'Aquila, Central Italy). Seismol. Res. Lett., 80/6, 940–950.

Faure Walker, J.P., Roberts G.P., Sammonds P. & Cowie P.A. (2010) - Comparison of earthquakes strains over 102 and 104 year timescales: insights into variability in the seismic cycle in the central Apennines, Italy. Journal of Geophysical Research, Vol. 115, B10418. doi:10.1029/2009JB006462.

Follieri M., Magri D., Sadori L. & Villa I.M. (1991) - Palinologia e datazione radiometrica 39Ar/40Ar di un sondaggio nella piana del Fucino (Abruzzo). Workshop evoluzione dei bacini neogenici e loro rapporti con il magmatismo Plio-Quaternario nell'area tosco-laziale. Pisa, 12-13 Giugno 1991, 90-92.

Frezzotti M. & Giraudi C. (1992) - Evoluzione geologica tardopleistocenica ed olocenica del conoide complesso della Valle Majelama (Massiccio del Velino - Abruzzo). Il Quaternario, 5 (1), 33-50.

Frezzotti M. & Giraudi C. (1995) - I depositi del Pleistocene superiore e dell'Olocene; evidenze di tettonica e di paleosismicità. In Serie di Studi e Ricerche, monografia sul "Lazio meridionale". Sintesi delle ricerche geologiche multidisciplinari dell'ENEA, Dipartimento Ambiente, Claudio Carrara Ed.

Galadini F., Galli P., Giraudi C. and Molin D. (1995) - Il terremoto del 1915 e la sismicità della piana del Fucino (Italia Centrale). Boll. Soc. Geol. It., 115.

Galadini F., Galli P. & Giraudi C. (1997a) - Geological investigations of Italian earthquakes: new paleoseismological data from the Fucino Plain (Central Italy). Journal of Geodynamics, 24, 87-103.

Galadini F., Galli P. & Giraudi C. (1997b) - Paleosismologia della Piana del Fucino (Italia Centrale), Il Quaternario, 10 (1), 1997, 27-64.

Galadini F. & Galli P. (1999) - The Holocene paleoearthquakes on the 1915 Avezzano earthquake faults (central Italy): Implications for active tectonics in Central Apennines. Tectonophysics, 308, 143-170.

Galli P., Giaccio B. & Messina P. (2010) - The 2009 Central Italy earthquake seen through 0.5 Myr-long tectonic history of the L'Aquila faults system. Quat. Sci. Rev., 29, 3768–3789, http://dx.doi.org/10.1016/j.quascirev.2010.08.018.

Galli P., Giaccio B., Messina P. & Peronace E. (2016) - Three magnitude 7 earthquakes on a single fault in central Italy in 1400 years, evidenced by new palaeoseismic results. Terra Nova.

Galli P., Giaccio B., Messina P., Peronace E. & Zuppi G.M. (2011) - Palaeoseismology of the L'Aquila faults (Central Italy, 2009, Mw 6.3 earthquake): implications for active fault linkage. Geophys. J. Int., 187/3, 1119-1134, http://dx.doi.org/10.1111/j.1365-246X.2011.05233.x.

Galli P., Messina P., Giaccio B., Peronace E. & Quadrio B. (2012) - Early Pleistocene to late Holocene activity of the Magnola fault (Fucino fault system, Central Italy). Bollettino di Geofisica Teorica ed Applicata, 53 (4), 435-458.

Galli P. & Molin D. (2014) - Beyond the damage threshold: the historic earthquakes of Rome. Bull. Earthquake Eng., 12, 1277-1306. Doi: 10.1007/s10518-012-9409-0.

Giaccio B., Galli P., Messina P., Peronace E., Scardia G., Sottili G., Sposato A., Chiarini E., Jicha B. & Silvestri S. (2012) - Fault and basin depocentre migration over the last 2 Ma in the L'Aquila 2009 earthquake region, central Italian Apennines. Quat. Sci. Rev., 56, 69–88, http://dx.doi.org/10.1016/j.quascirev.2012.08.016.

Giraudi C. (1988) - Evoluzione geologica della Piana del Fucino (Abruzzo) negli ultimi 30.000 anni. Il Quaternario 1(2), 131-159.

Giraudi C. (1995) - I detriti di versante ai margini della Piana del Fucino (Italia Centrale): significato paleoclimatico ed impatto antropico. Il Quaternario, 8 (1), 203-210.

Gori S., Dramis F., Galadini F. and Messina P. (2007) - The use of geomorphological markers in the footwall of active faults for kinematic evaluations: examples from the central Apennines. Boll. Soc. Geol. It., 126, 365-374.

Grunthal G. (Editor) (1998) - The European Macroseismic Scale EMS-98, Vol. 15, Conseil de l'Europe, Cahiers du Centre Europeén de Geodynamique et de Seismologie, Luxembourg, 101 pp.

Herrmann R.B., Malagnini L. & Munafò I. (2011) - Regional moment tensors of the 2009 L'Aquila earthquake sequence. Bulletin of the Seismological Society of America, 101/3, 975–993.

Improta L., Villani F., Bruno P.P., Castiello A., De Rosa D., Varriale F., Punzo M., Brunori C.A., Civico R., Pierdominici S., Berlusconi A. & Giacomuzzi G. (2012) - High-resolution controlled-source seismic tomography across the Middle Aterno basin in the epicentral area of the 2009, Mw 6.3, L'Aquila earthquake (central Apennines, Italy). Italian Journal of Geosciences, 131/3, 373-388.

Lavecchia G., Boncio P., Brozzetti F., De Nardis R., Di Naccio D., Ferrarini F., Pizzi A. & Pomposo G. (2010) - The April 2009 Aquila (Central Italy) seismic sequence (Mw 6.3): a preliminary seismotectonic picture. In: Guarnieri P. (Ed.), Recent Progress on Earthquake Geology. Nova Publishers, ISBN 978-1-60876- 47-0, pp. 1-17.

Lavecchia G., Brozzetti F., Barchi M., Menichetti M. & Keller Joao V. A. (1994) - seismotectonic zoning in east-central Italy deduced from an analysis of the Neogene to present deformations and related stress fields. Bull. Geol. Soc. America, 106, 9, 1107-1120.

Locati M., Camassi R. & Stucchi M. (eds) (2011) - DBMI11, the 2011 version of the Italian Macroseismic Database. Milano, Bologna. Accessed 18 Mar 2015.

Magri D. & Follieri M. (1989) - Primi risultati delle analisi polliniche dei sedimenti lacustri della piana del Fucino. Atti del Convegno di archeologia "Il Fucino e le aree limitrofe nell'antichità". Avezzano 10-11 Novembre 1989, 45-53.

Messina P. (1996) - Tettonica mesopleistocenica dei terrazzi nord-orientali del Fucino (Italia centrale). Il Quaternario, 9(1), 393-298.

Michetti A.M., Brunamonte F. Serva L. & Vittori E. (1996) - Trench investigations of the 1915 Fucino earthquake fault scarps (Abruzzo, Central Italy): Geological evidence of large historical events. Journal of Geophysical Research, 101 No. B3, 5921-5936.

Milana G., Azzara R.M., Bergamaschi F., Bertrand E., Bordoni P., Cara F., Cogliano R., Cultrera G., Di Giulio G., Duval A.M., Fodarella A., Marcucci S., Pucillo S., Régnier J. & Riccio G. (2011) - The contribution of seismic data in microzonation studies for downtown L'Aquila. Bull. Earthquake Eng. 9, 741-759. DOI 10.1007/s10518-011-9246-6.

Milli S. & Moscatelli S. (2000) - Facies analysis and physical stratigraphy of the Messinian turbiditic complex in the Valle del Salto and Val di Varri (central Apennines). Giornale di Geologia, 62, 57–77.

Monaco P., Totani G., Amoroso S., Totani F. & Marchetti D. (2013) - Site characterization by seismic dilatometer (SDMT) in the city of L'Aquila. Rivista Italiana di Geotecnica, Anno XLVII, n. 3, 8-22. ISSN 0557-1405. Pàtron Editore, Bologna, Italy.

Morewood N.C. & Roberts G.P. (2000) - The geometry, kinematics and rates of deformation within an en chelon normal fault segment boundary, central Italy. Journal of Structural Geology, 22, 1027–1047.

Quaternary geology and paleoseismology in the Fucino and L'Aquila basins

S. Amoroso-F. Bernardini-A.M. Blumetti-R. Civico-C. Doglioni-F. Galadini-P. Galli-L. Graziani-L. Guerrieri-P. Messina-A.M. Michetti-F. Potenza-S. Pucci-G. Roberts-L. Serva-A. Smedile-L. Smeraglia-A. Tertulliani-G. Tironi-F. Villani-E. Vittori

Moro M., Gori S., Falcucci E., Saroli M., Galadini F. & Salvi S. (2013) - Historical earthquakes and variable kinematic behaviour of the 2009 L'Aquila seismic event (Central Italy) causative fault, revealed by paleoseismological investigations. Tectonophysics, 583, 131–144. http://dx.doi.org/10.1016/j.tecto.2012.10.036.

Mostardini F. & Merlini S. (1988) - Appennino centro-meridionale: Sezioni geologiche e proposta di modello strutturale. Mem. Soc. Geol. It., 35, 177-202.

MS–AQ Working Group (2010) - Microzonazione sismica per la ricostruzione dell'area aquilana. Regione Abruzzo – Dip. Prot. Civile, L'Aquila, 3 vol. and CD-Rom, <www.protezionecivile.gov.it/jcms/en/view_pub.wp?contentId=PUB25330> (in Italian).

Narcisi B. (1993) - Segnalazione di un livello piroclastico di provenienza etnea nell'area del Fucino (Italia Centrale). Il Quaternario, 6, 87-92.

Narcisi B. (1994) - Caratteristiche e possibile provenienza di due livelli piroclastici nei sedimenti del Pleistocene superiore della piana del Fucino (Italia Centrale). Rend. Fis. Acc. Lincei, S. 9, 5(2), 115-123.

Nijman W. (1971) - Tectonics of the Velino-Sirente Area, Abruzzi, Central Italy: modification of compressional structures by subsequent dilatatation and collapse. Koninkl. Ned. Ak. Von Weten, S.B., 74, n. 2.

Oddone E. (1915) - Gli elementi fisici del grande terremoto marsicano-fucense del 13 gennaio 1915. Boll. Soc. Sism. It. 19, 71-216.

Palumbo L., Benedetti L., Bourlès D., Cinque A. & Finkel R. (2004) - Slip history of the Magnola fault (Apennines, Central Italy) from ^{36}Cl surface exposure dating: Evidence for strong earthquake over Holocene. Earth Planet. Sci. Lett., 225, 163-176.

Pantosti D., D'Addezio G. & F. Cinti (1996) - Paleoseismicity of the Ovindoli-Pezza fault, central Apennines, Italy: a history including a large, previously unrecorded earthquake in the Middle Ages (860-1300 A.D.). J. Geoph. Res. 101, 5937-5960.

Papanikolaou I., Roberts G. & Michetti A.M. (2005) - Fault scarps and deformation rates in Lazio–Abruzzo, Central Italy: comparison between geological fault slip-rate and GPS data. Tectonophysics, 408 (1-4), 147-176.

Patacca E. & Scandone P. (1989) - Post-Tortonian mountain building in the Apennines. The role of the passive sinking of a relic lithosphere slab, in The Lithosphere in Italy. Advances in Earth Science Research, edited by A. Boriani et al., pp. 157–176, Acc. Naz. Lincei, Roma.

Patacca E., Scandone P., Bellatalla M., Perilli N. & Santini U. (1991) - La zona di giunzione tra l'arco appenninico settentrionale e l'arco appenninico meridionale nell'Abruzzo e nel Molise. Stud. Geol. Camerti, Spec. Vol. 1991/2, pp. 417–441, Camerino, Italy.

Patacca E. & Scandone P. (2001) - Late thrust propagation and sedimentary response in the thrust belt-foredeep system of the Southern Apennines. In Anatomy of an Orogen: The Apennines and Adjacent Mediterranean Basin, edited by G.B. Vai & I.P. Martini, pp. 401–440, Kuwler Academic Publishers, Dordrecht, Netherlands.

Piccardi L., Gaudemer Y., Tapponier P. & Boccaletti M. (1999) - Active oblique extension in the central Apennines (Italy): evidence from the Fucino region. Geophys. J. Int., 139, 499-530.

Piroddi E., Mattogno C., Properzi P. & Tironi F. (1984) – L'Aquila: una piccola città media. Proceedings of the International Association of Urbanists "Les Acteur de la mise en oeuvre de l'urbanisme dans les villes Moyennes", Braga, 1-5 settembre 1984.

Pucci S., Villani F., Civico R., Pantosti D., Del Carlo P., Smedile A., De Martini P.M., Pons-Branchu E. & Gueli A. (2015) - Quaternary geology of the Middle Aterno Valley, 2009 L'Aquila earthquake area (Abruzzi Apennines, Italy). Journal of Maps, 11-5, 689-697, ISSN: 1744-5647. Doi: 10.1080/17445647.2014.927128.

Radmilli A.M. (1956) - Il Paleolitico Superiore nella Grotta Clemente Tronci presso Venere dei Marsi, Territorio del Fucino. Bollettino Società Geologia Italiana, LXXV: 94-116.

Radmilli A.M. (1981) - Storia dell'Abruzzo dalle Origini all'età del Bronzo. Ed. Giardini, Pisa, 451pp.

Raffy J. (1970) - Étude géomorphologique sur le Bassin d'Avezzano (Italie central). Mediterranee, 1, 3-18.

Raffy J. (1979) - Le versant tyrrhénien de l'Apennin central: étude géomorphologique. Thèse inédite, 705 pp.

Raffy J. (1981-82) - Orogenése et dislocations quaternaires du versant tyrrhénien des Abruzzes (Italie central). Rev. Geol. Dinam. et Geogr. Phys., 23(1), 55-72.

Ricci Lucchi F. (1986) - The Oligocene to recent foreland basins of the Northern Apennines. IAS Spec. Publ., 8, 105–139.

Roberts G. P. & Michetti A.M. (2004) - Spatial and temporal variations in growth rates along active normal fault Systems: an example from Lazio-Abruzzo, central Italy. Journal of Structural Geology, 26, 339-376.

Rovida A., Camassi R., Gasperini P. & Stucchi M. (a cura di) (2011). CPTI11, la versione 2011 del Catalogo Parametrico dei Terremoti Italiani. Milano, Bologna, http://emidius.mi.ingv.it/CPTI. DOI: 10.6092/INGV.IT-CPTI11

Salvi S. & Nardi A. (1995) - The Ovindoli fault: a segment of a longer, active fault zone in Central Abruzzi, Italy, Bull. Ass. Eng. Geol., Special Publication No. 6 "Perspectives in Paleoseismology", 101-113.

Santo A., Ascione A., Di Crescenzo G., Miccadei E., Piacentini T. & Valente E. (2013) - Tectonic-geomorphological map of the middle Aterno River valley (Abruzzo, Central Italy). Journal of Maps. Doi: 10.1080/17445647.2013.867545.

Saroli M., Moro M., Borghesi H., Dell'Acqua D., Galadini F. & Galli P. (2008) - Nuovi dati paleosismologici dal settore orientale del bacino del Fucino (Italia Centrale). Il Quaternario, Italian Journal of Quaternary Sciences, 21(1B), 2008 - 383-394.

Schlagenhauf A., Gaudemer Y., Manighetti I., Palumbo L., Schimmelpfennig I., Finkel R. & Pou K. (2010) - Using in situ Chlorine-36 cosmonuclide to recover past earthquake histories on limestone normal fault scarps: a reappraisal of methodology and interpretations. Geophys. J. Int., 182, 36-72. Doi:10.1111/j.1365246X.2010.04622.x.

Schlagenhauf A., Manighetti I., Benedetti L., Gaudemer Y., Finkel R., Malavieille J. and Pou K. (2011) - Earthquake supercycles in Central Italy, inferred from 36Cl exposure dating. Earth Planet. Sci. Lett., 307, 487-500, doi:10.1016/j.epsl.2011.05.022.

Schwartz D.P. & Coppersmith K.J. (1984) - Fault behavior and characteristic earthquakes: examples from the wasatch and San Andreas Fault Zones. J. Geophys. Res., 89 (B7), 5681–5698, http://dx.doi.org/10.1029/JB089iB07p05681.

Scrocca D., Doglioni C. & Innocenti F. (2003) - Contraints for an interpretation of the italian geodynamics: a review. Mem. Descr. Carta Geol. It., 15-46.

Serva L., Blumetti A.M. & Michetti A.M. (1988) - Gli effetti sul terreno del terremoto del Fucino (13/1/1915); tentativo di interpretazione della evoluzione tettonica recente di alcune strutture. Mem. Soc. Geol. It. 35, 893-907.

Serva L., Blumetti A.M., Guerrieri L. & Michetti A.M. (2002) - The Apennine intermountain basins: the result of repeated strong earthquakes over a geological time interval. Proceedings of the Conference "Evoluzione Geologica e Geodinamica dell'Appennino in memoria del Prof. Pialli". Boll. Soc. Geol. It., Vol. Spec. n°1 (2001), 939-946.

Stokel G. (1981) – La città dell'Aquila. Il centro storico tra il 1860 e il 1960. Edizioni del Gallo Cedrone, L'Aquila.

Tallini M., Di Fiore V., Bruno P.P., Castiello A., Punzo M., Varriale F., Del Monaco F., Tarallo D., Cavuoto G. & Pelosi N. (2011) - Sismica a riflessione ad alta risoluzione per il modello del sottosuolo e la stima della pericolosità sismica del centro storico dell'Aquila. Proceedings of 30th Conference Gruppo Nazionale di Geofisica della Terra Solida (GNGTS), Trieste 14-17 novembre 2011 (In Italian).

Tertulliani A., Leschiutta I., Bordoni P. & Milana G. (2012) - Damage Distribution in L'Aquila City (Central Italy) during the 6 April 2009 Earthquake. Bulletin of the Seismological Society of America, 102/4, 1543–1553, http://dx.doi.org/10.1785/0120110205.

Tertulliani A., Arcoraci L., Berardi M., Bernardini F., Camassi R., Castellano C., Del Mese S., Ercolani E., Graziani L., Leschiutta I., Rossi A. & Vecchi M. (2011). An application of EMS98 in a medium-sized city: The case of L'Aquila (Central Italy) after the April 6, 2009 Mw 6.3 earthquake. Bull. Earthq. Eng. 9, 67–80. Doi10.1007/s10518-010-9188-4.

Totani G., Totani F., Monaco P., Tallini M., Del Monaco F. & Zia G. (2012) - Site investigations and geotechnical problems in the Southern part of the historic centre of L'Aquila. In: M. Maugeri and C. Soccodato (eds), Proc. 2nd Int. Conf. on Performance-Based Design in Earthquake Geotechnical Engineering, Taormina, Italy, Paper No. 2.13, 315-328. Pàtron Editore, Bologna (CD-ROM).

Tucker G.E., McCoy S.W., Whittaker A.C., Roberts G.P., Lancaster S.T. & Phillips R. (2011) - Geomorphic significance of post-glacial bedrock scarps on normal fault footwalls. Journal Geoph. Res., Earth Surface, 116, F01022, 14 PP., 2011. Doi:10.1029/2010JF001861

Vannoli P., Burrato P., Fracassi U. & Valensise G. (2012) - A fresh look at the seismotectonics of the Abruzzi (Central Apennines) following the 6 April 2009 L'Aquila earthquake (Mw 6.3). Ital. J. Geosci., 131/ 3, 309–329, http://dx.doi.org/10.3301/IJG.2012.03.

Vittori E., Di Manna P., Blumetti A.M., Comerci V., Guerrieri L., Esposito E., Michetti A.M., Porfido S., Piccardi L., Roberts G.P., Berlusconi A., Livio F., Sileo G., Wilkinson M., Mccaffrey K.J.W., Phillips R.J. & Cowie P.A. (2011) - Surface faulting of the 6 April 2009 Mw 6.3 L'Aquila earthquake in Central Italy. Bull. Seismol. Soc. Am., 101/4, 1507–1530. http://dx.doi.org/10.1785/0120100140.

Wallace R.E. (1978) - Profiles and ages of young fault scarps, north-central Nevada, Bull. Geol. Soc. Am. 88 (1977) 1267–1281.

Wells D.L. & Coppersmith K.J. (1994) - New empirical relationships among magnitude, rupture length, rupture width, rupture area and surface displacement, Bull. Seismol. Soc. Am., 84, 974–1002.